IMPLICATIONS OF POTASSIUM CHANNEL HETEROGENEITY FOR MODEL VESTIBULO-OCULAR REFLEX RESPONSE FIDELITY

JAMES MCGUINNESS

Submitted in Partial Fulfilment of the Requirements for the Degree of Doctor of Philosophy

Division of Computing Science and Mathematics
University of Stirling

September 2014

DECLARATION

I, James McGuinness, hereby declare that this work has not been submitted for any other degree at this University or any other institution and that, except where reference is made to the work of other authors, the material presented is original.

September 2014

ABSTRACT

The Vestibulo-Ocular Reflex (VOR) produces compensatory eye movements in response to head and body rotations movements, over a wide range of frequencies and in a variety of dimensions. The individual components of the VOR are separated into parallel pathways, each dealing with rotations or movements in individual planes or axes. The Horizontal VOR (hVOR) compensates for eye movements in the Horizontal plane, and comprises a linear and non-linear pathway. The linear pathway of the hVOR provides fast and accurate compensation for rotations, the response being produced through 3-neuron arc, producing a direct translation of detected head velocity to compensatory eye velocity. However, single neurons involved in the middle stage of this 3-neuron arc cannot account for the wide frequency over which the reflex compensates, and the response is produced through the population response of the Medial Vestibular Nucleus (MVN) neurons involved.

Population Heterogeneity likely plays a role in the production of high fidelity population response, especially for high frequency rotations. Here we present evidence that, in populations of bio-physical compartmental models of the MVN neurons involved, Heterogeneity across the population, in the form of diverse spontaneous firing rates, improves the response fidelity of the population over Homogeneous populations. Further, we show that the specific intrinsic membrane properties that give rise to this Heterogeneity may be the diversity of certain slow voltage activated Potassium conductances of the neurons. We show that Heterogeneous populations perform significantly better than Homogeneous populations, for a wide range of input amplitudes and frequencies, producing a much higher fidelity response. We propose that variance of Potassium conductances provides a plausible biological means by which Heterogeneity arises, and that the Heterogeneity plays an important functional role in MVN neuron population responses.

We discuss our findings in relation to the specific mechanism of Desynchronisation through which the benfits of Heterogeneity may arise, and place those findings in the context of previous work on Heterogeneity both in general neural processing, and the VOR in particular. Interesting findings regarding the emergence of phase leads are also discussed, as well as suggestions for future work, looking further at Heterogeneity of MVN neuron populations.

ACKNOWLEDGEMENTS

Special thanks are extended to Dr Bruce P. Graham, for his constant support, advice and motivation in the production of the work presented here.

Thanks are also extended to Michael Hines, John W. Moore, and Ted Carnevale for their work developing the NEURON Simulation environment, used for the production of all results presented. Special thanks go to Hines and Carnevale for advice on parallelisation, the event delivery system of NEURON, and the proper coding of Noise in our models.

Thanks must also be extended to Tom Morse of the Yale.edu for the implementation of the Medial Vestibular Nucleus neurons used in the work, in the NEURON simulation environment. And to R. Quadroni and T. Knopfel for the mathematical basis from which these models derived.

Some results presented were obtained using the EPSRC funded ARCHIE-WeSt High Performance Computer (www.archie-west.ac.uk). EPSRC grant no. EP/K000586/1. Thanks go to Richard Martin for facilitating this access, and for help when nothing worked.

Finally, I would like to thank my parents, James and Margaret McGuinness, for their financial and emotional support in completing the work here.

TABLE OF CONTENTS

LIST OF FIGURES

LIST OF TABLES

LIST OF ACRONYMS

- VOR - Vestibulo-Ocular Reflex
- hVOR - Horizontal Vestibulo-Ocular Reflex component
- SCC - Semi-Circular Canal
- MVN - Medial Vestibular Nucleus
- CVN - Central Vestibular Nuclei
- PSTH - Peri-Stimulus Time Histogram

1

INTRODUCTION AND AIMS OF RESEARCH

1.1 INTRODUCTION

The Vestibular system is responsible for the maintenance of head and body posture, as well as the stabilisation of images in the visual field during motion, and the internal sense of balance and posture. Head and body movements are detected by sensory organs of the ear, in both rotational and linear planes, and processed along numerous parallel pathways in order to produce compensatory neck and eye movements, internal representations of head and neck position and angle, and to maintain balance [26]. The Vestibular system is considered to be phylogenetically ancient [33], being found throughout the fossil record largely unchanged [123], including some of the earliest extant species, such as the myxine and lamprey [63], and is found to be remarkably similar across species [1]. It has been extensively studied in a wide variety of organisms, and a vast amount of data and theory has been produced regarding the function and mechanisms by which it acts.

One component of the Vestibular system is the Vestibulo-Ocular Reflex (VOR), which produces compensatory eye movements in response to head and body movements, in order to maintain visual gaze stability, and focus on objects in the visual field during movements [47]. Specifically, the VOR detects head movements, either rotational or linear, and produces eye movements that directly compensate for these movements, thus keeping the eyes stable in relation to the head movements. For example, rotations of the head to the left produce compensatory rotations of the eye to the right, to maintain focus and stability of gaze. Generally, the VOR is a linear system, translating sensory input directly to motor output [7]

The VOR is organised into numerous parallel pathways, each acting on separate neuronal arcs, specialised and optimised to the features of the stimuli they respond to, the linearity of their response, and the capacity for adaptation of their response [128] [85] [105]. One such pathway is the linear Horizontal VOR pathway, which translates rotations of the head in the horizontal plane (left and right) into compensatory eye movements in this plane [98]. This response is achieved over a relatively simple three-neuron arc involving the neurons of the Medial Vestibular Nucleus (MVN)

as the middle stage of processing [129]. In addition, hVOR has a well characterised anatomy and physiology [89], therefore presenting it as an ideal system for investigation, particularly in investigation of the role of variability in neural systems.

The hVOR compensates for a wide range of frequencies of head rotations, producing a fast and accurate response to these movements. However, individual MVN neurons involved in the response cannot sufficiently code for wide dynamic range of responses seen, and Homogeneous populations are unable to account for the response produces. Thus, a population coding strategy is likely utilised by the system [89], and population Heterogeneity likely plays a role in the population responses.

Significant neuronal variability (Heterogeneity) is seen among the neurons identified as being responsible for the hVOR [109], and it is theorised that the variability seen across the populations is necessary for their dynamic properties [5], and particularly for the precise, wide frequency response required of the VOR [68]. However, no specific means by which population Heterogeneity arises, and the particular intrinsic membrane properties involved in this Heterogeneity have not been found. For true understanding of the coding strategies used in the VOR, and in neural systems in general, it is important to identify and quantify population Heterogeneity, and to explore the possible functional role of this Heterogeneity.

Here we investigate the role of population Heterogeneity, in the form of diversity of spontaneous firing rates across a population, in producing the necessary high fidelity response of the MVN neuron populations. Specifically, we hypothesise that population Heterogeneity in the form of the diversity of slow Voltage activated Potassium channel conductances across a population of MVN Type B neurons, creating a population of neurons with a distributed rate of spontaneous firing, leads to improved response fidelity of these Heterogeneous populations to high frequency inputs, over Homogeneous populations. In this way, we investigate and provide a description of the specific intrinsic membrane properties of MVNB neurons that are required for their observed functioning. We also look at the possible role of Noise in the response fidelity and performance of MVN neuron populations.

We approach this through the simulation of bio-physical, compartmental models of MVN neurons, using a realistic strategy for inducing population Heterogeneity, and compare the response fidelity of these populations with Homogeneous populations receiving the same inputs. Although previous research has suggested a functional role for Heterogeneity, both generally [72] and in the VOR specifically [5], and previous modelling studies have shown a functional role for

diversity of spontaneous firing rates [68], we suggest here for the first time the specific intrinsic membrane properties (diverse Potassium conductances) that give rise to this Heterogeneity, and its impact on the high frequency response of the hVOR.

Chapter 2 provides an overview of the Vestibular System, and the Vestibulo-Ocular Reflex in particular, identifying the pathways involved, and the specific neural populations making up these pathways. The exact pathway involved in the linear aspect of the hVOR, which we investigate, is elaborated upon, as well as the necessary understanding still required for describing the function of this pathway, and the contribution of the research here to this understanding.

We then provide an overview of the role of Variability in neural systems, looking at both the role of Noise and Heterogeneity, their implications for neural processing, and specific means by which they may benefit neural processing. Particular attention is given to the role of Heterogeneity, and the possible mechanism of desynchronisation by which it may improve neural population responses. This overview is then placed into the context of the hVOR, looking particularly at the role that ionic channel Heterogeneity, and its possible role in producing the dynamic responses seen in the populations of neurons involved.

Chapter 2 concludes with a thorough examination of the motivations and aims of the current research, the usefulness of the modelling approach applied, and the importance of understanding the area investigated.

Chapter 3 presents a description of the specific neurons modelled in the work presented, along with the basis by which these neurons have been modelled. We show that the model of the neurons accurately reproduce behaviour of real MVN neurons, and that they allow for an in depth exploration of the function of Heterogeneity in these neurons, though the manipulation of ionic conductances in order to model Heterogeneity plausibly.

Details of the modelling methods, in regards to input and the modelling of Heterogeneity are then presented, along with a brief overview of the parallelisation method implemented to allow for the large number of simulations required to be performed. This chapter concludes with an overview of the analysis methods and performance methods applied to produce results of the simulations.

Chapter 4 presents the results of our simulations, across several stages, using the various methods by which inputs have been generated and Heterogeneity has been modelled. We present results across 3 stages of simulations, looking at a general role for diverse firing rates in response

fidelity, before a more particular investigation of Heterogeneity produced through the variance of specific slow Potassium conductances is presented.

We then present an analysis of our results, in regards to the response fidelity of populations, the possible mechanisms by which fidelity is improved, the role of Noise in response fidelity and its relation to Heterogeneity, and interesting features of our results in regards to the emergence of a "phase lead" in the response of the Heterogeneous populations we have simulated here, and a discussion of this phenomenon in regards to phase leads observed in the real VOR response.

Finally, Chapter 5 presents a discussion of the results and analysis presented, outlying the findings we have made. These findings are placed into the context of other studies looking at Heterogeneity, both generally and in the VOR in particular. Possible shortcomings, and avenues for further research are also provided.

2

BACKGROUND

2.1 VESTIBULAR SYSTEM AND OVERVIEW OF VESTIBULAR REFLEXES

2.1.1 *Introduction*

The Vestibular system is responsible for the detection of head movements and the generation of reflexes of crucial importance to the everyday activities of a vast range of organisms , including the stabilisation of the visual axis (gaze stabilisation, through the Vestibulo-Ocular Reflex, or VOR), and the maintenance of body and head posture (Vestibulo-Spinal and Vestibulo-Collic reflexes). Further to this, the Vestibular system provides organisms with their subjective sense of movement, balance and spatial orientation. The Vestibular system is made up of two types of inner ear organs that act as the sensors that detect movements, the three semicircular canals (Horizontal, Anterior, and Posterior), and the otolith organs (Utricle and Saccule). The former are responsible for the detection of rotational movements, and angular acceleration, while the latter are responsible for detection of linear acceleration (gravitational and translational movements). These sensory organs innervate the neural structures responsible for the control of balance, eye movements, and posture, via the Vestibular nerve fibres and Second order, or Central, Vestibular nuclei.

These Vestibular Sensory Organs are located in the petrous part of the temporal bone, in the labyrinth of the inner ear in most mammals, in close proximity to the cochlea (auditory sensory organ), although the vestibular system is recognised as one separate from the auditory systems of the inner ear. The Vestibular system is considered to be phylogenetically ancient, as one of the oldest parts of the inner ear, remaining largely unchanged across the fossil record.

The Vestibular system plays a crucial role in ensuring postural equilibrium, through the production of appropriate movements during both self generated locomotion and rotations, and any externally applied forces leading to disturbance of posture or balance. Investigation of the Vestibular system through behavioural, clinical, neurophysiological, and theoretical studies have provided a substantial understanding of the function and role of the Vestibular system in many common activities.

One of the major aspects of the Vestibular system, the Vestibulo-Ocular Reflex (VOR) functions to stabilise gaze and maintain clear vision and gaze fixation during movement, through the production of compensatory movements of the eyes. That is, the VOR measures head movements, through the Vestibular Sensory Organs, and generates eye movements through a compensatory Oculomotor response, equal in magnitude but opposite in direction to the head movements compensated for. The relative simplicity of the pathways responsible for mediation of the reflex, along with the extent to which the reflex has been characterised, have made the VOR an eminent model system for the investigation of the relationship between neurons, neural circuits or pathways, and observed behaviour.

This chapter provides background and description of the Vestibular system, the function and role of the reflexes produced by the system, and the components involved in these reflexes, before moving on to detail the Vestibulo-Ocular reflex specifically, followed by discussion of the role of Variability in neural processing and the VOR itself.

2.1.2 *The Receptors of the Vestibular Sensory Organs*

2.1.2.1 *Semi Circular Canals*

The three semicircular canals (Horizontal, Anterior[1], Posterior) are half circular, interconnected membranous tubes filled with Endolymphatic fluid, and are able to sense angular accelerations in the three orthogonal planes. They are sensitive to angular accelerations (rotational movements of the head) [108], and are organised such that they can detect rotations of the head around each of the three possible axis of rotation) [56](Figure 2.1). The semicircular canals are made up of a circular path of continuous fluid terminating at the ampulla by an elastic, water tight membrane known as the cupula. The sensory epithelium of these semicircular canals is located on the ampulla, and contains hair cells, each of which projects cillia from their surface, into the Endolymphatic fluid surrounding them. These hair cells produce a tonic (or constant) release of neurotransmitter, which in turn produces spontaneous activity in the Vestibular nerve fibres to which they synapse. They function as the initial sensory apparatus for the Vestibular system through the detection and transduction of a mechanical force (angular acceleration) into an electrical signal (excitation and inhibition of Vestibular nerve afferents onto which they synapse). The tonic release of neurotransmitter, from these hair cells, is mediated and modified by the extent and direction of deflection of the cupula [52]. Although the stimulus on the semicircular

1 Sometimes referred to as the Superior canal

canals is angular acceleration, the neural output from the sensory cells represents the velocity of rotation [26]. This is due to the mechanics of the canals (largely the increase in viscosity of the fluid located in the canal, due to its small diameter), the output of the hair cells is representative of the velocity of rotation, rather than the acceleration (which serves as the stimulus to the Otolith organs) [50] [29]. The combination of the input from the three canals serves to produce a three-dimensional representation of instantaneous velocity of head rotation in space. The semicircular canals are, therefore, fundamentally angular accelerometers that act as velocity transducers in the physiological range of sinusoidal rotations. However, the VOR is not a sustained reflex; after many seconds of steady rotation the stimulus for eye movement will die down [26].

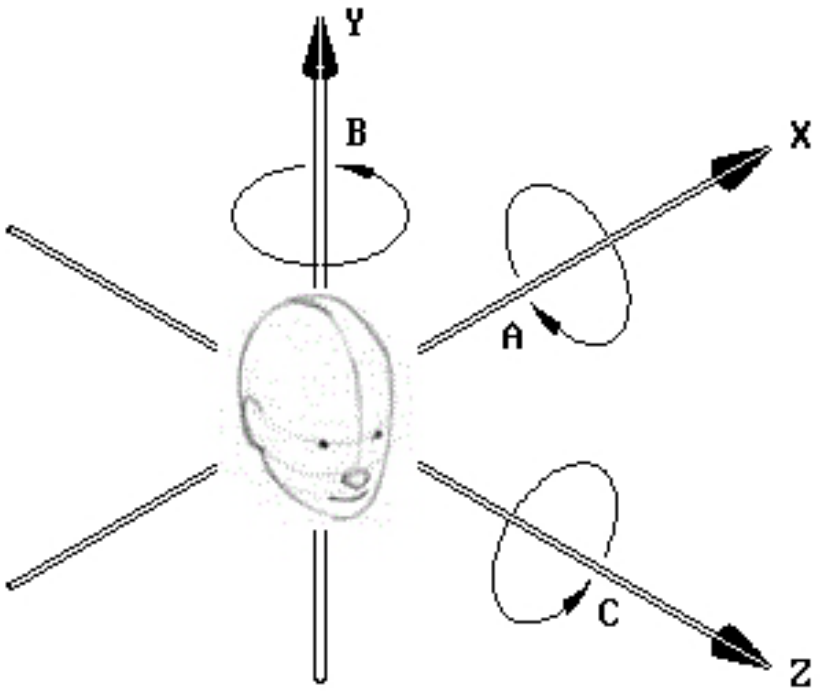

Figure 2.1: 3 Axis of Rotation around the Head. Movement A, around Axis X or the Sagittal Plane. Movement B, around Axis Y or the Transverse Plane. Movement C, around Axis Z or the Coronal Plane

2.1.2.2 *Otolith Organs*

Whereas the semicircular canals are sensitive to angular acceleration, or rotational movements, the Otolith organs, comprising the Utricle and Saccule, are sensitive to linear acceleration. Much like the semicircular canals, the sensory epithelium of the Utricle and Saccule contain hair cells which produce a constant release of neurotransmitter, producing spontaneous activity in the Vestibular-nerve afferents which are innervated by these organs. The deflection/bending of cilia

emerging from the hair cells of the sensory epithelium produces excitation or inhibition of the hair cells, causing increased or reduced neurotransmitter release, which in turn modifies the spontaneous activity of the vestibular afferents [43] [44] [45]. The Otolith organs detect both linear acceleration due to movement, along with the direction and extent of gravity [43] [44] [45].

2.1.2.3 *Vestibular Sensory Organ Hair Cells*

Two types of hair cells are found in the Vestibular sensory organs, and are the means by which acceleration and movement are detected and measured, and the spontaneous activity of the Vestibular afferents is mediated. Flask-shaped Type I haircells are present only in amniotes (birds, mammals, reptiles), while the Cylindrical Type II haircells are the phylogenetically older of the two types, and are present in both amniotes and non-amniotes [35]. These two cell types show distinct and specific properties. As an example, differences between the two cell types include differing densities of Potassium channels, with larger amounts of Calcium activated Potassium channels contributing to a greater sensitivity to high frequency stimulation [36] [35] [73] [83] [136]. As will be shown in the following section (Primary Vestibular Afferents), Type I and Type II haircells supply inputs to Irregular and Regular vestibular-nerve afferent fibres respectively.

2.1.3 *Primary Vestibular Afferents*

2.1.3.1 *Two Types of Vestibular Afferents: Regular and Irregular*

Vestibular-nerve afferents innervate (receive signals from) the Vestibular sensory organs (Type I and Type II hair cells), and enervate (carry signals to) the Second order, or Central, Vestibular nuclei. Functional grouping of the Vestibular-nerve afferents, into Regular and Irregular groups, is based on the regularity of the afferents spontaneous firing rate, or rate of resting discharge, based on a normalised coefficient of variation (CV* of the Interspike Intervals) [53]. That is, Regular afferents show little variation in the Interspike Intervals (ISIs) of their resting discharge rate (CV* of ISIs <0.1), while Irregular afferents show (CV* of ISIs >0.1) [53] (Figure 2.2, lower section). Further to this functional grouping, Vestibular-nerve afferents are also distinguished in that regular and irregular units have distinct morphological, or physical, properties (Figure 2.2, upper section). In both the otoliths and semicircular canals, Regular afferents are found to have a smaller axon diamater than Irregular afferents, and are found to provide bouton endings to type II haircells located at the periphery of the vestibular neuroepithelium. Further to this, Irregular units can be divided into two groups: those that provide calyx endings to Type I haircells located

at the center of neuroepithelium (C-irregulars) and the rest provide a mixed innervation of calyx endings to type I haircells and bouton endings to type II haircells (dimorphic or D-irregulars) [9].

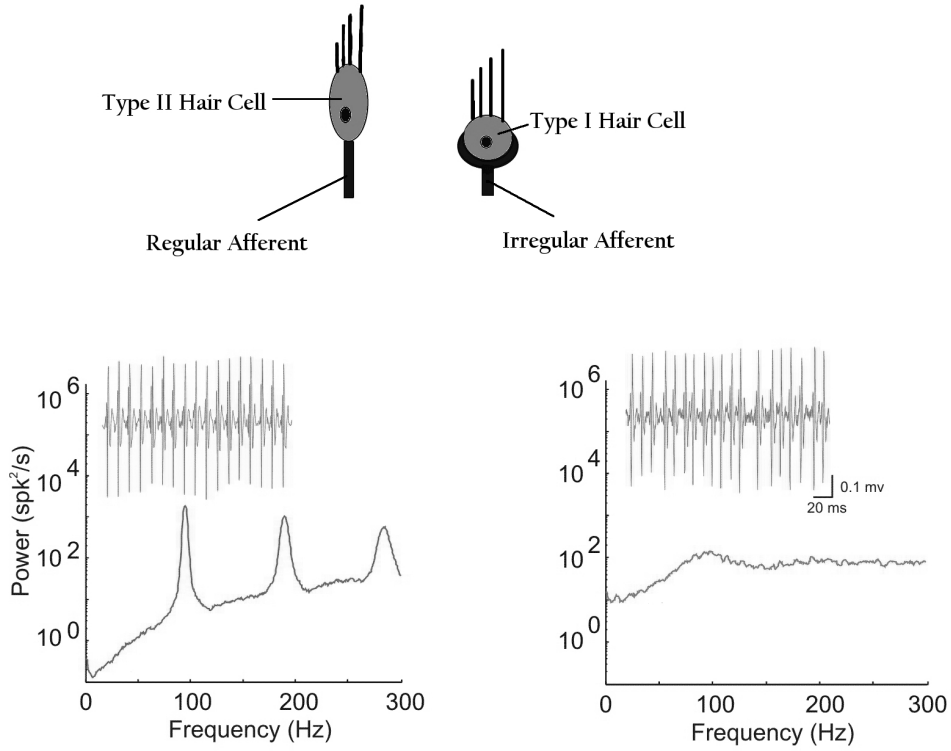

Figure 2.2: Regular and Irregular Afferents and their ISI Activity. Regular Afferents (Left) are innervated by Type II Haircells (upper section), and their power spectrum displays peaks at the resting discharge rate and its harmonic values (lower section). Irregular Afferents are innervated by Type I Haircells and, as they have an irregular Interspike Interval (ISI), their power spectrum does not show any definite peaks. Hair cells and their afferents show unique morphology and shape, with Type I displaying a rounded or flask shaped hair cell, with Calyx endings for the afferents, while Type II show a longer shape and Bouton endings to their afferents. ISI data reproduced from [26]

2.1.3.2 *Signals in Response Movements*

Vestibular-nerve afferents innervating the Otolith organs transmit information regarding the linear acceleration undergone by the Otolith organs, with both gravitational forces and translational movements, across a wide range of frequencies, eliciting similar responses from the afferents [43]. While the dynamic response of Otolith afferents is largely in phase with the rotational acceleration, with increased sensitivity caused by increased frequency of movement [4] [43] [44] [45], the response of Vestibular-nerve afferents innervating the Semicircular canals is, contrastingly, largely in phase with the velocity of the rotation imposed upon the Semicircular canals [42] [70]

[69] [112]. This difference is largely due to the specific mechanical properties of the Semi-circular canals.

Experimental studies which have focussed on the Vestibular-nerve afferents innervated by the Semicircular canals have shown that these Regular and Irregular Semicircular canal afferents use differing coding strategies for transmitting information regarding the velocity of rotations, mainly due to the level of variability of resting discharge of these Regular and Irregular afferents [111]. As the resting discharge variability is greater for Irregular afferents when compared to Regular afferents, Irregular afferents show a higher power in the power spectrum of their resting discharge, over physiologically relevant frequencies, resulting in a low signal to noise ratio, and minimal information in their specific spike timings, especially at lower frequencies [111]. By contrast, the lower variability of the Interspike intervals of Regular afferents resting discharge produces a higher signal to noise ratio, and thus a higher level of information in individual spike times [111]. In light of these differences in the information conveyed by spike timing between the two groups of Vestibular-nerve afferents, it can be seen that they use different encoding strategies for transmission of information regarding the velocity of rotation to the Second order, or Central, Vestibular nuclei [111]. Regular afferents convey the majority of information in their spike times, utilising a temporal code in order to transfer information about the velocity of rotation [111]. In comparison, the response of Irregular afferents is thought to be quantified through a rate coding strategy, with Gain[2] increases as a function of the frequency of rotation [70] [69] [112]. Therefore, it can be seen that while Regular afferents provide information about head movements through the use of a temporal code, Irregular afferents provide information about head movements (particularly at high velocities) through the use of rate encoding [69] [70].

In line with this, studies have attempted to study the implications of these differing coding strategies at the level of the Vestibular afferents, and apply this to the processing in the Second order, or Central, vestibular nuclei level [89]. For example, it was found that through combining the activities of multiple neurons under investigation, the information transmission of the Second order neurons was increased [89].

In order to maintain both perceptual and postural stability, and for behaviour to be guided accurately, it is necessary for the Vestibular signals produced by the external world acting upon an organism, and those resulting from the organism's own actions, to be differentiated by the organism's nervous system. However, studies have shown that the afferents of the Semi-circular

2 Where Gain refers to the ratio of the 'output' from the afferents and Second order neurons compared to the input provided to them

canals, involved in the linear rotational VOR, encode both externally produced movements (i.e., passive movements) and self-generated movements (i.e., active movements) in a similar fashion [28] [112]. As will be discussed in the following section (Second Order, or Central, Vestibular Neurons) the differentiation of active and passive movements within the Vestibular system begins to occur at the following level of signal processing, the Vestibular nuclei.

2.1.4 *Second Order, or Central, Vestibular Neurons*

2.1.4.1 *Four Main Nuclei of the Central Vestibular Complex*

The Vestibular afferents communicate via the vestibular branch of the eighth cranial nerve with targets in the brainstem and the cerebellum which are responsible for much of the processing necessary to compute head position and motion. Specifically, the targets in the brainstem are collectively known as the Second order, or Central, Vestibular complex or the Vestibular Nuclei.

The Second order, or Central, Vestibular complex comprises four primary nuclei (Figure 2.3): the Inferior (descending) Vestibular nucleus (IVN), the Lateral Vestibular nucleus (LVN), the Medial Vestibular nucleus (MVN), and the Superior Vestibular nucleus (SVN) [100] [129]. Although no absolute segregation of inputs from afferents is evident, the MVN and SVN primarily receive inputs from the horizontal and superior Semi-circular canals respectively [100] [129]. Utricular afferents mainly terminate in the IVN, although also send projections to the LVN, MVN, and SVN [100]. Alongside the direct projections of Vestibular-nerve afferents that converge on the Central Vestibular nuclei, inputs originating from cerebellar, cortical, and other brainstem structures also converge on the Central Vestibular nuclei, providing information on visual and somatosensory inputs, as well as information on eye movements.

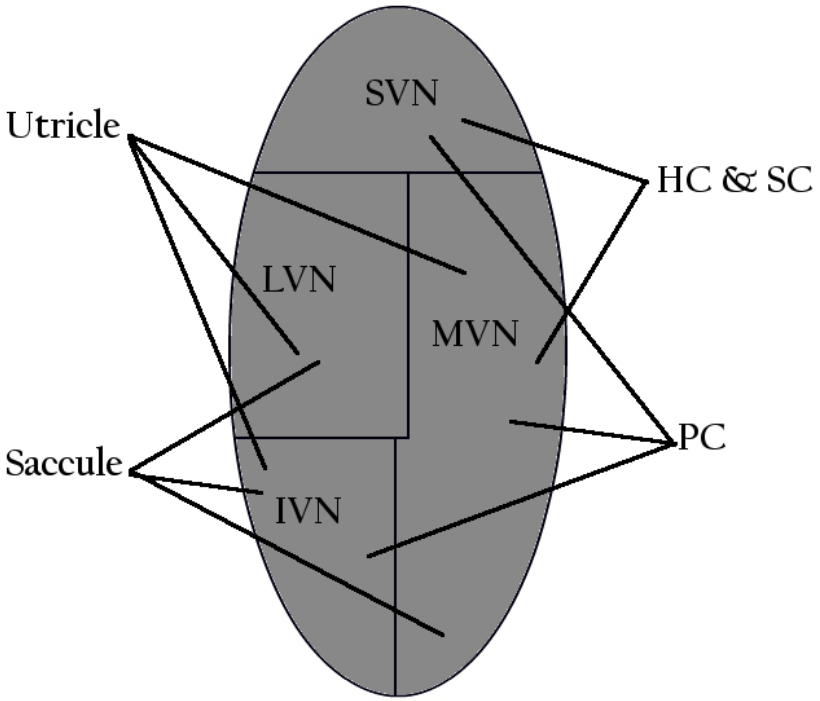

Figure 2.3: Central Vestibular Nuclei and their Vestibular Inputs. Abstraction of the Vestibular nuclei complex, and the general segregation of areas within them. The Utricular afferents primarily terminate in the Inferior Vestibular Nuclei (IVN), but also in the Lateral and Medial Vestibular Nuclei (LVN, MVN). Saccule innervated afferents terminate in the LVN, IVN, and MVN. Superior and Horizontal Canal afferents terminate mainly in the MVN and SVN

2.1.4.2 *Responses to Passive Movements*

The sensitivities of neurons in the Central Vestibular nuclei to rotational movements have been quantified extensively in various subjects, and have been shown to be consistent with the projections described in the section above (Four Main Nuclei of the Central Vestibular Complex). Neurons sensitive to horizontal rotations are primarily found in the MVN and LVN [75] [23] [27] [48] [116]. Neurons sensitive to vertical rotations have been recorded primarily in the SVN and MVN [32] [131]. Neurons sensitive to rotations in both the horizontal and vertical systems can be divided into 3 main classes based on their responses to voluntary eye movements and passive whole-body rotations. These classes being: Position-Vestibular-Pause (PVP) neurons (responsible for the performance of the Vestibulo-Ocular reflex), Vestibular-Only (VO) neurons (involved in Vestibulo-Spinal reflexes), and Eye-Head (EH) neurons (involved in smooth pursuit movements of the eyes).

2.1.4.3 *Vestibular Ocular Reflex*

The Vestibulo-Ocular reflex (VOR) effectively stabilises gaze during everyday movements, such as head or body rotations or locomotion, by moving the eye in the opposite direction to the motion that occurs, with precisely the same time course [129] [75] [10]. This elementary three-neuron arc pathway consists of projections from the Vestibular-nerve afferents to neurons in the Central Vestibular nuclei, which in turn project to the extraocular motoneurons [129] [75] [68]. The relative simplicity of this three-neuron arc makes the VOR apt for investigation.

In addition, the relative simplicity of the reflex, and three-neuron arc producing it, leads to the reflex's fast response time, with compensatory eye movements lagging behind head movements by 6ms, on average, in primate subjects [74] [98]. Despite the reflex serving to stabilise vision, the VOR is driven entirely by information regarding head rotation conveyed by the Vestibular system, and does not depend upon any visual input. Thus, the reflex works in the absence of any visual input, such as in complete darkness or when the eyes are closed [47].

As the Vestibulo-Ocular Reflex is the main focus of the work being presented, a more complete exploration and analysis of the reflex shall follow in the section (Section 2.2).

2.1.4.4 *Other Vestibular Reflexes*

In addition to the role played by the Vestibular system in stabilising gaze through the action of the VOR, the Vestibular system also plays a significant role in the coordination of postural reflexes. The Vestibulo-Collic reflex (VCR) works in a similar fashion to the VOR, but serves to stabilise head and body position in relation to movement, such as locomotion, and is critical for the maintenance of head and body posture during daily activities [134]. This stabilisation is achieved through the generation of head movements in the opposite direction to that of current head velocity in space, mediated by the projection of Vestibular-only (VO) neurons from the Vestibular Nuclei to the cervical spinal cord [134].

The Vestibular sensory organs (the three approximately orthogonal semicircular canals, (Anterior, Horizontal,Posterior) and the two otolith organs (Utricle, Saccule)) provide the most important input for the detection of head movement, the afferents of which serve to evoke the Vestibulo-Collic reflex (VCR)[3] [134]. Specifically, for angular head velocity in space, Vestibular hair cells located within the Semicircular canals of the inner ear detect head velocity, and in turn the Vestibular afferent neurons of the vestibular nerve project information regarding this velocity

3 the VCR involves control of neck muscles for correction of the orientation of the head

to Vestibular-Only (VO) neurons in the Vestibular nuclei, which similarly encode information regarding head velocity [110]. Further, VO neurons show little sensitivity to eye movements and are modulated during passive whole body rotational movements [110]. In addition, VO neurons are likely responsible for the control of Vestibulo-Spinal reflexes[4] [26] [110].

2.2 THE VESTIBULAR-OCULAR REFLEX

2.2.1 *Introduction and Basic Overview of the Vestibulo-Ocular Reflex*

The Vestibulo-Ocular reflex (VOR) is a reflexive eye movement that acts to ensure that images are stabilised on the retina during head movement, via the production of eye rotations that are compensatory to the detected head movements [49]. That is, in an ideal VOR that compensates for any arbitrary head movements in 3-Dimensional space, eye rotations are generated in the opposite direction to, but at the same speed as, the head movements being compensated for. The result of this compensatory eye movement is that the eye remains stationary in space, relative to head or body movements, and stabilisation of images on the retina is achieved and maintained [47]. For example, head rotation to the left (with gaze fixated upon an object or target) produces eye rotation to the right in order to compensate for that head rotation, and to ensure the focusing of the image on the fovea of the eye [57].

The VOR acts over both brainstem and cerebellar pathways to generate the necessary compensatory eye movements [84] and achieves the necessary compensation through the control of eye muscles driven by input from the Otolith and Canal structures of the vestibular system [128]. That is, head (or body) movement is detected by the Vestibular apparatus of the ear, it is relayed to the brainstem and cerebellar interneurons, and it is then used to drive eye movements through stimulation of the eye muscles [47].

The VOR is of paramount importance to effective and normal functioning of an organism during everyday movements of the head or body, allowing for gaze fixation and image stabilisation to be maintained during these activities [56]. That is, for example, the VOR allows predatory organisms to maintain visual contact with prey organisms and objects or obstacles in their visual field during hunting movements, or, similarly, allow prey organisms to maintain visual contact with predatory organisms or obstacles during movements required for evasion. Indeed, as organisms are almost constantly undergoing head movements, the VOR is necessary for maintaining gaze fixation during any and all everyday activities [47]. Loss of the VOR function can have severe

4 These reflexes are responsible for maintaining of head and body posture and balance.

and detrimental consequences for an organism, for example a patient with vestibular damage finds it difficult or impossible to fixate on visual targets while the head is moving, a condition called oscillopsia. Such a condition would leave a subject or organism with severe detriments in activities such as the reading of text, or maintaining gaze fixation on a food source (or other object of interest) while moving.

The VOR has five main constituent stages of input generation, signal transmission, and processing. Firstly, head movement is detected by the Vestibular apparatus of the inner ear, the three Semi-Circular canals and the Otolith organs, which produce inputs to the reflex, corresponding to head angular velocity, linear acceleration, and orientation of the head with respect to gravity. Secondly, this activity, the altered neurotransmitter release from the hair cells of the Vestibular apparatus (through the deflection of the cilia of the hair cells), is transmitted, via synapses, to the Vestibular afferents of the VIIIth Cranial nerve (Scarpa's Ganglion, or the Vestibular Nerve Ganglion). Thirdly, these Vestibular afferents synapse with neurons in the Central Vestibular Nuclei (of the brainstem) as well as with targets in the Cerebellum (involved in higher order Vestibular systems). Fourth, the Central Vestibular neurons project to and synapse with Vestibular efferent targets in the Oculomotor nuclei (as well as the Abducens nuclei), which, in the fifth stage, synapse with and provide input to the 12 Oculomotor muscles responsible for eye movements [129] [10] [128] [75]. This general organisation is illustrated in Figure Number 2.4.

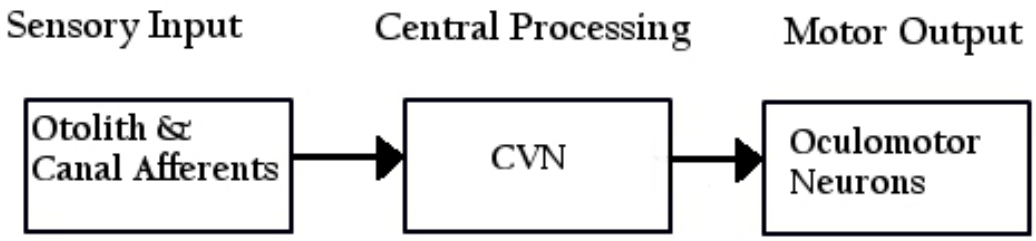

Figure 2.4: Schematic illustration of the major stages of the Vestibulo-Ocular Reflex. Sensory Input from the Otolith and Canal afferents is sent to the Central Vestibular nuclei (CVN), and then to the Oculomotor nuclei, to produce motor output

This organisation is sometimes referred to as the Elementary three neuron arc of the VOR [129], referring to the three stages of neurons involved - Vestibular afferents (located in the VIIIth Cranial nerve), Central Vestibular Nucleus neurons (located in the brainstem), and the Oculomotor Nuclei and Vestibular efferents (in the Oculomotor nerve and Abducens nuclei, IIIrd and VIth Cranial

nerves, respectively). This three neuron arc follows the structure of other observed elementary three neuron arcs, with sensory neurons (Vestibular afferents), interneurons (Central Vestibular neurons), and motor neurons (Vestibular efferents) [129].

At the gross phenomenological level, the VOR shows two major components, each compensating for one of two types of movement of the head: the angular or rotational VOR compensates for rotational movements, is generated by activity arising from the Semi-Circular canals (SCCs), and is primarily responsible for stabilisation of gaze; and the linear or translational VOR which compensates for translational movements of the head (for example, during locomotion), and is generated by activity in the Otolith organs (Utricle and Saccule) and is primarily engaged in situations when the organism is viewing near objects (due to the relative change in position on the retina of objects nearby, compared to that of distant objects) [56] [47]. Both rotational and translational movements activate the VOR (Rotational and Linear VOR). With a rotational movement, the head can move relative to the body (that is the head rotates while the body does not, such as when rotating the head around the neck to the left or right), or can move in tandem with the neck body (such as when the whole upper body is rotated). Translational movements occur when the entire body (including the head) is moved in tandem (such as when stepping sideways).

Further to this separation of the VOR into two major components, these components themselves can be further separated on the basis of the planes of movement and axis of rotation upon for which they produce compensatory eye movements, and upon the planes and axis upon which the movements generating them are derived [76] [95]. The rotational VOR can be separated into three components, each responsible for detecting and compensating for rotations in one of the three major axis of rotation [76]. The Horizontal Semi-Circular Canals provide inputs regarding the rotation of the head in the Yaw axis, which drive the Horizontal component of the angular or rotational VOR (hVOR) [121]. Similarly, the Superior and Posterior Semi-Circular Canals provide information on, and produce compensatory eye movements for, rotations in the Pitch (Vertical rotational Vestibulo-Ocular reflex (vVOR)) and Yaw (Torsional rotational Vestibulo-Ocular reflex (tVOR)) axes [75]. Examples of these three components include: turning the head left or right, rotating it around the transverse plane (hVOR); nodding, rotating the head around the sagittal plane (vVOR); and bringing the ear in contact with the shoulder, rotating the head around the coronal plane (tVOR).

In these components, the Neural signal generated in the Semi-Circular Canals from rotational canal stimulation, and transmitted to the cell bodies in the Vestibular Nucleus, closely approximates the mechanical responses of the Vestibular end organs involved [78]. That is, the velocity of head rotation is transmitted, via the Vestibular afferents to the Central Vestibular nuclei. From there, information regarding the velocity of head rotation is transmitted to the Vestibular efferents, and then to the Oculomotor muscles which generate the required compensatory eye movements [76].

Similarly to the separation of the rotational VOR into components involved in compensating for rotation in each of the three axis of rotation, the linear or translational VOR can be separated into two components, one providing compensation for movements in the horizontal plane of movement, and the other for movements in the vertical plane [3] [4]. The horizontal linear VOR is driven by the Utricle, and the vertical linear VOR by the Saccule [129]. In these translational VOR components, linear movements detected by the Otolith organs are transmitted to the Vestibular afferents (which generate activity matching linear acceleration), which in turn are transmitted to the Central Vestibular neurons (which generate activity matching linear velocity) [3] [4]. This information is then transmitted, via the Vestibular efferents, to the Oculomotor muscles that generate the necessary compensatory eye movements [76].

Therefore, the VOR is separated into two distinct components, the rotational or angular VOR and the linear or translational VOR, each dealing with a distinct form of head movement (rotational movements, and linear movements). Each of these major components can be further separated into components corresponding to the planes of movement and axis of rotation for which they compensate, and the Vestibular sensory organs from which the signals transmitting the velocity of head movement arise (three axis of angular rotation, two planes of linear movement), to give five distinct components of the VOR.

Further to this functional and anatomical separation of the components of the VOR, it has been found that the three neuron arcs involved in each of these components of the reflex are composed of distinct functional subgroups of neurons, with different intrinsic membrane properties and response dynamics [128].

The existence of functionally distinct parallel pathways is commonly seen in sensory systems [52], and it has been proposed that the VOR is organised into such parallel pathways, with the various components of the reflex each arising from separate structures of the labyrinth, separate structures in the Vestibular nuclei, and, ultimately, stimulating separate extraocular muscles

[128]. Although not all the details that are seen to characterise the parallel processing of other sensory systems are to be seen in the VOR, there is organisation of the system into parallel pathways composed of distinct populations of neurons with different dynamic properties [127]. In addition, it has also been shown that, as well as organisation into distinct populations, these distinct populations receive distinct inputs [62] [13], and produce distinct outputs [129] [75]. The two components (rotational and translational) act in parallel to each other, and arise from separate labyrinthine end organs in the ear, with the rotational reflex receiving inputs from the Semi-circular Canals (which act as angular accelerometers), and the translational reflex receiving input from the Otolith organs (Utricle and Saccule, which act as linear accelerometers) [63]. For this reason, the rotational component is sometimes referred to as the Canal-Ocular component, and the translational component is sometimes referred to as the Otolith-Ocular component [3]. However, some overlap in the pathways may be present, due to the convergent nature of inputs to the Central Vestibular Nuclei [101]. This convergence may be necessary when, for example, some involvement of Otolith-Ocular pathways in compensation for head rotation may be apparent in the Canal-Ocular component when compensation is performed while the head is tilted from the earth vertical axis [3]. The functional significance of this overlap is still unknown (if it indeed has any functional significance, as will be discussed when the Pathway model of the VOR is presented in a following section).

Two features are required of the VOR, and are apparent in its normal functioning, in order for it to be useful in maintaining gaze stabilisation and object fixation in the visual field. Firstly, it must be fast. Any significant delay in compensatory eye movements produced by the VOR would lead to inaccurate visual information and a distortion of the visual field for an organism. This requirement is met by the organisation of the VOR circuitry into the three neuron arc described previously, and the direct nature by which the VOR process (generally) occurs. For example, studies of Squirrel monkey rotational VOR responses, for movements in the horizontal axis, show an average delay of 7ms when performed in darkness [98]. Further, this 7ms delay would be consistent with the delays in processing measured from the individual neural components of the VOR [98] [10]. The 7ms has been supported with further studies [74]. Similar delays (of 6ms) have also been found for components of the rotational VOR other than the hVOR [95]. Latency of the linear or translation VOR have been found to be around 34ms, which, although being greater than the rotational VOR latency, is still much shorter than the latency of visually guided eye movements, which is around 80ms [14].

Secondly, the VOR must be accurate and must derive from Vestibular inputs only (and not visually guided movements, due to the latency of these as previously mentioned). That is, compensatory eye movements must be equal in magnitude to head movements, in order for the reflex to produce clear vision. Evidence of this accuracy, in the absence of visual stimuli (that is, deriving entirely from Vestibular inputs) can be seen in values of 90% [98] and 80% [7] of head movement compensated for, by opposite eye movements in the dark. Both of these characteristics of the reflex must be met by the supporting neuronal circuitry that produces them.

The VOR also presents as an ideal system for investigation for several reasons. Firstly, the VOR and the vestibular system in general can be considered to be phylogenetically ancient [33]. The development of the Vestibular system was an important evolutionary event, allowing both vertebrates and invertebrates to maintain posture, balance, equilibrium and spatial orientation, all while moving within their environments [63]. The Vestibular system evolved in organisms a very long time ago, and is present across a wide range of the fossil record [123], including some of the earliest extant species, such as the myxine and lamprey [63]. This is also evidence of remarkably successful design of the Vestibular system, that has changed little throughout Phylogeny.

As such, the Vestibular system and VOR are present in, and have been studied in, numerous species, including the Squirrel monkey [97] [98], the Macaque [137], the Mouse [7], the Cat [78], the Rat [64], the Toad-fish [13], the Guinea Pig [29], the Chinchilla [138], and the Human [29]. Further to this, the Vestibular apparatus and VOR circuitry show remarkable similarities across species [1]. Due to this, there is a great deal of information that can be used specifically for theoretical and modelling studies of the Vestibular system and VOR. In addition, the Vestibular system and VOR have a well characterised anatomy and physiology [89], therefore presenting it as an ideal system for investigation, particularly in investigation of the role of variability in neural systems.

Secondly, the relative simplicity of the three neuron arc involved in the VOR, and its direct nature, makes the reflex an ideal candidate for investigation, especially in regards to the strategies and mechanisms by which the nervous system codes and transmits information from the sensory to the motor space. For example, the horizontal rotational VOR transmits sensory input, converting it to motor output, almost directly and with little to no subsequent processing. That is, the hVOR has no extensive downstream processing that can be seen in other systems, and the sensory input is converted to motor output, through only a single layer of interneurons [68]. Generally, the VOR is a linear system, translating sensory input directly to motor output [7].

2.2.2 *Vestibular Sensory Apparatus and Vestibular Afferents*

The Vestibular sensory apparatus includes the bony labyrinth of the ear (which consists of the Semi-Circular canals (SCCs) and the Otolith organs), and the motion sensors of the Vestibular system, the hair cells located within the SCCs and Otolith organs. The SCCs are organised almost orthogonally to each other, such that they can detect head rotation in any of the three planes of movement. Due to the mechanical forces that act upon the hair cells during angular rotation they act as angular accelerometers, and work in a push-pull arrangement with the corresponding labyrinth of the opposite ear. The Horizontal SCCs detect rotation exclusively in the lateral plane, Anterior SCCs detect forward or downward rotation of the head, and the Posterior detects rotation when the head tilts backwards. It is generally stated that the Canals work in pairs in order to detect acceleration and compensate for movement (horizontal SCCs of right and left labyrinth for horizontal rotations, left and right anterior SCCs for vertical rotations where the head tilts forward or downward, right and left posterior SCCs for backward or upward head tilting, and the so-called Left Anterior Right Posterior (LARP) and Right Anterior Left Posterior (RALP)[5] movements around the Yaw axis). The planes upon which angular motion is detected by the SCCs are close to the planes of the extraocular muscles (that cause eye movement) such that relatively simple neural connections between the sensory neurons and the neurons responsible for motor output can be traced [12].

One end of each SCC displays a significant widening of diameter, thus forming the ampulla containing the cupula. Each canal is filled with Endolymphatic fluid. The presence of the cupula produces a difference in Endolymphatic fluid pressure, due to the physical forces at play during head motion, which causes movement of the hair cells embedded in the cupula [47]. These hair cells are specialised biological sensors (which contain many cilia and are embedded in the gelatinous cupula), which convert the deflection the cilia undergo from fluid displacement, caused by head motion, into changes in their level of neurotransmitter release. That is, when hair cells are deflected towards or away from their longest process, the levels of neurotransmitter released is either increased or decreased respectively, thus producing excitation or inhibition of the Vestibular afferent cells to which they synapse [50] [42]. This excitation and inhibition in complimentary hair cells is illustrated in Figure 2.5. It has been hypothesised that canal size of a species is linked to the form of locomotion most commonly associated with that species [123].

5 Such as when the head tilts sideways, bringing the ear into contact with the shoulder. This causes excitation and increased activity from the ipsilateral Anterior canal (due to its downward movement) and the contralateral Posterior canal (due to its upward movement).

Thus, primates that exhibit fast and agile locomotion possess larger canals, in relation to body size, compared to species that exhibit slower and more cautious movements [123].

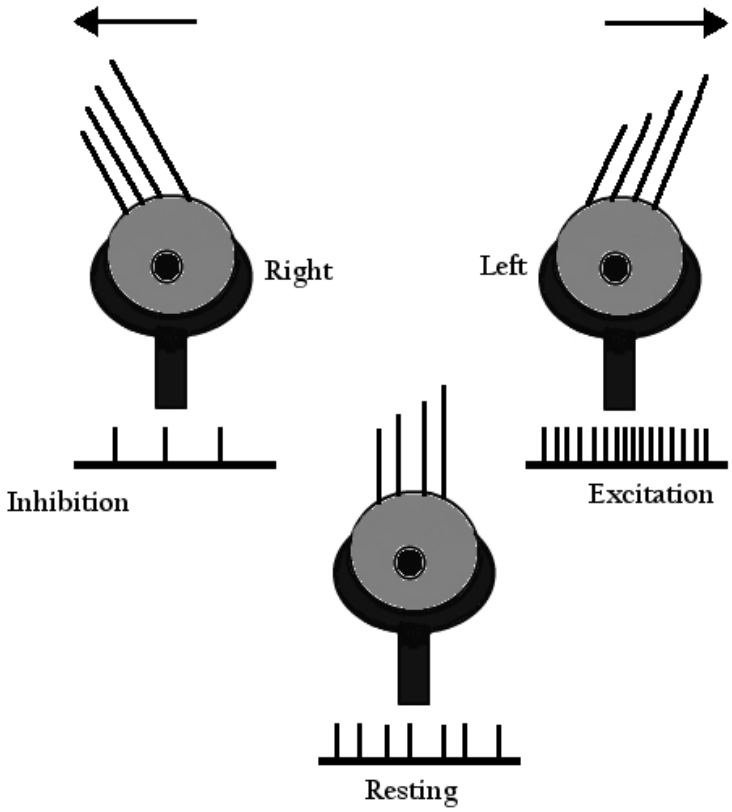

Figure 2.5: Excitation and Inhibition of Hair Cells, and the Firing Rate Modulation of Vestibular Afferents. A rotation to the left side causes the hair cells of the Left HSCC to deflect towards their longest process (longest hair of the cell), thus causing increased neurotransmitter release from the cell, and excitation in the Vestibular afferent, which shows a greater frequency of firing (spike train below each illustration). The hair cells of the right HSCC deflect away from their longest process, thus causing inhibition in the Vestibular afferents of that side, and the reduced frequency of firing. An undeflected hair cell and its resting discharge is shown for comparison.

The hair cells of the Otolith organs function similarly to those of the SCCs [134]. The hair cells of the Utricle and Saccule are embedded in the Maculae of the Otolith structures, and the Otolithic structures contain endolymphatic fluid similar to the structures of the SCCs. However, the maculae of the Otolithic structures contain calcium carbonate crystals known as ocotonia which possess significantly more mass than the endolymphatic fluid surrounding them. This differential in mass causes the maculae to be sensitive to gravity [43] [44] [45]. This is in contrast to the cupula of the SCCs, which are insensitive to gravity, as they possess the same density as the endolymphatic fluid that surround them.

Through the orientation of the SCCs and Otolith organs, these sensory apparatus respond selectively to head motions in particular directions and axis of rotation.

2.2.3 *Second Order Vestibular Neurons and Central Processing*

Due to the pairing of the SCCs, there is a push-pull arrangement involved in the changes of neurotransmitter released, and a subsequent excitatory and inhibitory effect on the firing rate of the corresponding Vestibular afferents innervated by the SCCs. For example, rotation on the horizontal axis to the left causes increased neurotransmitter released in the left horizontal SCC, and an increase in the resting discharge rate of the left Vestibular afferents and the Vestibular Nucleus neurons, and a reduction of neurotransmitter release and resting discharge of the right horizontal SCC and the Vestibular afferents and Vestibular Nucleus neurons which they innervate [103]. That is, increased neurotransmitter release leads to excitation of the ipsilateral (on the same side) Vestibular afferents and Vestibular Nuclei neurons, and inhibition of the contralateral (the opposite side) Vestibular afferents and Vestibular Nuclei neurons.

In the horizontal SCCs, ampullopetal flow (deflection of the cupula towards the ampulla) is excitatory, and ampulloflugal flow (deflection of the cupula away from the ampulla) is inhibitory. Although it was considered that the inhibitory element of a coplanar pair had a considerable effect on the VOR, it has since been shown that, under normal circumstances and especially at high velocities, the inhibitory component may make little contribution to bilaterally generated VOR components. For example, after unilateral neurectomy, ampullopetal flow and the excitation arising from it, in a single horizontal SCC (even in the absence of the ampulloflugal flow and inhibition from the opposite horizontal SCC) generated near normal VOR responses [57].

One way in which the coplanar pairing of the SCCs and their push-pull arrangements may be of advantage, is the provision of sensory redundancy [47]. If damage or disease affects the SCCs of one member involved in a pairing, the Central Vestibular nucleus neurons will still receive information on rotations and their velocity from the contralateral member of the pair. Secondly, the pairing any changes to neural firing that occur on both sides of the pair, due to changes in body temperature or chemistry, can be ignored [47].

The Otolith organs also have a similar push-pull arrangement of Vestibular sensors, with a further feature of the pairing, in that head tilting causes increased afferent discharge from one part of the macula involved, while reducing afferent discharge from a portion of the same macula [46].

The vestibular afferents project to two main targets, the Vestibular Nuclei complex in the brainstem, and the cerebellum. The Vestibular nuclei are the primary processors of vestibular input, and are responsible for implementing the fast, direct connections between the motor output neurons and the incoming Vestibular afferent information, whereas the cerebellum acts as an adaptive processor, altering vestibular processing if required for optimal vestibular performance [47].

As previously described, the Vestibular complex is composed of four main nuclei: the medial vestibular nucleus (MVN), the superior vestibular nucleus (SVN), the lateral vestibular nucleus (LVN), and the inferior (or descending) vestibular nucleus (IVN). While there is no absolute segregation of inputs from afferents, there is considered to be a separation of function between the routes taken by or distinct and separate pathways for each component of the VOR [130] (see discussion on Pathways Model of the VOR). The MVN and SVN receive inputs mostly from horizontal and vertical semicircular canal pairs respectively [135] [130], and are the main relays for the VOR, whereas the LVN is the main nucleus involved in the Vestibulo-Spinal Reflex (VSR). The utricular afferents terminate mainly in the IVN, while also sending projections to the LVN, MVN, and SVN. Saccule innervated afferents mainly project to the LVN and IVN. In addition to these direct projections from vestibular afferents, neurons in the vestibular nuclei also receive inputs from cortical, cerebellar, and other brainstem structures [32].

Specifically for the horizontal rotational VOR, head rotation velocity is transmitted, via Vestibular afferents, to the MVN neurons. These MVN neurons increase their discharge for ipsilateral horizontal angular acceleration, and decrease their discharge for contralateral acceleration [103]. That is, the neural signal transmitted to the cells of the MVN, from horizontal rotational canal stimulation, closely resembles the mechanical responses of the Vestibular organs that are stimulated [78].

The two sides of the Vestibular Nucleus complex are connected by a series of commissures, which allow for information to be shared across the two sides of the brainstem, and implements the push-pull pairing of the Vestibular inputs.

2.2.4 *Oculomotor Muscles and Vestibular Efferent System*

The VOR output neurons are the motor neurons of the Oculomotor nuclei, which drive the Extraocular muscles, and generate movements of the eye to compensate for head movement. The VOR works on all six muscles responsible for eye movement. These six muscles of the eye

work in pairs, forming three muscle pairs that work together to allow for specific eye movement. Discharge of the neurons of the Oculomotor nuclei are directly translated into active-state tension in these muscles, which produces the required compensatory eye movement [10]. For example, in the hVOR, the lateral and medial rectus muscles work together to respond to and compensate for left and right head rotation and maintain the direction of gaze, with rotation to one side causing contraction of the medial rectus muscle of the eye on that side, and the lateral rectus muscle of the other eye. These Extraocular muscles are shown in Figure 2.6.

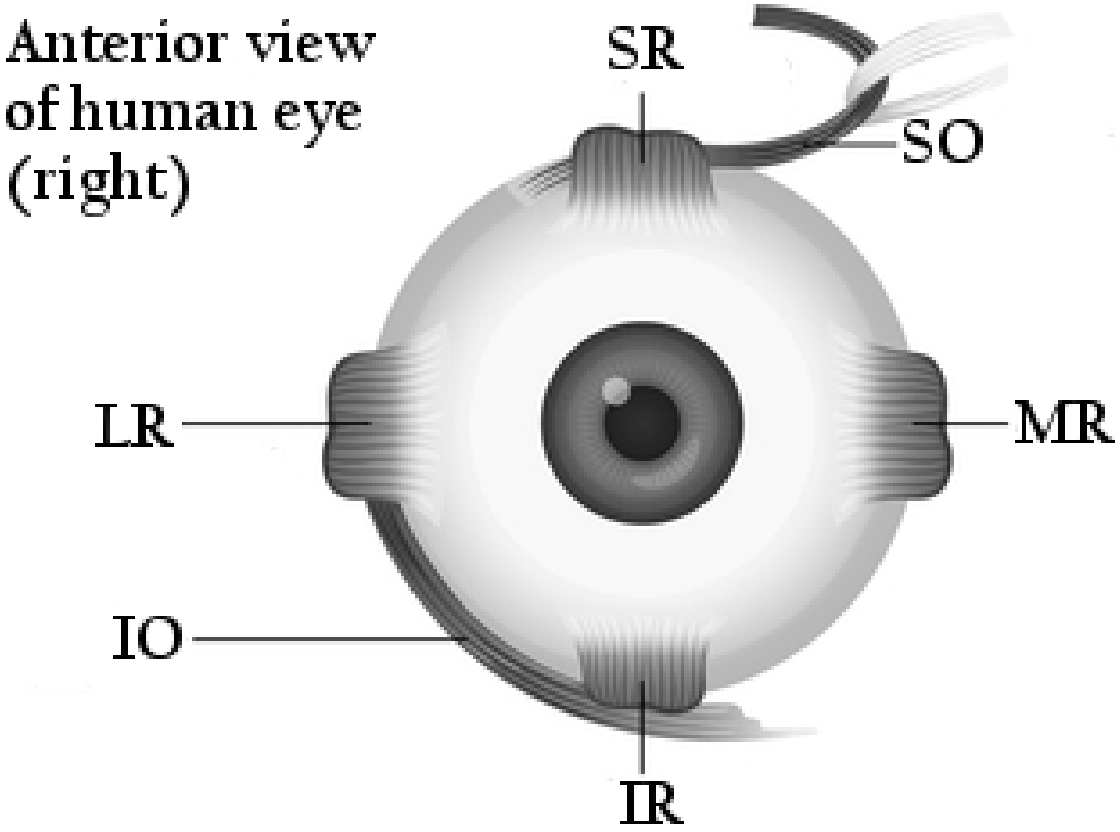

Figure 2.6: Arrangement of Extraocular Muscles of the Eye. This figure shows the arrangement of the 6 Extraocular muscles of a (human) right eye, from the Anterior view. The Medial Rectus (MR) produces inward movement, the Lateral Rectus (LR) outward movement, Superior Rectus (SR) and Inferior Rectus (IR) produce upward and downward movements respectively. The Superior Oblique (SO) produces combined downward and outward movements, and the Inferior Oblique (IO) produces combined upward and inward movement. Image modified from that appearing at http://www.rudyard.org/human-eye-muscles/

As stated previously, different regions of the Vestibular nuclei project to the different Oculomotor nuclei (cranial nerves III, IV, and VI). Signals from these nuclei then result in contraction (through excitation) and relaxation (through inhibition) of the appropriate extraocular muscles.

Excitation of the Anterior canal results in contraction of the ipsilateral Superior Rectus (SR) and contralateral Inferior Oblique muscles, causing upward eye movements (in response to detected downward head movements) and relaxation[6] of the ipsilateral Inferior Rectus (IR) and contralateral Superior Oblique (SO) muscles. Excitation of the Posterior canal results in contraction of the ipsilateral SO and contralateral IR muscles and relaxation of the ipsilateral IO and contralateral SR muscles, thus resulting in a downward eye movement (in response to detected upward head movement). Finally, excitation of the lateral canal results in contraction of the ipsilateral Medial Rectus (MR) and contralateral Lateral Rectus (LR) muscles and relaxation of the contralateral MR and LR muscles. This results in a horizontal eye movement toward the ear opposite the excited canal, and opposite to the direction of head movement [129]. These connections, between the Semicircular canals and the extraocular muscles are summarised in Table 2.1.

Canal	Excitation	Inhibition	Effect
Horizontal	Ipsi. MR, Contra. LR	Ipsi. LR, Contra. MR	Rotation of eye to Contra. side to Head Rotation
Anterior	Ipsi. SR, Contra. IO	Ipsi. IR, Contra. SO	Upward eye movement
Posterior	Ipsi. SO, Contra. IR	Ipsi. IR, Contra. SR	Downward eye movement

Table 2.1: Excitatory and Inhibitory connections between Canal types and Extraocular muscles[129]. Ipsi. and Contra. refer to Ipsilateral and Contralateral respectively.

One major difference between the torsional and vertical components of the rotational VOR, and the horizontal component, is in the number of canals involved in these components. During both head tilts backwards and forwards, and torsional rotations, four canals are stimulated, leading to their excitation or inhibition. In forward head tilts, both Anterior canals are excited, leading to upward eye movements, while both Posterior canals are inhibited, leading to relaxation of the muscles allowing for upward eye movement. This arrangement is reversed for backward head tilts, with both Posterior canals undergoing excitation, and both Anterior canals undergoing inhibition. In the torsional movements[7] the Anterior canal ipsilateral to the head movement, and the Posterior canal contralateral are excited, and the contralateral Anterior and ipsilateral Posterior canals are inhibited. In contrast to these movements, purely lateral rotations (evoking the hVOR) involve only two canals [57], with the ipsilateral Horizontal canal exhibiting excitation, and the contralateral

6 This relaxation is caused by the inhibition relayed to the contralateral muscles, and allows the eye to move in the required direction. That is, it relaxes the muscles in opposition to those that contract when the movement occurs.

7 LARP and RALP movements, such as when rotating the head so that the ear moves towards the shoulder. In this case, the ear moved towards the shoulder is considered the ipsilateral ear

Horizontal canal exhibiting inhibition. This difference, and the involvement of different canals between the tVOR and vVOR, and the hVOR, has lead to differences being recorded between these two sets of components, with the tVOR and vVOR more closely resembling each other than they do the hVOR [11]. That is, the vVOR and tVOR show a closer resemblance to canal characteristics that drive them, than the hVOR. This would be the case if the tVOR and vVOR components both arise from the same canals, as is the case.

In addition to the motor output of the VOR, Vestibular efferent neurons are found in the Abducens nucleus (ABN) area of the brainstem, and receive inputs from the Vestibular nuclei, as well as directly from Vestibular afferent neurons [51]. In addition, excitatory Vestibular efferent neurons project back to Vestibular sensory organs (hair cells of the Vestibular apparatus), increasing their resting discharge [51] [61]. Although the exact function of these back projecting efferent neurons is unknown, particularly in alert primates, it is thought that they may be involved in increasing the dynamic range of Vestibular afferent responses [26].

2.2.5 *Summary and Example of Horizontal Rotational Vestibulo-Ocular Reflex*

The rotational VOR works to stabilise images on the retina through the detection of head rotation and the application of compensatory eye movement, such that the eyes maintain focus on their target and the visual field remains stable. The VOR works for both angular rotations of the head around the neck, and linear movements of the whole body. Thus, rotational Vestibulo-ocular reflex (rotational VOR) responds to angular motion of the head and results from stimulation of the semicircular canals, whereas the linear Vestibulo-ocular reflex (linear VOR) responds to linear motion of the head and results from stimulation of the otolith organs. These two components are further subdivided, on the basis of the planes of movement upon which they act, into five further components.

As it is the main concern of the rest of the current work, we concentrate now upon the Horizontal Rotational VOR (hVOR), and provide an overview of the particular activity involved in the functioning of this aspect of the VOR. As stated previously, the hVOR is generated by the push pull activity of the two Horizontal semi-circular canals (HSCCs). Rotations in a given direction cause excitation, and an increased release of neurotransmitter, from the hair cells of the HSCC on the side rotated towards, and inhibition in the opposite HSCC. This excitation represents the acceleration of the head, and is transmitted, via the Vestibular afferents, to the ipsilateral Medial Vestibular nuclei (MVN) of the brainstem. This signal is then transmitted by

the Position-Vestibular-Pause (PVP) neurons of the MVN to the ipsilateral oculomotor nucleus to drive contraction in the ipsilateral medial rectus, and to the contralateral Abducens nucleus to drive the contralateral lateral rectus. The inhibition, from the contralateral HSCC, serves to inhibit the opposing muscles. Thus, a rotation to the left excites the right HSCC, which, through the 3 neurons, excites the left medial rectus and the right lateral rectus, pulling the eye to the right. Figure 2.7 shows an overview of this excitatory hVOR pathway.

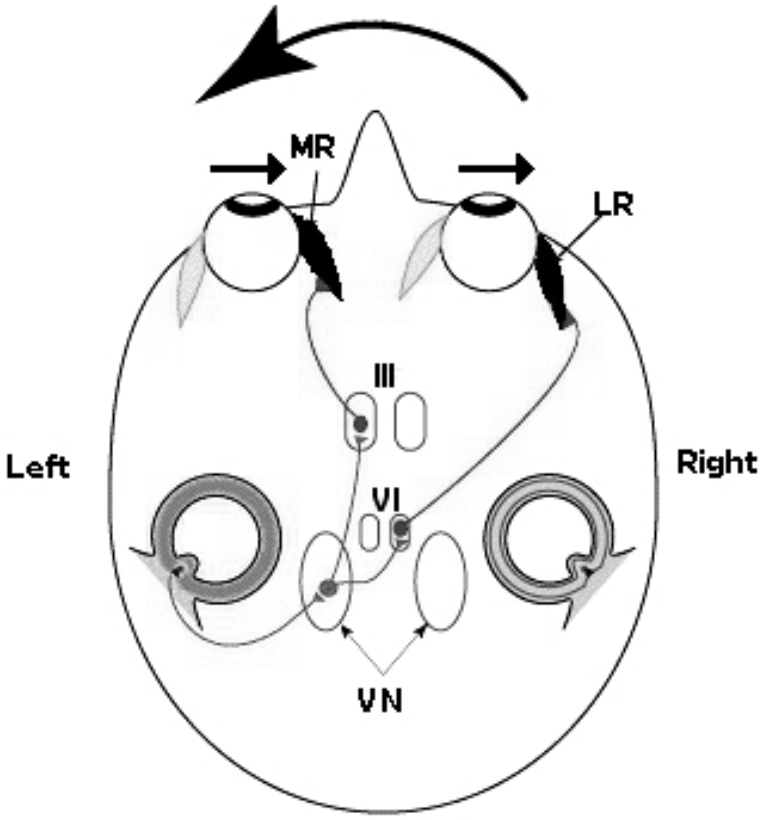

Figure 2.7: Excitatory Example of Horizontal VOR Activity. Head rotation to the left causes excitation in the left Horizontal Semi-circular canal, which sends excitatory impulses to the left Vestibular Nuclei (VN). This excitatory signal causes contraction of the Left Medial Rectus (MR, via the Oculomotor Nucleus, or IIIrd Cranial Nerve) and the Right Lateral Rectus (LR, via the Abducens Nuclei, or VIth Cranial nerve)

2.2.6 *Pathways Model of Vestibulo-Ocular Reflex*

From the preceding discussion, it is evident that the VOR can be separated into five major components, each dealing with head movements around a given axis or along a given plane (three Canal-Ocular responses, and two Otolith-Ocular responses). Further to this, each of these responses can be separated on the basis of the direction of movement for which they compensate

(and not just the plane or axis), the specific Vestibular end organs which drive them, and the specific Oculomotor muscles upon which they act. For example, the hVOR can be separated into the response which rotates the eyes to the right in response to head rotations to left, and the response which moves the eyes to the right in response to head rotations to the right. From this, we can consider that separate parallel pathways exist, that allow for separate neural coding of different head motion components [128]. However, studies have shown that this is not the end of the separation of the VOR responses, and that these individual directional responses can themselves be separated into multiple channels or pathways, based on evidence regarding the existence of Linear and non-Linear aspects of the response, and their relation to the adaptation of the response.

The existence of Linear and non-Linear components for these responses was first proposed by Minor et al. from a study recording the hVOR response of Squirrel monkeys to high acceleration rotations [98]. It was found that differences for Gain[8] and Phase of the hVOR were apparent for sinusoidal rotations less than and greater than 4Hz, with Gain increasing as the frequency of rotation increased above 4Hz[9], thus suggesting the existence of a Low and High frequency Gain control element [98]. It has been suggested that, while the Linear component is responsible for the Linear transfer of Head velocity to compensatory eye movements, that the non-Linear component is involved with Gain adjustment [24], or the reduction of retinal slip and the smooth pursuit of targets [130] [95]. This separation has also been suggested to occur in the vVOR and tVOR components [95].

Although originally it was considered that any adaptive mechanism involved in the VOR arose from a single Gain altering element, it has since been found that the mechanism of adaptation in the VOR is more complex than this, and that it most likely involves the presence of frequency selective adaptive channels [85] [105]. Lisberger et al. studied the effect of spectacle induced adaptation on VOR response and found that, when adapted towards a Gain of 0 or 2[10] for a given frequency of passive sinusoidal rotation, the VOR exhibited large changes in gain at the adapted frequency, but much smaller changes in Gain for frequencies other than that adapted to. That is, when magnifying or minimising spectacles where used, and a single frequency was then used to force adaptation, the VOR showed large changes in Gain for that frequency, but much smaller changes in Gain for adjacent frequencies [85]. However, when adaptation was allowed to occur

8 Gain in this situation refers to the ratio of Eye velocity/Head velocity.
9 For frequencies <4Hz Gain remained constant. Past 4Hz, as the frequency increased, the Gain also increased.
10 Magnifying or minimising spectacles where used to increase or decrease the gain.

naturally[11] significant Gain changes were seen across all frequencies when the VOR was tested [105].

A directionally differential adaptation was also found in the Squirrel monkey vVOR, in that the Up and Down components showed different magnitudes of adaptation [65]. In this particular case, however, the adaptive elements of these two components were not found to be entirely independent of each other, as a symmetrical adaptation regime (where both the up and down responses underwent adaptation) showed a greater effect than an asymmetrical adaptation regime [65].

Further to the frequency selective appearance of adaptation in the VOR, it has also been found that the non-Linear component shows a greater modification in response to spectacle induced adaptation than the linear component, suggesting either that the non-Linear channel is more open to adaptation than the Linear channel, or that the Linear channel is more resistant to adaptation [24]. Finally, the difference in delay of the modified and unmodified channels, after adaptation, suggests the existence of separate pathways or channels being involved [106].

Although currently unknown, it has been suggested that the site of adaptation is the Medial Superior temporal area [130], or possibly the Cerebellar flocculus and Ventral paraflocculus [86], and that it occurs after the Central Vestibular nuclei stage of Linear pathway [25]. Further, the direct mechanism of adaptation is currently unknown, though it has been suggested that cerebellar projections may alter Vestibular afferent synapse activity without altering or compromising the direct, linear VOR performance [93], although the site of this adaptation has been contradicted, and it may be that adaptation occurs after the Central Vestibular stage of the reflex pathway [25]. In support of the latter, it has been found that adaptive changes in the Gain of the VOR are accompanied by only small changes in Vestibular sensitivity and no changes in the sensitivity of the MVN neurons [84].

What this suggests, therefore, is that there does exist two parallel pathways for each head motion component: a Linear transfer function; and a non-Linear gain adjustment [24] (or augmentation of the Linear to mitigate for retinal slip [95]), and that both components exhibit separate adaptive aspects[12] [25]. Further, these two pathways involve different Central vestibular neurons, with the Linear component involving the Position-vestibular-Pause neurons of the Vestibular nuclei, and the non-Linear involving the floccular target cells [105].

11 Through spontaneous natural head movements and not through a regime of adaptation
12 Separate processes drive the adaptation of the Linear and non-Linear pathways, as opposed to a single adaptive process.

From the above evidence, we can conclude that there does exist a direct, linear component to the VOR, showing little delay in response, and providing high fidelity compensations for head rotations. That is, underlying the adapted or modified pathways, or the components involved in Gain adjustment, or smooth pursuit eye movements, there is a direct, unmodified pathway of the hVOR[13], which changes sensed angular head rotations into compensatory eye movements, via the Vestibular afferents, PvP cells of the Medial Vestibular nucleus, and the neurons of the Oculomotor nucleus [130] [106]. Further, it has been proposed that these separate three neuron arcs are composed of distinct functional subgroups of neurons, with differing response dynamics, arising from intrinsic properties, at each synaptic level, and that, specifically the Central neurons (i.e., MVN PvP neurons) use intrinsic membrane properties (as well as emerging network properties) in order to transmit the required information for the VOR to be accomplished [128]. That is, the separate parallel pathways evident, allow for the separate coding of different components of head motion and the required compensation, and that the different neuronal elements involved provide a cellular basis for this parallel processing [102]. The role of intrinsic membrane properties in MVN has been supported in modelling studies of these neurons [5] [68].

This principle, of distinct and discrete channels involved in the processing information in neural systems, can be seen to follow the principles of Channel theory, which originally emerged from Communication theory [120], and has had a long and fruitful history of modelling neural information processing [60].

2.3 VARIATION AND HETEROGENEITY

In this section we look at the sources, effects, and possible benefits of two forms of variability that are present in Neural systems, Noise and Heterogeneity. We then look at their possible significance to, and involvement in, the Vestibular-Ocular reflex.

2.3.1 *Noise in Neural Systems*

Noise is often described as "random or unpredictable fluctuations or disturbances that are not part of a signal" or "more generally any distortions or additions which interfere with the transfer of information" [40], or "a signal that varies as a function of time, the value of which at any given time is drawn randomly from some distribution" [38]. Although we have been aware of sensory noise for some time, recently attention has been given to the role of cellular and motor noise [40]

13 that is, adaptation of VOR components is thought to occur in a different pathway to the direct and linear response [86].

[38] and to the role of noise in nervous system functioning [99]. Noise is an inescapable problem for information processing in neural systems, effecting multiple aspects of neuronal behaviour [40]. Experimental and computational work has been done recently showing the effects of noise in neural systems, and the principles by which nervous systems can overcome the detrimental effects of noise [40]. Further, although noise is often considered as a detriment to information processing, disrupting patterned activity and causing interference of encoding, recent work has shown a potentially beneficial and constructive role for noise in neural information processing [132] [91] [38].

Overtly, noise can be seen in nervous systems through the trial-to-trial variability of neuronal spike timing [38]. This trial-to-trial variability is the difference between observed spike timing produced when the same 'experiment' or stimulus is repeated with the same neuron [90]. That is, between trials, where the same stimulus is applied, and the same overt behaviour or output is observed, the actual neural processing that occurs may not be identical between trials. As an example of this noise induced variability, we can imagine a neuron receiving a sub-threshold input, with noise added – if the amplitude of the noise is sufficient, the sub-threshold input can be augmented such that it exceeds threshold, and a spike is generated. Similarly, the rate at which a neuron fires, or its periodicity can also be altered through noise [38].

Noise in a nervous system is inescapable, for example, from stochastic processes in molecular components, sensors that detect individual quanta, and complex networks of noisy neurons, and noise has implications for the computational power of the brain. However, despite this (or, perhaps, because of this) noise, neural systems, and brains, are able to function reliably and accurately, presumably, because evolution has occurred in the presence of noise, and the constraints that have arisen due to noise [40]. To function in the presence of noise, nervous systems have developed various strategies by which to deal with this inherent noisiness [40], and further, it has been proposed that the noise seen in nervous systems is a benefit to neural processing [59] [6] [17].

2.3.1.1 *Sources of Noise*

There are primarily three sources of cellular noise in the nervous system (as categorised by [40]): Electrical noise; Synaptic noise; and Motor Noise. This review will deal only with Electrical and Synaptic noise at the cellular level, but not with Motor noise at the cellular level. In addition, it should be noted that cellular noise is only one of three forms of noise in nervous systems, with

the others being Sensory and Motor noise. Discussion of these other sources of noise are beyond the scope of this review, and not directly relevant to the modelling used.

Firstly, electrical noise can have an effect on both local and network computation, as it can cause fluctuations in both membrane potentials (local) and the timing of Action potentials (network). The primary cause of electrical noise, is channel noise [115]: Noise, or fluctuations in membrane potential, caused by electrical currents produced by the random or stochastic opening of voltage or ligand gated ion channels [40]. These fluctuations can effect both the local computations derived from ion channel dynamics and local membrane potentials, as well as the timing, initiation and propagation of Action Potentials. Further causes of electrical noise are: cross talk, or ephaptic coupling (where communication occurs between neurons when neuronal membranes are closely apposed but not contiguous); Johnson noise (caused by thermal agitation of charge carriers);and Shot noise (where finite signal particles give rise to statistical fluctuations in detection) [40].

In experimental studies, it is important to consider electrical noise, as it has tended to be overlooked, with synaptic noise receiving more attention [40]. As such, it can be largely absent from many simulation and modelling studies.

Synaptic noise arises at the synapses (the main sites for communication between neurons) within nervous systems. If a pre-synaptic cell is driven repeatedly, with identical stimuli, there will be a trial-to-trial variability in the post-synaptic response produced. This variability is due to the stochastic processes which are involved in signal transmission in nervous systems [40] [38]. One major phenomena responsible for synaptic noise is the miniature Post-Synaptic Current (mPSC), which is a fluctuation or change in post-synaptic currents or membrane potentials, seen in the absence of any pre-synaptic activity. These mPSC's have been interpreted as being the result of the spontaneous release of vesicles of neurotransmitter at the synaptic cleft [41]. Although there are other sources for synaptic fluctuations, they are generally caused by the stochastic nature of, or random events in, the machinery involved in synaptic transmission: spontaneous opening of Calcium stores, leading to vesicle release; noise in the Calcium channels; spontaneous triggering of the vesicle release mechanisms; fusion of the vesicle with the cell membrane [40] [39]. Regardless of the cause, the spontaneous or stochastic release of a vesicle leads to a post-synaptic current.

In addition to this, there is also a variance in the post-synaptic response to vesicle release due to variance in the amount of neurotransmitter that can be released. For example, the duration of calcium channel opening, which drives vesicle release, can vary, leading to a variance in the

number of vesicles released and the probability of vesicle release (this calcium channel duration can vary due to Action potential Width, which is affected by axonal noise [39]).

Further, noisy biochemical mechanisms can effect post-synaptic response in several other ways. Firstly, the mechanisms involved in synaptic communication involve small numbers of molecules, and are therefore subject to thermodynamic noise. Secondly, variability in neurotransmitter volume release can vary due to vesicle size differences. Thirdly, there is thermodynamic noise present in the diffusion of substances across the synaptic cleft, or after uptake by the post-synaptic cell. Fourthly, the location of vesicle release in the synaptic cleft can cause variance. Fifthly, there is channel noise (as described above) in post-synaptic receptors. Finally, there is synaptic adaptation and plasticity, which can lead to changes or variance in the vesicle release probability [39].

2.3.1.2 *Strategies For Dealing With Noise*

It can be difficult or costly to remove noise once it has been added to a signal (and, a system may not want to remove noise, for the possible benefits arising from it), and may be unavoidable for a signal to become noisy [40]. Several strategies, or principles, have been put forward as to how nervous systems are able to minimise the negative consequences of noise present, two of which will be dealt with here: Averaging; and the use of prior knowledge.

Averaging can be applied when there is a redundancy of information (where there is superfluous or duplicate information) across an input, or within some information processing system in a nervous system. Averaging could be present, particularly, in a system were several 'units' receive the same signal, but independent sources of noise. In this situation, when the signal + noise is averaged, the shared or common signal (seen across the inputs) will be predominant in the processed output, over the independent noise, because the shared/common input will tend to be amplified or remain stable, while the noise will tend to cancel itself out. In this way, it can be seen that simple averaging works best when each input or signal is subject to noise that is similar (in amplitude or spectrum) across each unit [6].

Averaging is perhaps most commonly posited as one of the first steps seen in sensory processing. For example, in auditory processing, the stereocilia of auditory hair cells, are disturbed by sound vibrations and open mechanically gated ion channels in response. The random fluctuations in individual stereocilia movement is averaged across a single hair cell however, because stereocilia are mechanically coupled, and so move together to a certain extent, and so the random fluctuations are averaged out across the input [81]. Similarly, in visual systems, we can see that inputs are

averaged over photo-receptors with adjacent, or overlapping receptive fields [40]. Averaging can be seen as a viable strategy in both of these systems, because both hair cells, and photo-receptors are what are called graded-potential neurons, in that they do not use Action Potentials to communicate, but rather communicate through graded synapses. This graded communication allows for the largely straightforward averaging and noise 'removal' for post-synaptic units receiving information from the hair cells or photo-receptors.

Prior knowledge can also be used to alleviate the negative consequences of noise in neural systems. If a system has some 'knowledge' of the structure of the signals it receives, and/or the noise which corrupts that signal, this knowledge can be used to distinguish the noise from the signal. This is commonly known as the matched-filter principle, and can be seen in nervous systems where units or systems use prior knowledge about their expected inputs to attenuate the impact of the noise corrupting those signals [40].

Nervous systems would not have to utilise these strategies in isolation, and, indeed, there is evidence that they are combined, especially when there is a variance in the parameters (the 'volume' or amplitude or spectrum) of a corrupting noise signal (as Averaging tends to work best when there is little variance in the 'volume' of the noise, or noise that comes from independent sources, but shares similar properties) [40]. Through the combination of the two strategies, prior knowledge of the 'volume' of the noise signals can be used to improve or facilitate weighted averaging of the input signals.

These two strategies can also be combined, into a mathematical framework of optimal statistical estimation and decision theory, known as Bayesian Inference. Bayesian inference involves the assignation of probabilities to propositions calculated by taking prior knowledge and noisy observations. In order to make use of sensory information, nervous systems must represent and use information about uncertainty [80]. There is a growing evidence that biological organisms use Bayes optimal perceptual computation, which leads to the Bayesian Coding hypothesis: nervous systems represent sensory information in the form of probability distributions [80]. However, although there is definite evidence that biological organisms use Bayesian inference to deal with uncertainty in perception and action [40], and numerous computational theories have been put forward as to how this may be achieved in neural systems, there currently exists very little evidence or information on the (possible) neural mechanisms that would be involved [80].

2.3.1.3 *Benefits of Noise*

However, noise is not just a problem that must be attenuated or dealt with by neural systems. It can also be a benefit to neural processing [90] [38]. As was briefly mentioned previously, noise can play a part in the reliability of a neurons firing – evoking an Action Potential at a particular time, either across trials of a single neuron, or across multiple neurons in a population. This is because the noise can cause a threshold to be reached, even when the input(s) to the neuron is sub-threshold, and the average noise amplitude is zero. This is especially likely to occur over multiple trials, either of the same neuron, or across a population, and can elicit a spike pattern which reflects the bio-physical properties of the neurons involved [38]. Also, when averaging is applied to such a system, and inputs are averaged over time, the noise helps to produce an effectively smoothed non-linearity, improving neural network behaviour [40].

Similarly, noise can also lead to an improvement in the periodicity or regularity of neuron firing, producing a more clock like pattern of spiking (spikes separated by fixed time intervals) [38]. In a situation were a sub-threshold varying input is subject to noise, the noise could cause threshold to be reached, and induce firing only during the peak of the signal [38]. This can be considered an example of Stochastic Resonance.

There is also evidence for the role of noise in neural synchrony. Noise induced synchrony, however, is highly dependent upon the characteristics and connectivity of the network involved, as well as the 'units' (neurons) involved [17] [38]. These factors can bias a network towards synchrony. There is currently growing theoretical and experimental evidence for noise induced synchrony, and the importance of synchronous firing to performance in some neural systems[14]. For example, it was found, through human Electroencephalogram (EEG) studies, that increases in synchronous neural activity in different regions of a neural system, were correlated with increased levels of awareness and attention [96]. Similarly, it was found that decreases or disruptions of synchronous firing led to a diminished ability for odour discrimination in bees [126].

Finally, no discussion of the constructive role of noise would be complete without at least the introduction of the phenomena of Stochastic Resonance (SR). A very broad definition of SR states that it is observed when increases in the levels of unpredictable fluctuations, leads to an increase in the metric of the quality of signal transmission, rather than a decrease [90]. However, there is some argument as to the validity of this definition, as it essentially states that increasing noise leads to increased performance, without any further elaboration, and such a situation would lack

14 However, neural synchronisation is not always a desired phenomenon, as will be discussed shortly when the possible benefits of Neural Heterogeneity are introduced

the properties necessary for a bona-fide 'resonance' [90]. A narrower, but more useful, definition of SR would be that it is the improvement in detection of a weak, periodic signal, through the introduction or utilisation of optimal levels of noise [90]. For example, it was found that Crayfish use SR to enhance detection of nearby predators – that is, the weak periodic force is the water vibrations caused by a nearby fish's tail, the noise is the water turbulence, and Crayfish are able to detect the vibrations caused by the fish (predator) more easily with the background of water turbulence [34]. Further, evidence has also been found suggesting the action of SR in human visual perception [31] [113].

Specifically in regards to the functioning of the VOR, previous modelling work has suggested a role for Noise in the high fidelity response of MVN neurons to high frequency inputs [68].

2.3.2 *Heterogeneity in Neural Systems*

2.3.2.1 *General Overview of Neural Heterogeneity*

Neuronal heterogeneity refers to the variation in any one of a number of a neuron's parameters within a population, and is known to increase the information content of a population of neurons [21] [109]. Neural systems display significant heterogeneity in neuron properties, even among same class neurons, and this may have substantial implications for the information processing of those systems. Neurons within the same area of the brain, and of the same qualitative type, can vary across numerous parameters. Although this cell-to-cell variability, or diversity in neural populations, was documented by some of the first researchers into the function of variability, the fact that neurons and populations of neurons are heterogeneous has largely been ignored, in favour of research on the role of Noise, and it is only recently that the functional role of heterogeneity has been investigated [72].

For example, it is known that neuronal responses within a cortical area are characterised by their high degree of heterogeneity, and that even cells within the same functional column are known to have highly heterogeneous response properties when the same stimulus is presented. It has been found that the heterogeneity of the neuronal responses is beneficial for sensory coding of stimuli [21]. In modelling studies, it has been shown that heterogeneity can optimise network information transmission for temporal or rate coding, even in realistic conditions, and improve population coding of neural ensembles [92]. It has also been found that heterogeneity in the intrinsic biophysical properties[15] of cochlear nucleus neurons reduces the redundancy involved

15 Heterogeneity of the Neural population's parameters, rather than just their responses to stimuli

in their firing patterns, and increases their representation of temporal information [2]. Finally, it has also been found that diversity or heterogeneity amongst sensory receptors can allow for the establishment and improvement of population codes [87].

2.3.2.2 *Desynchronisation as a Benefit of Heterogeneity*

One possible mechanism by which heterogeneity (and noise) may improve neural performance, is through the desynchronisation of a population's response to a common input [16] [72]. Although synchronisation of a population is sometimes of great benefit to the encoding or decoding of the signals handled by that population [96] [126], this is not always the case. If we consider a (simulated) population of entirely identical, homogeneous neurons, receiving a common input with no variation or noise (either in the input or acting upon them), and beginning with the same initial conditions, it can be seen that, as they function entirely deterministically, such a population would exhibit entirely synchronised firing patterns. That is, because they start at the same place in their phase space, and because the input is identical between members, and each member of the population obeys the same set of differential equations, they will travel on the same trajectory in their phase space. That is, at any time, every member of the population will be at the same point in their periodicity, and their spike times will be identical to each other - the population would be entirely synchronised. This would introduce an immense amount of redundancy in the information carried by the population, as any information present in the population response will be present in the response of a single neuron.

Adding independent noise to the common input received by each member of the population will desynchronise the members, by causing a shift in their individual neuronal phases. That is, the small changes in the neuron states across the population will produce slight delays or advancements in the firing of the neurons, and their responses will be, somewhat, out of phase from one another.

The above example is entirely artificial, and somewhat idealised[16], and in a real (or more realistically simulated) population, we can imagine small differences in the starting conditions (and thus the periodicity) of the members would lead to a diminishment of the synchronisation in the population, as members will not follow precisely the same trajectories in their phase space. However, this is not the case, as sub-threshold inputs to a group of neurons will force synchronisation upon them. That is, sub-threshold inputs will force members of the population

16 In that the neurons are precisely the same, with precisely the same initial conditions, and they receive precisely the same inputs

towards a stable equilibrium point, and with the return of a signal above the threshold of the population, members will begin to fire at approximately the same time, and show approximately identical responses.

Heterogeneity introduced into the population (for example, in the form of changes to their firing threshold, the level of input required to cause an action potential) acts to desynchronise the population and its response [16]. Heterogeneity increases the range of the distribution of the population's phases and periodicity, shifting the firing times of each member either forward or back. That is, neurons with a lower threshold will fire earlier than those with an average threshold, and those with a higher threshold will fire later, thus causing a desynchronised response from the population. In this way, heterogeneity encourages desynchronisation, which operates by affecting the temporal properties of neuronal firing across the population [72].

2.3.2.3 *Heterogeneity in the Vestibulo-Ocular Reflex*

Heterogeneity has been observed in the populations of neurons involved in the VOR. Although primarily this has been observed in the Vestibular afferents [109] [37], it has also been found in the Central Vestibular neurons involved in the reflex [117]. It has been found that the variability of populations in the Vestibular system, promote the fidelity of its encoding [114]. This variability, or heterogeneity, has been observed in both the individual responses of neurons in these populations, as well as in the intrinsic properties of the neurons involved [117]. Further to this, the primary form of this heterogeneity has been found, in experimental studies, to be in the specifics of the Potassium (K^+) currents involved in the spontaneous activity of these neurons. This has been supported by findings from modelling work, which found that the timing of repetitive discharge (of model Vestibular afferent neurons) was governed by a K^+ conductance [122].

Studies of Vestibular afferent populations have shown that they display diversity in their responses to inputs [37] [83], and heterogeneity in their K^+ conductances [109]. It has been suggested that the diversity of firing patterns observed, reflects the diversity of intrinsic membrane and ion channel properties of the neurons involved, and that neuron morphology (shape and size of the neuron) cannot adequately explain the heterogeneity of observed discharge rates [37] [83]. Candidates for the intrinsic membrane or ion channels involved in heterogeneity have largely been shown to be K^+ conductances [109]. Further, it has been shown that this diversity is due, not to the type of conductances involved, but due to the proportion or density of the conductances and channels producing them [20].

Vestibular afferents, isolated from bother their peripheral inputs and Central vestibular targets, showed cell-to-cell variability in the magnitude of their K^+ conductances, but very little variability in the magnitude of their Sodium (Na^+) conductances[17] [109]. Thus it has largely been concluded, for Vestibular afferents, that a combination of heterogeneous K^+ conductances, along with a broad range of hair cell responses, leads to the observed diversity of firing rates seen in the afferents, and that this diversity is responsible for the wide range of frequencies over which the VOR functions [109] [83].

Although commonly thought that the wide range of firing responses observed in Central vestibular neurons to identical inputs arose from the types of inputs which these neurons received (circuit properties), it has been shown that the intrinsic properties of these neurons plays a significant role in the diversity of their responses [117]. That is, the diversity of firing dynamics reflected the heterogeneity of intrinsic membrane conductances, along with differences in synaptic input. Specifically, it was found that the K^+ conductances of these neurons played a significant role in the generation of their diversity of response, and that, rather than a discrete categorisation of responses being present, a continuous distribution of responses was found [117]. However, due to the lack of a topographical segregation, and the lack of a specific K^+ current antagonist[18] during spiking of the neurons, no functional role of the heterogeneity could be definitively assigned [117].

2.4 Motivations of the current work

Now that we have identified the channel or pathway responsible for the fast, direct, linear hVOR, and looked at the possible role of noise and heterogeneity in its functioning, we now look at the observed characteristics and properties of the neurons involved in this component of the VOR, before expressing the aims of, and motivation for, the work to be presented.

2.4.1 *Segregation and Classification of Vestibular Afferent and Medial Vestibular Nucleus Neurons*

A primary function of the nervous system is to transform and relay sensory input to motor output (as in the case of the Elementary 3 Neuron arc, as well as more complex behaviours), through the specialised synaptic and cellular processes and structures involved [7]. That is, the neurons involved are specialised to the behaviours they contribute to. Functionally distinct,

17 Thus eliminating heterogeneity of Sodium conductances as a possible candidate for the cause of diverse firing rates
18 A Potassium current blocker

parallel pathways are commonly seen in sensory and sensory-motor systems [60], and so work has been performed to attempt to uncover such functional segregation in the vestibular system (i.e. [52] [62] [121]. Although, primarily, this work has concentrated on the segregation of the afferent neurons (the vestibular nucleus neurons, innervated by the Canal and Otolith organs), some work has also been performed to categorise, and identify functional segregation, within the Vestibular nuclei.

The identification and classification of neuron types, within a circuit, is fundamental to the understanding the relevance of neural circuitry to behaviour, as it is the diversity of neurons that supports complex processing, with neural types specialised to the finely tuned behaviours they support [7]. Thus, the identification and classification of neuron types is a critical step in understanding the behavioural relevance of their connections and cellular properties. In the case of the Vestibular Nuclei, located in the brainstem, identification of neuron types (and thus determination of their properties and consequences for behaviour) is hampered by a lack of a clear anatomical segregation [8]. This has been highlighted as one of the clear limitations of anatomical studies - that they can only produce positive results when clear segregation of units is present, with different neuron types projecting to topographically distinct regions [52]. As such, many studies seeking to identify segregation and classification for the Vestibular system have made use of electrophysiological techniques, and opportunities to investigate testable hypotheses through modelling and simulation have arisen. In addition, the neural basis for systems can be hard to identify and to investigate in in-vivo, and in vitro, and so motivation for modelling is provided [56].

The primary segregation and categorisation that has been identified, for both afferent and central neurons (that is, Vestibular Nerve neurons and Vestibular Nuclei neurons), is the segregation into Regular and Irregular neurons. Shimazu and Precht categorised neurons in the Medial Vestibular nucleus depending upon the regularity of their discharge to horizontal angular head acceleration [121]. They identified two neuron types in the MVN: the regular or 'tonic' type; and the irregular or 'kinetic' type. Regular, 'tonic' neurons were found to have regular, even spacing between their action potentials produced by head rotations, whereas the 'kinetic', irregular neurons showed irregular spacing between action potentials [121]. In addition, it was noted that Vestibular Nuclei neuron responses were similar to those of Vestibular afferents.

Similar to Vestibular Nuclei neurons, identification and categorisation of Vestibular afferent neurons has focussed on the segregation of the neurons into regular and irregular types [52] [62]

and the contributions of these types of afferents to the inputs to Vestibular Nucleus neurons [13]. Initially it was found that Vestibular afferents differ in the regularity of their action potentials, their level of resting activity or spontaneous discharge and their dynamic properties. Primarily, it has been found that there is some distinction between regular and irregular afferents and the pathways to which they contribute, and the type of central neurons which they innervate [62]. However, the delineation of afferents to central neurons has not been found to be clear, with most central Vestibular Nuclei neurons receiving a mix of regular and irregular inputs [62]. Although, it was found that the net contribution to the VOR central neurons (i.e. MVN neurons) came from irregular afferents, and a possible relation between regular and irregular afferents and central neurons (that is, irregular afferents input predominantly to irregular central neurons, and regular afferents innervate regular central neurons predominantly) was also found.

The identification of the separation of MVN neurons into regular and irregular types was furthered when evidence was found for further distinctions of irregular and regular MVN neurons, based primarily on the characteristic action potential shape of the two types of neurons, as well as further specifics about their dynamics [118] [119]. As well as further identifying the differing properties and dynamics between regular and irregular MVN neurons, the electrophysiological and chemical studies performed, and the data gathered from these studies, have formed the basis for the construction of models of these neurons (as will be shown in the following section, dealing with the models used for the current work).

It has been shown that MVN neurons possess intrinsic membrane characteristics, which allow for complex integrative properties, and that they can be typed (in relation to these integrative properties) into 2 classes of MVN Neuron, differing primarily in the shape and pattern of the neuron's 'after hyperpolarisation' (AHP. The repolarisation phase seen in neurons following an action potential, where membrane potential rapidly moves from the high positive value at the peak of the action potential, to a highly negative value, usually more polarised than the neuron's resting potential) [118] [119]. It was found that MVN Type A neurons, matching the previously categorised regular or tonic MVN neurons, show a deep, single AHP, with the following depolarisation (return to resting potential after AHP) slowing after an inflexion point. Irregular MVN neurons were found to match MVN Type B neurons (as they have been classed), which show, in contrast to the single deep AHP of MVN Type A neurons, a double AHP, consisting of an initial brief and rapid phase of hyperpolarisation, followed by a brief phase of depolarisation, followed by a second longer and slower phase of hyperpolarisation [118] [119].

In addition, it was also found that the two types of MVN neuron differed in the amplitude of their AHP (MVNA neurons showing a much greater amplitude than type B), the 'width' of their Action Potentials (Type A showing longer action potentials than Type B), as well as the resting (in-vitro) discharge rates of the two types [118] [119]. However, on the subject of resting discharge rates, it has been shown that in-vitro and in-vivo discharge rates for MVNB neurons show significant discrepancies, possibly due to the absence of certain conditions in-vitro, which are present in-vivo (such as synaptic noise) [114], and so, although determining the basis for spontaneous activity is helpful, the actual discharge rates seen in in-vitro conditions are not a useful measure in themselves.

Further recordings of MVN neurons, from horizontal preparations of Rat dorsal brainstem, found a similar classification of MVN neurons, on the basis of their average action potential shapes [77]. Again, MVN neurons were classified into type A (single deep AHP), and type B (showing an early, fast AHP, followed by a delayed slow AHP) [77]. In addition to the classification into the two types of MVN neuron, differences were noted in the number of each type found (30% Type A, 70% Type B), as well as differences in the active membrane conductances (specifics of these conductances will be elaborated in the following chapter on the models used for the current work). These results were in line with previous classifications of MVN neurons. It has also been suggested that this classification of MVN neurons reflects their functional role in the VOR, with Type B neurons being responsible for High frequency head movement responses, and Type A for responses to low frequency head movements [111].

Further to the segregation of MVN neurons by their phenomenological properties, it has been shown that classification of MVN neuron types can be shown via a molecular framework, through the use of transgenic mouse lines [8]. Through the fluorescent labelling of neurons in two transgenic lines, two distinct subset of neurons were found, corresponding to the previous classification of Type A and Type B MVN neurons, with matching action potential shapes as those previously seen [8]. In addition, it was found that those neurons corresponding to the MVN Type B classifications were responsible for the translation of head motion into compensatory motor behaviour over a large, dynamic operating range [8].

2.4.2 *Motivations for and Outline of Current Work*

The relative simplicity of the pathways responsible for mediation of the reflex, along with the extent to which the reflex has been characterised, have made the VOR (and specifically the

linear components of the VOR) an eminent model system for the investigation of the relationship between neurons, neural circuits or pathways, and observed behaviour. The VOR also presents as an ideal system for investigation for several reasons. Firstly, the VOR and the vestibular system in general can be considered to be phylogenetically ancient [33]. The development of the Vestibular system was an important evolutionary event, allowing both vertebrates and invertebrates to maintain posture, balance, equilibrium and spatial orientation, all while moving within their environments [63]. The Vestibular system evolved in organisms a very long time ago, and is present across a wide range of the fossil record [123], including some of the earliest extant species, such as the myxine and lamprey [63]. This is also evidence of remarkably successful design of the Vestibular system, that has changed little throughout Phylogeny.

As such, the Vestibular system and VOR are present in, and have been studied in, numerous species, including the Squirrel monkey [97] [98], the Macaque [137], the Mouse [7], the Cat [78], the Rat [64], the Toad-fish [13], the Guinea Pig [29], the Chinchilla [138], and the Human [29]. Further to this, the Vestibular apparatus and VOR circuitry show remarkable similarities across species [1]. Due to this, there is a great deal of information that can be used specifically for theoretical and modelling studies of the Vestibular system and VOR. In addition, the Vestibular system and VOR have a well characterised anatomy and physiology [89], therefore presenting it as an ideal system for investigation, particularly in investigation of the role of variability in neural systems.

Secondly, the relative simplicity of the three neuron arc involved in the VOR, and its direct nature, makes the reflex an ideal candidate for investigation, especially in regards to the strategies and mechanisms by which the nervous system codes and transmits information from the sensory to the motor space. For example, the horizontal rotational VOR transmits sensory input, converting it to motor output, almost directly and with little to no subsequent processing. That is, the hVOR has no extensive downstream processing that can be seen in other systems, and the sensory input is converted to motor output, through only a single layer of interneurons [68]. Generally, the VOR is a linear system, translating sensory input directly to motor output [7].

However, in addition to identifying the characteristics and properties that can be used to categorise and identify different neuronal types involved in the Vestibular system, it is also important to identify the ways in which individual members of a population of a given class or type of neuron differ, and how that variability can be quantified across populations, and to identify the role and function of this heterogeneity. That is, significant variability is seen amongst

populations of identified neuronal types, and is seen amongst populations of MVN Type B (and MVN Type A) neurons [118] [119] [109], and it is theorised that the variability seen across the populations is necessary for their dynamic properties [5], and particularly for the precise, wide frequency response required of the VOR [68]. As such, it is necessary to identify and quantify the means by which populations of MVNB neurons may vary, and what significance and role such variance has on performance of the populations.

The fundamental mechanisms of sensory signalling are still largely unknown [109]. Evidence has been shown that suggests that, along with factors such as neuron morphology and size, diversity of ion channel expression, and the conductances arising from these channels, are responsible for heterogeneity in the populations involved [37], and that this heterogeneity is responsible for the diversity of responses seen [109] [83] [20]. It is still to be determined, however, which intrinsic membrane properties of the neurons involved in all stages of the VOR allow for the graded hair cell responses to be encoded into trains of action potentials, which are then transmitted through the Vestibular afferents, to the Central Vestibular neurons, and then to the Oculomotor neurons. There is good evidence, however, that the heterogeneity of the Vestibular afferent populations and their responses is due to the expression of K^+ conductances, and that these conductances are expressed heterogeneously across the populations involved [20].

Experimental limitations have precluded a thorough investigation of the role which neural heterogeneity may play in the performance of the VOR [117] [68], thus a modelling approach, especially involving models with high bio-physical plausibility such as those used in the current work, can help to investigate the function and possible benefit of such heterogeneity in the MVN response of the linear, direct hVOR. For example, the small number of neurons that show spontaneous discharge in cell cultures has limited such techniques in investigating the cause and diversity of such discharge [83].

Both modelling and electrophysiological studies of MVN Type B neurons have shown that single neurons display only a limited range of frequencies for which their response is linear, and follows the input faithfully [68] [89]. Therefore, single neurons cannot account for the behaviour of the MVN Type B neurons at this stage of the VOR, and a population response must be considered, especially for high frequencies.

Thus, we attempt here to investigate the possible role of MVN Type B population heterogeneity in the high frequency response of the fast, linear, direct and unmodified hVOR, using models with a high bio-physical plausibility, that allow us to model and manipulate specific ion channel

properties and parameters of the model neurons. Previous modelling work (i.e., [68] and [72]) has only made use of simpler models, such as leaky integrate-and-fire, and Fitzhugh Nagamo models of neurons, which suffer from limitations in the capacity for parameter setting of the model, the fitting of model behaviour to observed cause of that behaviour, as well as modelling of the neuron morphology [88]. For example, these simpler models do not allow for the consideration of the dendritic structure to be modelled as closely as the compartmental nature of the models used in the present work, thus we can model and distribute synaptic inputs dispersed across the dendritic tree (Chapter 3, Section 3.2.2), as they would be in the real neuron, or through the location ionic conductances, including them in some compartments, but not others. Simpler models of the neuron treat it as a single point in space, and so neglect the possible effects of this neuron morphology, an element of neuron behaviour that is almost certainly important in its function [88].

Also, the means by which the conductances of the models used here are modelled allows for more realistic and focussed representation and manipulation, such as the separation of similar conductances into their subtypes (i.e., slow or fast voltage activated Potassium conductances, or Calcium activated Potassium conductances) or through the varying of their activity and via density, parameters, or specifics of activation and deactivation of the channel. Thus we can model varying behaviour observed in MVNB populations with observed heterogeneity of the conductances involved to investigate the functional role of that heterogeneity.

Specifically, we investigate here the role of diverse spontaneous discharge rates across the population, modelled as an electrical bias supplied to the models in the early stages, and Heterogeneity in K^+ currents in latter stages. Along with population Heterogeneity we also investigate the possible role of noise in the population response. We also model inputs through a method that allows the dendritic structure of the neuron to be incorporated into the simulations.

3

METHODS

3.1 COMPARTMENTAL MODELS OF MEDIAL VESTIBULAR NUCLEUS NEURONS

3.1.1 *Introduction*

As has been discussed in the preceding chapter, at the level of the central vestibular nucleus neurons, a sensorimotor transformation occurs, between the sensory space (the semi-circular canals of the vestibular system) and the motor space (force exerted by the extraocular muscles) in order for the functioning of the rotational Vestibulo-Ocular Reflex (VOR) to be achieved. Specifically, when dealing with the horizontal VOR (hVOR), the central vestibular neurons responsible for this transformation are the Medial Vestibular Nucleus (MVN) neurons. Further, it has been proposed that this operation relies heavily on the membrane properties of the neurons involved [128], in addition to the network connectivity [61] and synaptic mechanisms [62]. However, without access to simultaneous recordings from a large number of Vestibular neurons, these membrane and network properties are difficult to illuminate.

Computational and modelling methods, however, provide an alternative approach to the investigation of membrane and network properties, and the extrapolation of these to network behaviours. That is, through modelling of the MVN neurons, we can investigate and explore the network and membrane properties involved in the VOR, and how these properties relate and contribute to the overall behaviour of the reflex, and particularly the high speed/frequency response of the VOR.

Therefore, in the work being presented, Bio-physically plausible compartmental models of Guinea Pig Medial Vestibular Nucleus (MVN) neurons, implemented in the NEURON Simulation environment, were utilised. The parameters and structure of the models were published previously [104], and were chosen in order to reproduce the behaviour and responses of MVN Type B neurons reported through electro-physiological recordings [118] [119]. Parameters not constrained by data obtained through these electro-physiological recordings were, instead, constrained by data obtained from other recordings, primarily from neurons located in the deep cerebellar nuclei and hippocampal CA3 pyramidal cells [104].

Two main considerations underlie the type and construction of model used in the current work. Firstly, a high level of biological plausibility was required from the mechanics and kinetics underlying the (membrane properties and their representation within the) model. Voltage gated ion channels utilised Hodgkin-Huxley Kinetics [67], while Ligand gated ion channels and Calcium modelling used Michaelis-Menten type Kinetics [94]. A relative advantage of this approach, is that it allows for the physical structure and parameters of the model to be related to actual electro-physiological data [104]. In addition, by modelling the individual parameters and variables of the model independently, it allows for the manipulation of these parameters in a plausible manner. However, this approach of requiring high biological plausibility in the models, does have the disadvantage of being computationally expensive, when compared to other, less plausible modelling methods.

The second consideration of the modelling strategy was the use of actual electro-physiological data, from previously published intracellular studies [118] [119] to constrain the parameter values of the models. That is, Hodgkin-Huxley and Michaelis-Menten type kinetics were used to model the membrane properties of the neurons, with the parameters of the kinetics constrained strictly by data from intracellular studies of actual Medial Vestibular Nucleus neurons. In addition, any parameters that were not constrained by data from these studies were constrained instead by data obtained from electro-physiological studies of other neuronal preparations, particularly neurons located in the deep cerebellar nuclei and hippocampal CA3 pyramidal cells [104].

One important result of the use of high plausibility modelling techniques, and the constraints to the parameters and structure applied to the model, is that, under specific conditions, the models are able to reproduce behaviour observed in electro-physiological studies that were not utilised during the construction of the models. This can be considered evidence for the predictability of the models utilised [104].

3.1.2 *Morphology*

The models used Compartmental modelling principles, in order to more accurately model the involvement of the neuron's dendritic structure in the behaviour of the neuron. That is, the spatial extent and complexity of the neuron's dendritic structure is modelled as multiple individual compartments, each of a given diameter and length. The dendritic tree is divided into cylindrical compartments, each given their own membrane resistance, as well as type and density of ion channels and other mechanisms. Each compartment is characterized by its capacity and

transversal conductivity, with adjacent compartments being coupled by the longitudinal resistance determined by their geometrical properties. This allows for the model to take into account the uneven distribution of ion channels and other mechanisms across the neuron's surface.

The Type B MVN neuron models feature 4 proximal dendrites, branching from the soma, each made up of 3 compartments. Proximal dendrites further split in to 2 distal dendrite branches, each of which is made up of 6 compartments. This compartmental structure is illustrated in Figure 3.1. Soma radius was 15.5µm, proximal dendrite radius and length 1.5µm and 99µm, and distal dendrite radius and length 0.5µm and 198µm [1]. The structure of the dendritic tree was chosen to match data available on MVNB neurons (including personal communications between Quadroni & Knopfel and M Serafin).

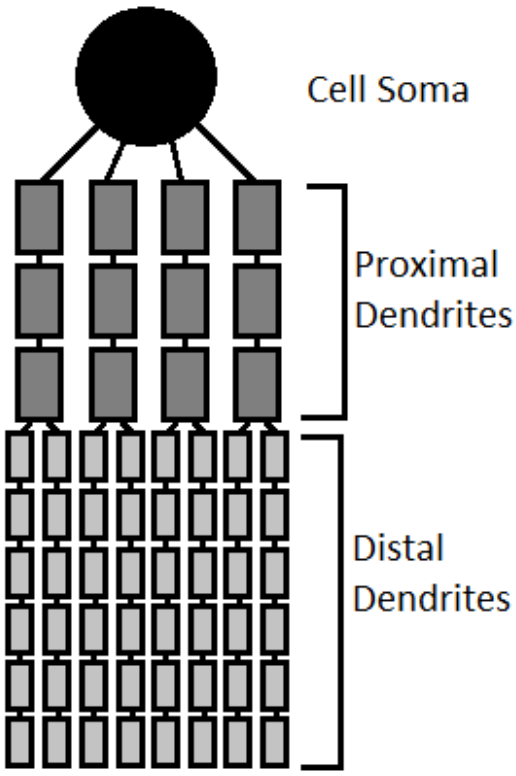

Figure 3.1: Compartmental Structure of the MVNB Neuron Models. The models consists of a cell Soma, with 4 Proximal Dendrites branching from this, which then branch into 2 Distal Dendrites each. Each Proximal Dendrite is made up of 3 compartments, while Distal Dendrite is made up of 6 compartments.

The shape of the MVNB neuron model, as implemented in the NEURON simulation environment, is shown in Figure 3.2.

1 These match the values provided by [104]

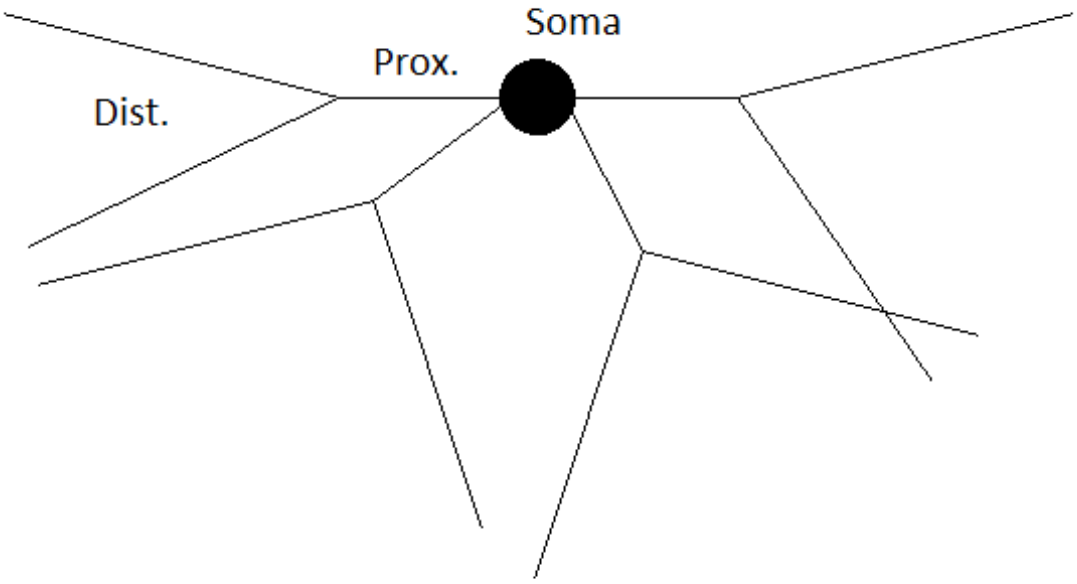

Figure 3.2: MVNB Model Shape as Implemented in NEURON. Soma is represented by the large circle at the top of the image, with Proximal dendrites (Prox.) branching from this. Proximal dendrites then branch into 2 Distal dendrites each (Dist.).

3.1.3 *Active Membrane Conductances*

The modelling of active membrane conductances is founded upon the general formalisations of Hodgkin and Huxley [67], in which each channel is controlled by (at least) one gate, and is considered activated when all gates are in the open state. The gate states are controlled by backwards and forwards rate functions, which in turn are dependent upon membrane voltage. In addition, the Calcium activated Potassium channel rate functions are, in part, dependent upon internal Calcium concentrations. That is, each channel is controlled by at least one gate, and is activated when all gates are open, each gate being in one of two states (open or closed), and the transition between states being determined from the forward and backward rate functions.

Each of the 61 compartments were allowed to contain up to 9 Active conductances. The characteristics of the modelled conductances were derived from intracellular recordings of MVN neurons from Guinea-pig brainstem slices, by Serafin and colleagues [118] [119], from which mathematical models, channel specifics, and rate functions were then formalised by Quadroni and Knopfel [104][2] These models were subsequently implemented in the NEURON simulation

2 The conductance density, reversal potential, and rate functions of the models implemented in NEURON correspond to those provided by [104].

environment, by Tom Morse of Yale.Edu, and made publicly available on the 'SenseLab' Model Database.

3.1.3.1 *General Observations from Intracellular Recordings*

Two studies detailing the intrinsic membrane properties [118], and their ionic basis [119], of Guinea-pig Medial Vestibular Nucleus neurons were used to constrain the parameters of the models detailed by Quadroni and Knopfel [104]. Firstly, we provide a general overview of the findings from these studies, before detailing the Active conductances observed, and the details of their modelling performed by Quadroni and Knopfel.

Intracellular recordings were taken from 170 neurons of the MVN from brainstem slices of the Guinea-pig, primarily to identify their intrinsic membrane characteristics. A resting potential of -50mV, and AP size of 60mV were observed. Two main sub-types of MVN neuron were observed, largely based on the characteristics of their After-hyperpolarisation (AHP, as discussed in the previous chapter)[3]. A small number of neurons tentatively classified as a third group (Type C) was found also, as a heterogeneous population that showed some, but not all of the characteristics of the Type A and B classes [118]. However, it is assumed that these neurons were part of the Type A or B classes, but due to their heterogeneity, they were not clearly classified as either. Further studies have not identified Type C neurons as separate from Type A or B [77] [8].

Type A neurons were characterised by a deep, single AHP, and, during spontaneous activity, displayed a slowing of AHP, suggesting the involvement of an active process (possibly an A-Like Potassium Rectification, causing a change in the depolarisation slope of the AHP, around midway through, reducing the strength of the AHP [119]) [118].

Type B MVN neurons showed a double, or bi-phasic, AHP (a rapid, brief repolarisation after an action potential, followed by a longer, slower AHP, or repolarisation, phase). This bi-phasic AHP was present in all MVN B neurons observed. A mean AHP amplitude of 10mV (both phases), an action potential duration of 0.29ms, and resting potential of 56.3mV were observed for MVN B neurons. In comparison, MVN A neurons showed much greater AHP amplitudes (22.2mV), and significantly longer action potential durations (0.5ms). Type B neurons showed Subthreshold Plateau potentials, which kept the cells close to their firing threshold. Both Types showed spontaneous activity, or regular resting discharge [118].

3 This classification of MVBN neurons into two types is largely in line with previous classifications mentioned previously, into Tonic and Kinetic, or Regular and Irregular, neurons. We mainly present details of the Type B neurons, as they are the focus of the current work, but include some discussion of Type A neurons for comparison and completeness.

Type B neurons had large, high threshold calcium spikes and prolonged calcium dependent plateau potentials, as well as Calcium dependent AHP and subthreshold persistent Sodium conductances, and low threshold Calcium spikes, leading to some bursting activity. In contrast, Type A neurons small, high threshold Calcium spikes (increased by Barium), but shared a Calcium dependent AHP [119].

Both MVN neuron types showed an anomalous rectification (drop in voltage response after prolonged Hyper-polarising pulses) blocked by the application of Caesium (K^+ channel blocker), along with the reduction of AHP (second phase of Type B) in the presence of both Cadmium and Cobalt (Ca^{2+} channel blockers) suggesting the involvement of Ca^{2+} Activated K^+ in this behaviour [119].

3.1.3.2 *Fast Inactivating Sodium Conductance*

The Action Potentials of Type B neurons are seen to be fast (0.29ms, as mentioned previously), suggesting that the Sodium conductance responsible for the initial phase of the Action Potential possesses both a fast activation and a fast inactivation, thus limiting the size of the outward current required for repolarisation of the cell. Further, as MVN Type B cells can show maximum firing rates of 400Hz, a fast recovery from inactivation is suggested in this conductance [118][118]. The rate functions for these channels were adjusted, in order for the shape of action potentials observed in electrophysiological recordings to be reproduced faithfully and accurately in the model neurons [104].

3.1.3.3 *Persistent Sodium Conductance*

This conductance is responsible for the subthreshold plateau potentials, which have been observed in MVN neurons to resist inactivation during strong depolarisation, and show sensitivity to QX314 (Bromide, a Na^+ channel blocker). Further, as long depolarising pulses have been shown to inactivate and/or block spiking in MVN neurons, but not the persistent Sodium current, it is suggested that this conductance is not the 'window current' (the small range of voltages where T-type (Transient) channels can open, but do not inactivate completely) of the Fast Inactivating Sodium Conductance, but rather this is a current/conductance generated by a separate and distinct set of channels [104]. This conductance was modelled using data obtained from Hippocampal Pyramidal cells, and did not include inactivation.

3.1.3.4 *Fast Voltage Activated Potassium Conductance*

This conductance is responsible for the initial phase of repolarisation after action potentials, seen in MVN Type B neurons. The underlying channel responsible for this conductance may correspond with observed delayed rectification [118], but may also incorporate other channels. This conductance must feature rapid deactivation at resting potential, in order for the biphasic after-hyperpolarisation observed in MVN Type B neurons. The shape of the action potentials, therefore, can be constrained by the rate functions of this conductance, with a fast activation, combined with a high activation threshold, leading to the very fast action potentials observed in Type B MVN neurons [104].

3.1.3.5 *Calcium Activated Potassium Conductance*

The second phase of after-hyper-polarisation seen in Type B MVN neurons is blocked by Apamin, Cadmium and Cobalt (all of which are Ca^{2+} channel blockers). Therefore, it is likely that this conductance is generated by a current derived from or generated by Ca^{2+} activated or dependent Potassium channels. A similar current has been seen in other types of neurons, and is not observed to be Voltage activated. The mathematical expressions used for this conductance are equivalent to Michaelis-Menten like Kinetics [104]. In addition, this conductance may also involve the dendritic structure. That is, after the initial, first, rapid phase of after hyper-polarisation the soma is highly polarised, and negatively charged. Calcium currents from the Dendrites to the Soma are generated, with Calcium flowing into the Soma, and this positive current influx is responsible for the brief depolarisation seen between the 2 phases. It has been proposed that this Calcium flow, from Dendrite to Soma, is responsible for the activation of this Potassium conductance, and the 2nd phase of MVN Type B after hyper-polarisation. The existence of this conductance and confirmation of the channel underlying it was also confirmed in electrophysiological studies not used in the construction or consideration of the model [77].

Modelling studies of MVN neurons[4] have provided further support for the role of a Calcium activated Potassium channel in shaping the second phase of AHP [5].

3.1.3.6 *Transient Potassium Conductance*

This conductance is present only in the Soma of Type B neurons, and is theorised to be similar to an A-Like conductance (Potassium channel, similar to 'shal' or 'shake' channels [104]). It

4 Using single compartment models, with Hodgkin Huxley and Active conductances

shows de-inactivation (that is, becomes available for activation) during hyperpolarisation, and rapidly activates with depolarisation. Additionally, this conductance is confirmed by the selective means by which it's blocked in Rat MVNB neurons, from studies not used in the creation or consideration of the model [77]

3.1.3.7 *Slow Relaxing Voltage Activated Potassium Conductance*

In cortical neurons, the persistent Sodium conductance is accompanied by a slow activating outward current. This slow current counteracts development of sub-threshold plateau potentials. This conductance may partially represent slow depolarisation activated Chlorine currents, electrogenic pumps and exchangers [104]. Slow kinetics are required for this conductance, in order to replicate Sodium dependent plateau potentials, and to accurately reproduce the relationship between injected current and firing frequency.

3.1.3.8 *Slowly Relaxing Mixed Sodium-Potassium Conductance*

Both Type A and Type B MVN neurons showed a 'sag' during injection of hyper-polarising current pulses. This anomalous rectification was eliminated by Caesium (Potassium channel blocker) [119]. This conductance is similar to conductances seen in cat cortical neurons and cerebellar purkinje cells [104].

3.1.3.9 *High Voltage Activated Calcium Conductance*

A high threshold inactivating Calcium (Ca2+) conductance, based on previous experimental work and models of hippocampal pyramidal cells, with altered time dependence of activation to recreate behaviour of MVN neurons in electrophysiological studies [104].

3.1.3.10 *Low Voltage Activated Calcium Conductance*

This conductance is unique to Type B MVN models (not present in pharmacological studies or models of MVN Type A neurons). Considered to be responsible for burst firing observed in Type B neurons, and is similar to those seen in thalamic and cerebellar nuclei neurons. The kinetics of this conductance are based on those described in experimental work and models constructed from this work [104].

3.1.4 *Model Behaviour*

For the work presented here, the mathematical models described in the literature [104] are incorporated into the NEURON simulation environment, with some slight modification (the inclusion of an empty 'dummy current' in order to avoid problems with numerical integration that were encountered).

The Quadroni & Knopfel model faithfully reproduces behaviour described by Serafin and colleagues [118] [119], as far as Action Potential size, length, shape and the specific course and shape of after-hyperpolarisation (AHP). The implementation of these models used in the current work also reproduce this behaviour. Figure 3.3 shows the Action potential shape of the model MVN Type B neurons. Further, the two phase AHP is reproduced through the interaction of currents generated by the fast voltage activated Potassium conductance (K-Fast) and the Ca^{2+} activated K^{+} (K-AHP), as well as Calcium currents flowing between the Soma and dendritic structures. The first component of the AHP is generated, mainly, by K-Fast, and the second by K-AHP, with the latter activating only after repolarisation, due to the delay of sub-membranous Calcium concentration compared to voltage. The brief depolarisation seen between the 2 phases of hyperpolarisation, is seen to be dependent upon the dendritic structure used in the models (that is, reducing the number of proximal dendrites branching from the soma body can lead to the elimination of this brief repolarisation, as well as reduction of the 2nd phase of AHP), as is due to the inward Calcium currents present in the dendritic structure [104].

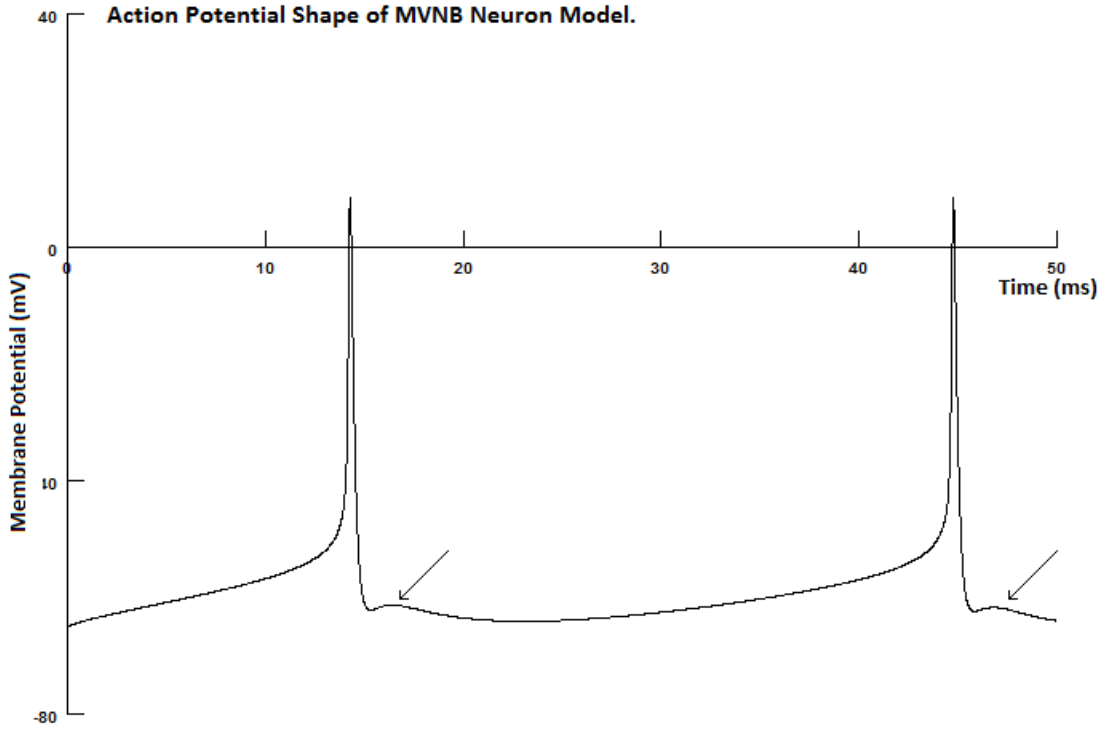

Figure 3.3: MVN Type B Action Potential Shape. Voltage trace of model MVN Type B neurons, showing Action Potential course. Arrows show the start of the second phase of the two phase After-Hyperpolarisation observed in experimental studies, and produced by the Ca^{2+} activated K^{+}. The Calcium currents activating this Potassium conductance are responsible for the brief period of depolarisation observed prior to the second phase of AHP.

Several properties of these conductances and the model are required to produce the distinctive shape of the 2 phase AHP. Firstly, K-Fast must display rapid deactivation, near resting membrane potential. This must be followed by a rapid repolarisation, in order to induce the large potential gradient between the soma and dendritic structure, and, thus, the brief depolarisation seen between the 2 phases of AHP. In addition the morphology of the model/neuron plays a part in producing the shape of the AHP, as the K-AHP conductance of the 2nd phase is activated by the Calcium conductances originating in the dendritic structure. Reducing the number of dendrites increases the spike and AHP amplitude (as there is decreased Calcium based currents flowing between soma and dendrite), and no dendritic structure leads to mono-phasic AHP.

Both MVN Type A and B neurons display spontaneous firing activity, or regular resting discharge [118]. This is replicated in the model cells, with standard or default rates of 15Hz (Type A) and 21Hz (B) (Our implementations show an spontaneous frequency of 20.904Hz for MVNB models). The persistent Sodium current of the models supports and produces the spontaneous

activity in Type B MVN neurons, whereas the slow potassium current builds up during long lasting depolarising current injections and, during spontaneous activity, it regulates activity the of cell, through opposition of the persistent Sodium current. The transient Potassium conductance has a low threshold to deactivation, and thus there is no delay to action potential generation after long lasting hyper-polarisation, as is seen in MVN Type A neurons [104].

3.1.4.1 *Induced Rhythmic Bursting Activity*

As well as recreating the behaviour observed in [118] and [119], the models of Quadroni and Knopfel successfully recreated behaviour observed in electro-physiological and pharmacological studies that were not used to create the model [104]. That is, the models were able to recreate behaviour seen in studies, the data and observations of which were not used to define the parameters of the model, or as a target of the model's behaviour. In studies involving the use of Apamin, which is known to block certain Calcium activated Potassium channels (SK channels, such as the K-AHP of the MVNB model), rhythmic bursting activity was observed from MVNB neurons [30]. In the Quadroni and Knopfel model, this behaviour was successfully induced by the removal of the K-AHP conductance (thus modelling the blocking action of Apamin on Calcium activated Potassium channels) [104]. This recreation of behaviour not used in the creation of the models was considered to be an indication of their validity and possible predictive ability [104].

The models used by the author in the current study also recreate this behaviour, as is seen in Figure 3.4. Removal of the K-AHP conductance leads to rhythmic bursting activity from the model, matching that observed in both the modelling work of Quadroni and Knopfel [104], and the pharmacological studies of de Waele and colleagues [30].

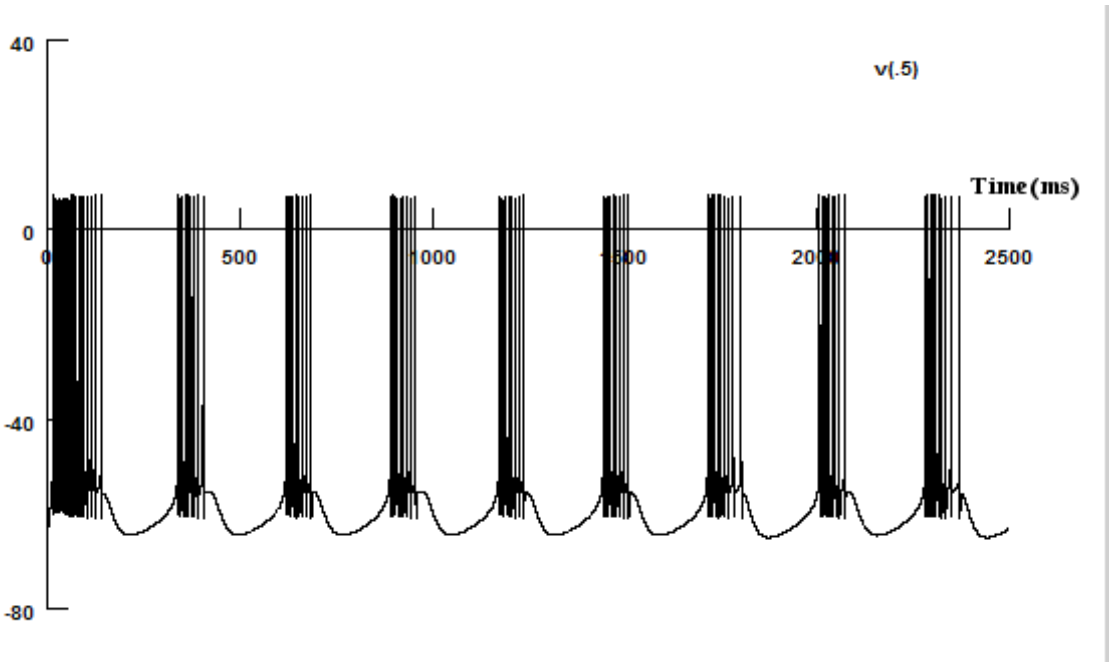

Figure 3.4: Rhythmic Bursting Activity Induced by K-AHP Removal.

In addition, the introduction of hyper-polarising current to the model and neuron, with K-AHP removed, reduced the frequency of the rhythmic bursting activity. Again, the models used here recreate this behaviour faithfully, as shown in Figures 3.6, 3.7, and 3.8.

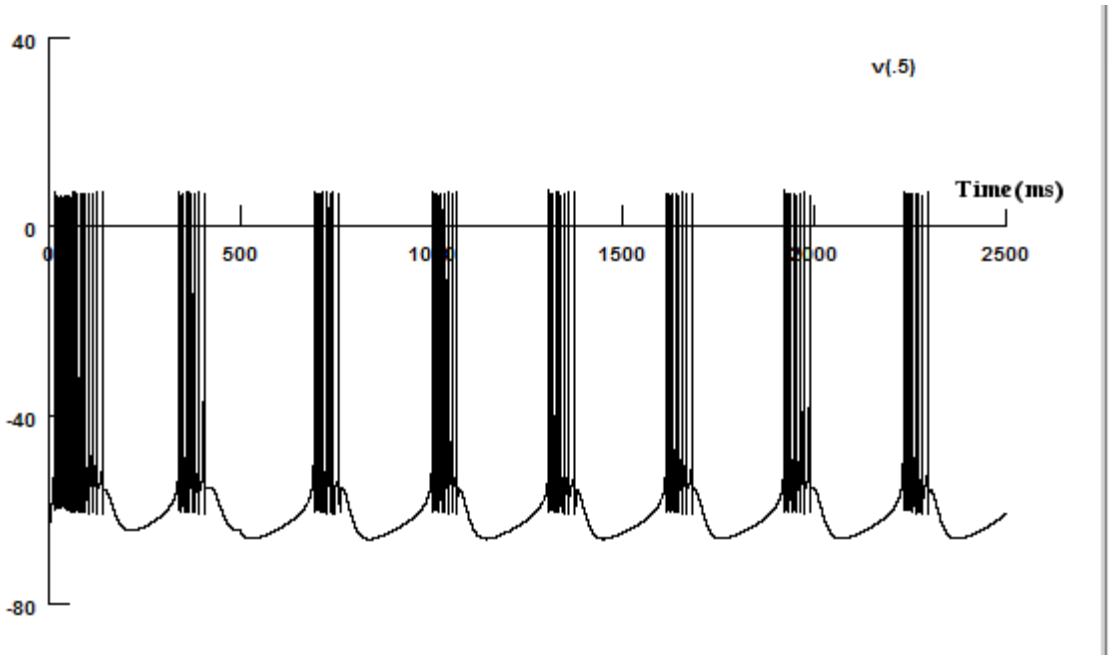

Figure 3.5: Effect of Hyper-polarising current injection of -25pA (0.025na) on Rhythmic Burst frequency. Current injection begins at 300ms

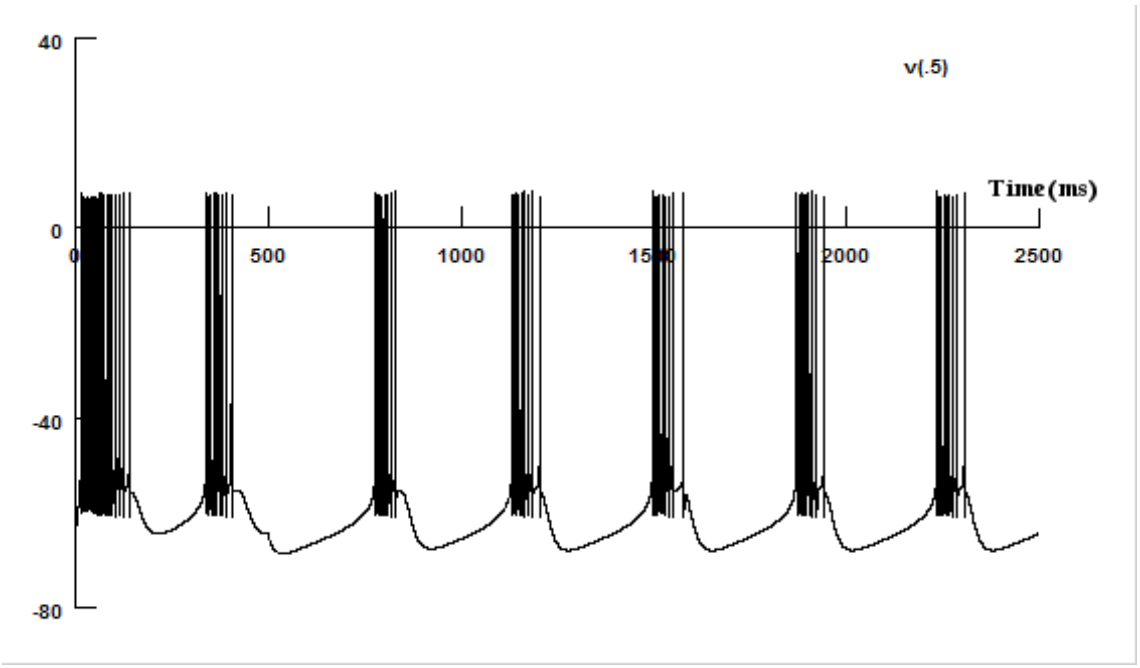

Figure 3.6: Effect of Hyper-polarising current injection of -50pA (0.05na) on Rhythmic Burst frequency. Current injection begins at 300ms

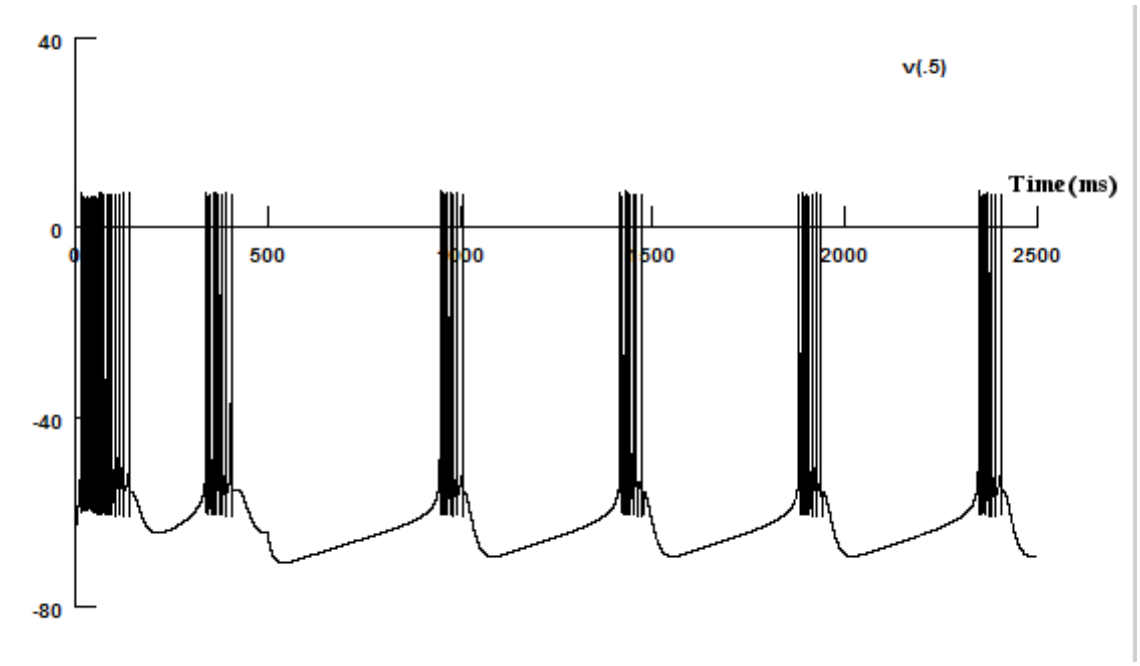

Figure 3.7: Effect of Hyper-polarising current injection of -75pA (0.075na) on Rhythmic Burst frequency. Current injection begins at 300ms

Rhtyhmic burst activity was modified further with hyper-polarising current, in that duration of the bursting activity decreases with with the inclusion of hyper-polarising current injection. This is shown in Figure 3.8.

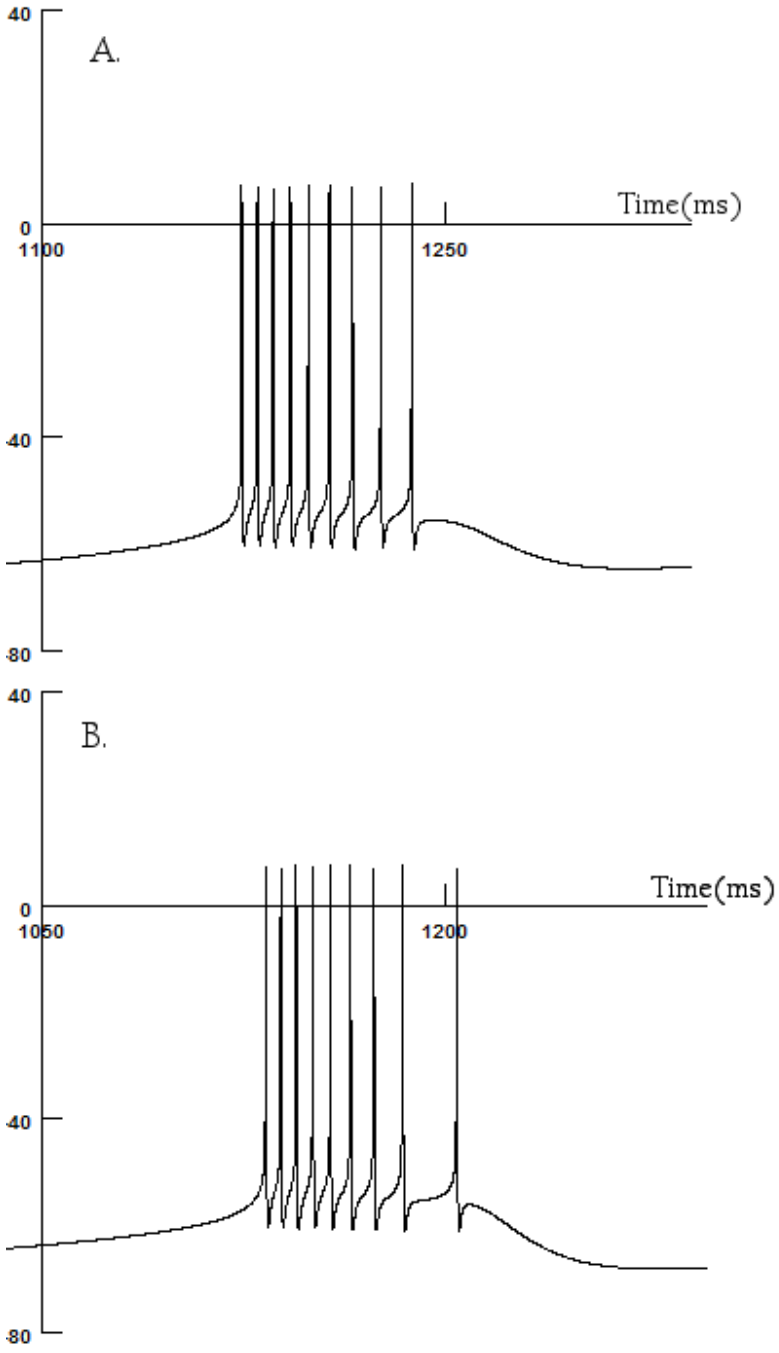

Figure 3.8: Comparison of Rhythmic Burst Length. Rhythmic burst activity, induced by elimination of the K-AHP conductance, is reduced in duration by hyper-polarising current injection. Top trace shows rhythmic burst length with current injection of -50pA (0.05na), lower trace shows no current injection.

The likely cause of this reduction in both rhythmic burst length and frequency is the effect of the hyper-polarising current in augmenting the already present hyper-polarisation caused

by the K-Slow channels, which builds up to terminate the burst. With hyper-polarising current augmenting the hyper-polarisation of the K-Slow channels, bursts are terminated sooner.

Finally, the rhythmic activity of MVNB neurons in SK channel blocking mediums was observed in other pharmacological studies characterising the ionic conductances of Rat MVN neurons that were not available during model creation, along with an alteration to the shape of the second phase of AHP in MVNB neurons, with the second phase eliminated in Apamin medium [77]. The models used here also recreate this behaviour, as shown in Figure 3.9.

Thus, our models accurately recreate behaviour obtained from studies used to create and parametrise the models, as well as from studies that were used in proofing, and in separate studies not used to proof the Quadroni & Knopfel models.

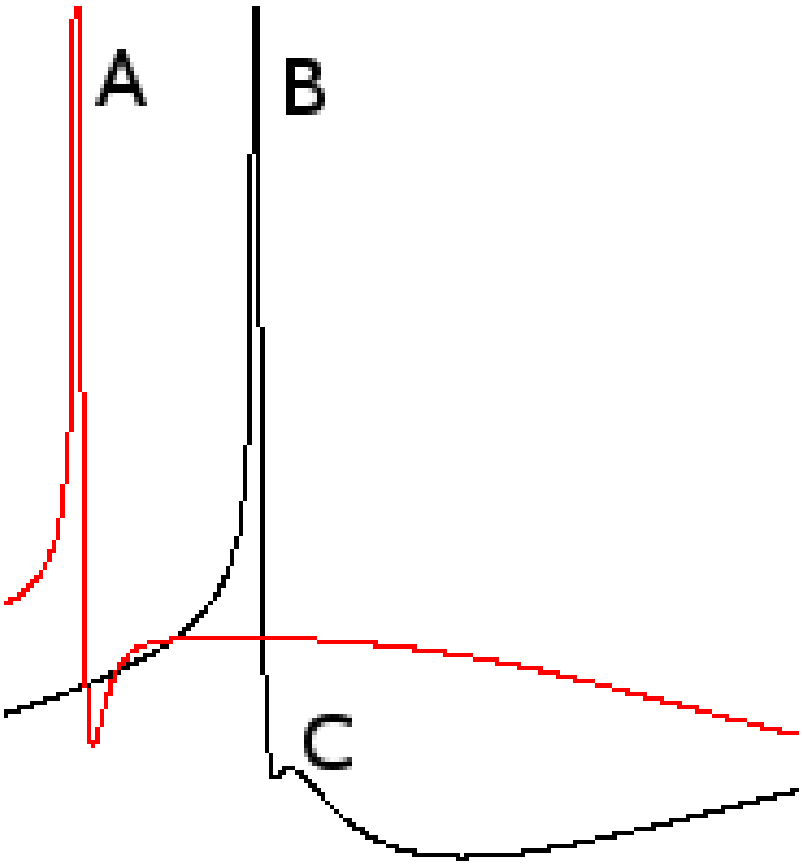

Figure 3.9: Action Potential Shape with eliminated K-AHP conductance (A) and in the standard model (B). Second phase in the standard simulation is marked (C) and missing from the simulation with eliminated K-AHP.

3.1.5 *Specific Behaviour of Slow Potassium Conductance*

As previously mentioned, it has been suggested that heterogeneity of MVN neuron populations is, at least in part, responsible for the diverse range of responses seen from MVN neurons [109] [83] [20], and the wide range of frequencies over which the hVOR operates [68]. We seek to investigate the implications of this population heterogeneity (for response fidelity), expressed as diverse spontaneous discharge rates, and firing rates in response to inputs, across a population of model MVN neurons. Heterogeneity of the Slowly relaxing Voltage Activated Potassium conductances (K-Slow), across populations, was investigated as the possible cause of the diversity of spontaneous discharge rates, in the current work.

This conductance was investigated as a possible cause of MVNB spontaneous discharge rate heterogeneity due the observed action of the conductance, and its relation to the persistent Sodium conductances present in neurons, and MVN neurons specifically. The persistent, inward Sodium conductance (NAp) is known to produce the spontaneous activity of MVNB cells [118] [119], through the generation of the sub-threshold plateau potentials, prolonged or persistent depolarisations of the cell constantly maintaining membrane voltage near threshold [71], thus increasing their spontaneous rate of activity [79]. These sub-threshold plateau potentials are sustained in MVN neurons, due to the persistent nature of NAp, and thus drive the constant spontaneous depolarisation of the cell responsible for the rate of their rhythmic activity, and supporting this spontaneous activity of the cell [118]. Therefore, the NAp conductance modulates and supports the spontaneous activity of model MVNB cells[104]. The K-Slow conductance, on the other hand, is seen to counteract the development of these sustained plateau potentials in neurons [124], and MVN (Type A and B) neurons specifically [118]. Thus, during spontaneous activity in the model cell, this conductance acts to regulate this activity of the cell by opposing the activity of the NAp conductance [104].

As previously described, Potassium(K^+) channel heterogeneity has been found to be the cause of the diverse firing rates seen in both Vestibular afferent neurons, and the MVN neurons involved in the hVOR. Vestibular afferents showed cell-to-cell variability in the magnitude of their K^+ conductances [109], and in Central Vestibular nucleus neurons it was found that the K^+ conductances of these neurons played a significant role in the generation of their diversity of response, and that, rather than a discrete categorisation of responses being present, a continuous distribution of responses was found, and it was found that, specifically the slow K^+ conductances and their continuous distribution affected the repetitive firing seen in populations [117]. However,

for Vestibular afferent neurons at least, very little variability in the magnitude of their Sodium(Na^+) conductances were found [109], thus eliminating variability of these Na^+ conductances as a possible candidate for the cause of the diverse firing properties of these populations. Therefore, alteration of the K-Slow conductance, but not the NAp conductance, was investigated as a possible cause of the diverse firing dynamics of MVNB neurons. Figure 3.10 shows the effects of manipulation of K-Slow conductances on the spontaneous activity of MVNB neurons.

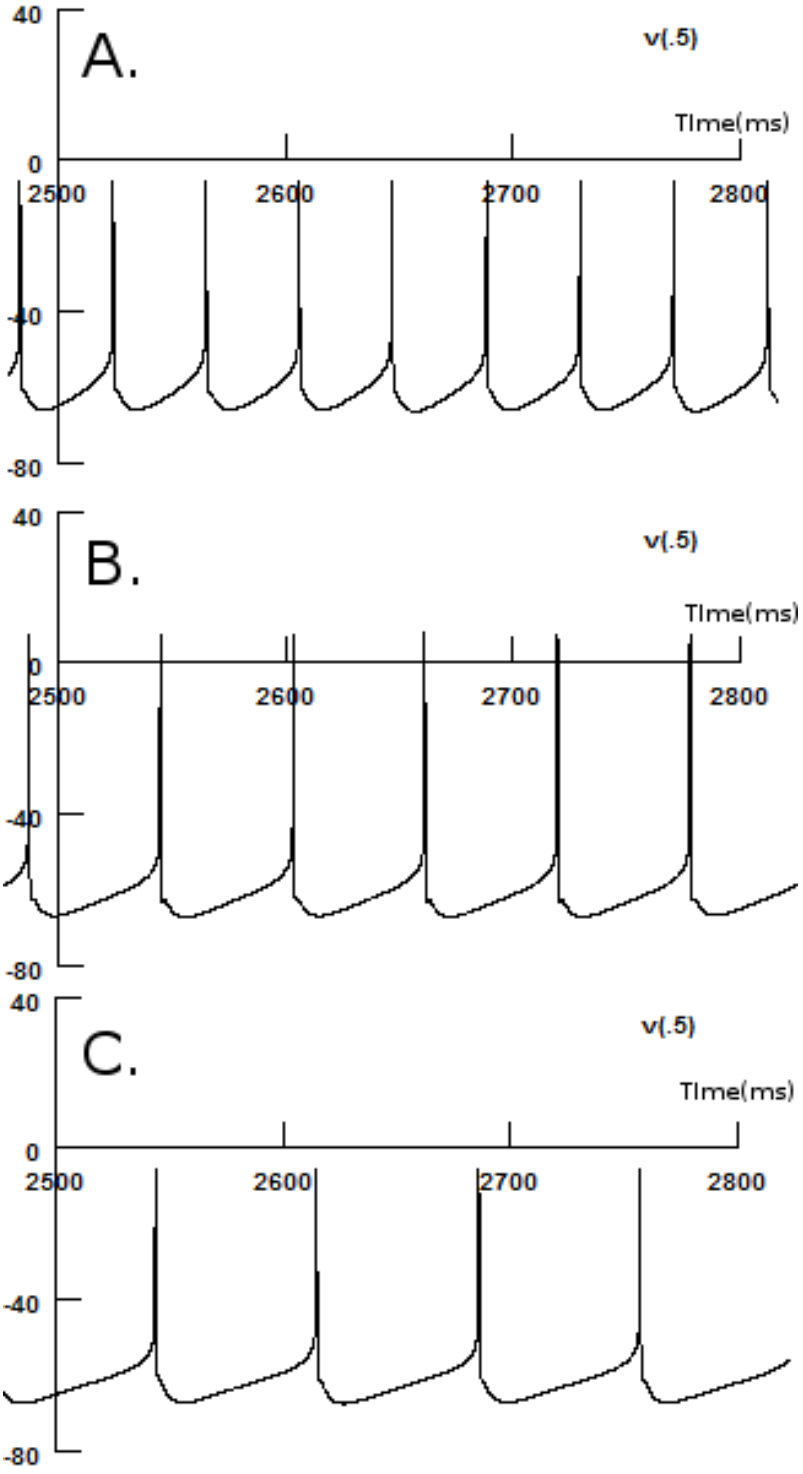

Figure 3.10: Comparison of spontaneous activity in MVNB Cells with altered K-Slow conductances. Voltage traces of simulated MVNB neurons, showing the effect of decreased K-Slow density (top trace, A., increasing firing frequency), unaltered (B.), and increased (C., decreased frequency of firing)

That is, the persistent inward Sodium conductance (NAp) acts to depolarise the cell constantly, supporting its rhythmic, spontaneous activity, whereas the outward slow Potassium conductance (K-Slow) hyper-polarises the cell, driving it away from threshold. Increasing the density or magnitude of K-Slow leads to greater hyperpolarisation, countering the depolarisation caused by NAp more strongly, thus decreasing the spontaneous activity of the cell. Similarly, decreasing the density of K-Slow causes less hyperpolarisation to oppose the depolarisation of NAp, increasing the spontaneous firing rate of the model cell.

3.2 METHODS OF HETEROGENEITY AND INPUT SIMULATION

Here we present the methods used in the work presented for the modelling and simulation of population heterogeneity, input to the cells, and noise present in the simulations.

3.2.1 *Population Heterogeneity Modelling*

3.2.1.1 *Bias Current*

The first method of simulating population heterogeneity, in the form of varied spontaneous firing rates, was the use of 'bias' added to the model, through current injection, in order to increase or decrease the spontaneous rate of fire. This method has been used previously, to investigate the role of heterogeneity in model MVNB neurons (using simpler, leaky-integrate-and-fire models) [68], as well as the general benefits and effects of population heterogeneity on information processing (with Fitzhugh-Nagamo neuron models) [72].

Hyper-polarising current injection to the cell model Soma serves to decrease spontaneous firing activity, counteracting the conductances that depolarise the neuron naturally and persistently. Thus, the effect of the persistent Sodium current NAp, which drives constant depolarisation of the neuron towards and past threshold for spiking, is reduced through the hyper-polarisation of the injected current. Similarly, the natural depolarisation is augmented by the injection of depolarising current, increasing the spontaneous rate of fire. The effect of this current injection is shown in Figure 3.11. To take account of any initial but transitory effect on the model from the current injection (it was observed that neurons showed a changing ISI rate while they "settled in" to the level of current injection provided) simulations using this method were allowed 500 milliseconds, until ISIs were constant, before any experimental input was provided. This was similar to an initial delay used in previous work[68].

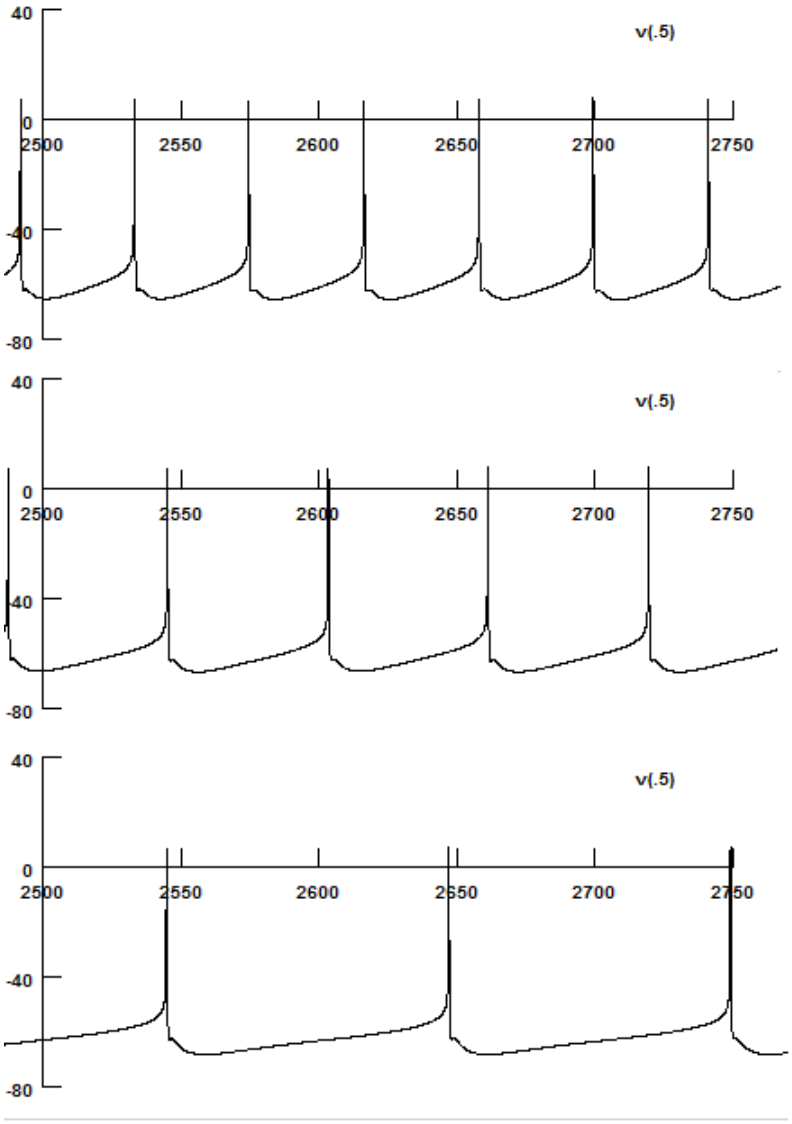

Figure 3.11: Comparison of Current Injection Bias Effect on MVNB Spontaneous Discharge Rate. Voltage traces of Model MVNB neurons receiving the depolarising and hyper-polarising current inject used as a bias to simulate firing rate heterogeneity. Top trace shows depolarising current of 50pA (0.05nA), middle trace shows no current, bottom trace shows hyper-polarising current of -50pA.

For our simulations, the relationship between amplitude of current injection and spontaneous firing rate was found, such a population of neurons could be simulated, with a chosen distribution of firing rates, and the required current required to the individual members of the population. Figure 3.12 shows the distribution of firing rates of a population of neurons with rates chosen from a normal (or gaussian) distribution (mean = 1, variance = 0.02778) using this bias current

injection method. This population was found to be normally distributed (Chi square goodness of fit test p = 0.0626) around a mean of 20.881Hz.

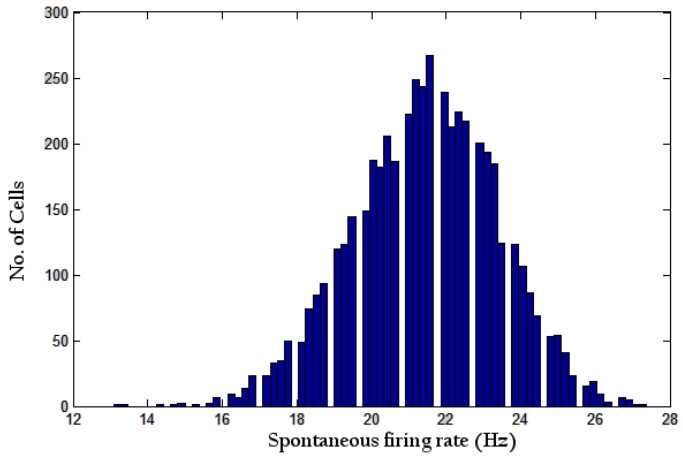

Figure 3.12: Actual Firing Rate Histogram of MVNB Population with rates chosen from Normal or Gaussian distribution, mean = 1, var = 0.02778, using the bias current injection method. This population is normally distributed, around the mean rate of 20.881Hz

3.2.1.2 *Conductance Manipulation*

As previously discussed, manipulation the slow Potassium conductance (K-Slow) effects the spontaneous firing rate of the neuron model. Increasing the density of the conductance, in both the Soma and Proximal dendrite compartments, decreases the spontaneous firing rate, while decreasing the conductance density increases spontaneous activity. Firing rate diversity of a population can effectively be modelled as diversity in these conductance densities.

Prior to actual experimental simulations, the exact relationship between the density of the K-Slow conductance and the resting/spontaneous discharge rate of the model was determined, such that the density of K-Slow conductances (in both the Soma and Proximal dendrite compartments of the model neuron), for a chosen resting discharge rate (for an individual member of the population of simulated neurons), can be determined. That is, as we are seeking to investigate the implications of MVN neuron population heterogeneity (in the form of a diverse spontaneous discharge rates across the population, with that diversity arising from K-Slow conductance heterogeneity), it is necessary for the relation between density of the K-Slow conductances of the models, and the spontaneous discharge rate to be determined. Once this relationship was known, the required density of K-Slow conductances (in both the Soma and Proximal dendrite compartments of the model) could be derived, in order to produce the required spontaneous

discharge rate for that member of the population. This relationship is shown in Figure 3.13, for both Soma and Proximal dendrite compartments.

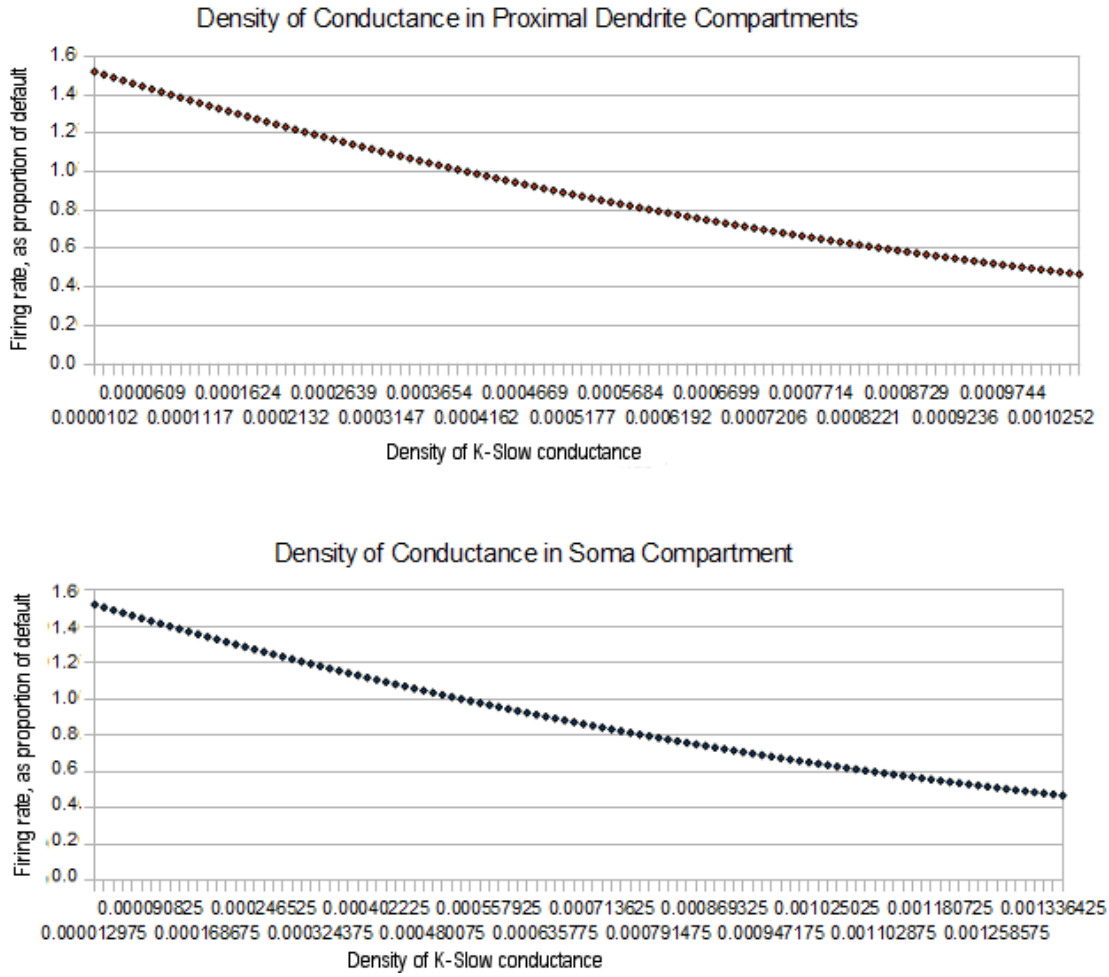

Figure 3.13: Relation between K-Slow Density and Spontaneous Discharge in MVN Type B Neuron Models. Density of K-Slow conductance, in Proximal Dendrite (top) and Soma (bottom) compartments, increases from left to right. Spontaneous discharge of the model is shown as a proportion of the default rate of discharge.

This data was obtained through manipulating the density of the K-Slow conductances for a number (104) of small populations of neurons (n=10), multiplying this density by factors between 0.025 and 2.6, the same factor being used to alter the Soma K-Slow density and the Proximal dendrite K-Slow density. This produced a range of populations with average firing rates (derived from their average instantaneous frequencies over 3 seconds of simulation, after 1.2 seconds settling, to forget initial conditions, and a further 3 seconds of simulation with inputs) between 10 and 33Hz (MVNB default spontaneous rate of fire = 20.904Hz).

From this data[5] it was found that the relationship between Density of K-Slow conductances and discharge rate could be expressed through the following equation: **Channel Density = (log(Firing Rate/a))/b**. For values of a and b listed in Table 3.1, for both Soma and Proximal Dendrite compartments. This equation could then be used to determine the required channel density, for both the Soma and the Proximal dendrites, for a given firing rate. That is, prior to simulation, each member of the population can be assigned a firing rate (for example, from a normal distribution) which can be used in the equation to determine the required densities of the K-Slow conductance in both proximal dendrite and Soma compartments, which can then be set in the model prior to simulation. There was a negligible error in the equation and procedure, in that actual spontaneous firing rate differed from the chosen rate by up to 1% due to the minor deviation from a perfect exponential relationship.

Compartment	a	b
Soma	1.56951	-884.46640
Prox. Dendrite	1.56957	-1130.68968

Table 3.1: Channel Density of K-Slow Equation Values. Values for a and b used to determine channel density required to produce a given spontaneous discharge rate.

Simulating a population (n=5000) of MVNB neurons with firing rates chosen from a normal distribution (mean = 1, variance = 0.02778) produces the distribution of firing rates shown in Figure 3.14. This distribution is indeed normally distributed (Chi square goodness of fit test p = 0.074) around a mean of 21.059Hz, as expected, confirming the validity of the rate/density procedure, Again, 1.2 seconds of delay was allowed before the data used to obtain this distribution was collected. This delay was used across all simulations using this method of conductance manipulation.

5 Using Least Squares method of Exponential regression

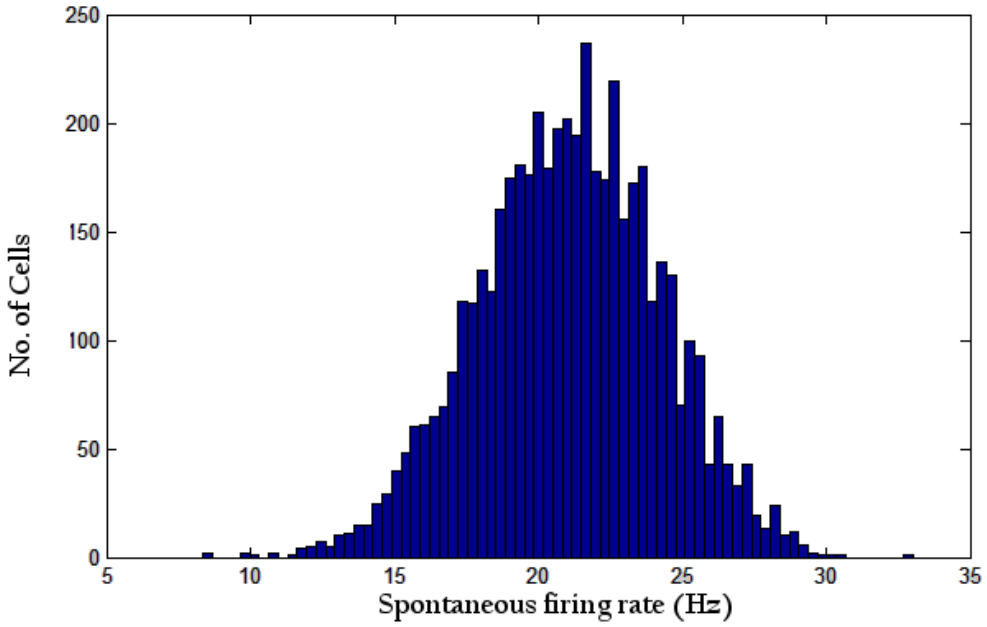

Figure 3.14: Actual Firing Rate Histogram of MVNB Population with rates chosen from Normal distribution, mean = 1, var = 0.02778 using the K-Slow manipulation method. This population is normally distributed, around the mean rate of 21.059Hz

3.2.2 *Input Simulation*

Input for our simulated populations took the form of sinusoidal waves of frequencies 8Hz, 12Hz, 16Hz, and 20Hz, matching the 'medium' to 'high' range of frequencies seen in the real VOR and Vestibular system [98]. In addition, as single neurons of the MVN involved in the VOR display only a limited range of frequencies for which their response is linear, and follows the input faithfully (up to 10Hz) [68] [89], this range of frequencies would allow us to investigate the ability of a population response (through the population's rate encoding of the inputs) for the VOR's high frequency response range. Use of sinusoidal abstractions for the input to Vestibular nucleus neurons is common throughout the literature [68] [114].

3.2.2.1 *Input through Current Injection*

The initial method of input simulation was the use of current injection. Input to the cells was approximated as a sinusoidal wave of one of the given experimental target frequencies (8Hz, 12Hz, 16Hz & 20Hz), and simulated as direct current, injected into the Soma of the model cell,

using a modified form of the NEURON simulation environment's Current Clamp point process (with the current injected following the required sinusoidal wave).

This method of input allowed us to easily control the mean and amplitude of the current injected into the cell, as well as allowing us provide independent noise to the input of each member of the population. That is, although the common input was identical across the population (as the current from each individual point process was identical across the population, as it followed the same equation), it was produced by individual processes attached to individual cells which could be modified, through the addition of Gaussian noise, across the population. This noise could be controlled (across the population as a whole or for individual members) in regards to its mean, amplitude and time constant. The NEURON simulation environment's Event delivery system was used to control the time constant of the noise, and ensure this did indeed remain constant.

Increased amplitude of the input signal represents an increased velocity of the movements being compensated for in the model VOR.

3.2.2.2 *Synaptic Spike Train Input*

The second method of input was through the use of simulated exponential synapses, producing excitatory input to the cells, following pre-generated spike trains. Excitatory, exponential synapses were distributed uniformly across the model cell's dendritic structure (Proximal and Distal dendrite compartments), with their excitatory events following pre-generated spike times produced to approximate a distributed sinusoidal input. That is, each model synapse produced excitatory inputs to the cell following separate spike trains, each synapse being assigned a spike train prior to simulation, from a large set of pre-generated spike trains. Thus, the input provided and the timing of the excitatory input events was not identical across the synapses of an individual cell, or across the population of cells as a whole. The distribution of synapses could be controlled in regards to their number and the weight of their excitatory conductances.

The synapse type used was the NEURON environment's Exp2Syn object, a 2 state kinetic scheme synapse described by a rise time (0.5ms), and decay time constant (3ms), which produces a synaptic current with an alpha function like conductance. These were activated by 'events' delivered through the NEURON environment's NetCon object, which was driven by pre-generated spike trains. That is, each synapse was activated at event times supplied by the NetCon object, and each NetCon object was provided with times from individual pre-generated trains read in to

the object prior to simulation beginning. Each Synapse was provided a random train chosen from a set shared across the population.

The spike trains provided to the populations were produced through a poisson process, using a thinning algorithm to give the exact spike times (were random spike times are produced, and discarded if they do not match the required frequency of the spike train at that time, to produce the required spike trains, and kept if they do match the required frequency closely enough). This process produced imhomogeneous poisson distributed spike trains, approximating the distributed input signal produced by Vestibular afferents, following a sine wave of one of the experimental target frequencies. These spike trains could be controlled in regards to their mean frequency, amplitude, as well as the inclusion of a refractory period, thus allowing us to pre-generate a range of spike train sets to investigate the effect of these factors on the population output, along with factors such as the number of synapses and their relative weight.

Figures 3.15, and 3.16 show the characteristics of the 3 spike train parameters used, at 8Hz and 16Hz, to demonstrate the process which the spike trains follow. Spike train inputs oscillate in the frequency of their spikes[6], by a given amplitude and around a given mean, with the oscillation following the target frequency of the input (the frequencies we expect our simulated populations to follow). Input train set A01 has a mean of 50Hz, and amplitude of 25Hz, thus simulating a Vestibular afferent population providing input at a mean rate of 50 spikes per second, and an amplitude of 25 spikes per second (50+/-25). Input A02 has a mean of 75Hz and amplitude of 25Hz (75+/-25). Input A03 a mean of 35Hz and amplitude of 20Hz (35+/-20). These distributions were chosen to roughly approximate those seen in the literature [82]. Differences in the mean and amplitude of these input spike trains represent differences in the velocity of the rotations being compensated for in our model VOR response, with increases in mean/amplitude representing an increased velocity of rotation.

6 Not to be confused with the Target frequency at which the spike trains oscillate

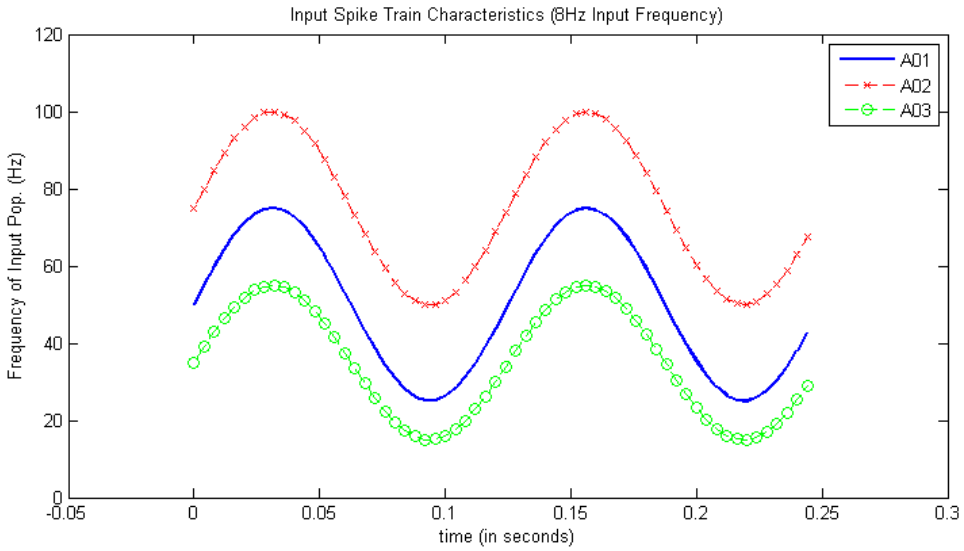

Figure 3.15: Input Train Characteristics for 8Hz Target Frequency. A01 had a mean frequency of 50Hz and and amplitude of 25Hz. A02 75 +/-25. A03 35 +/-20

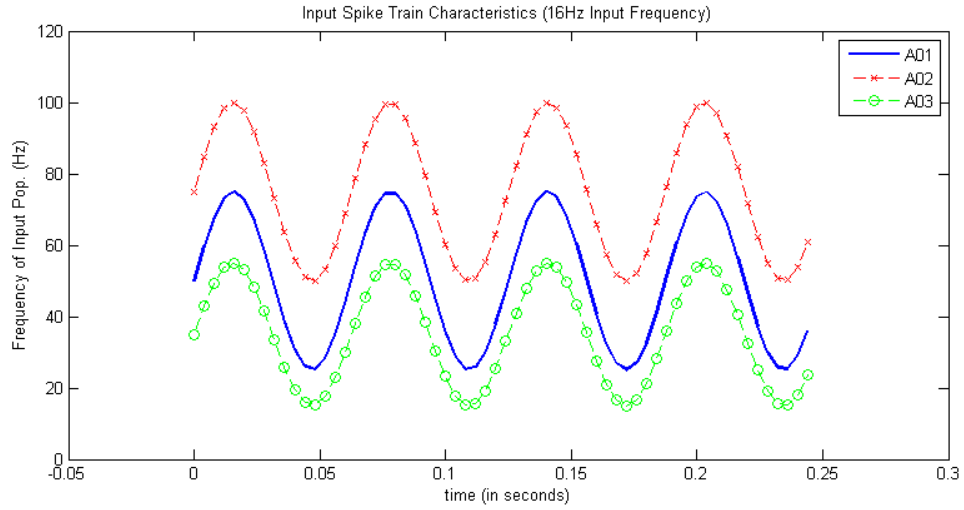

Figure 3.16: Input Train Characteristics 8Hz. Means and amplitudes are the same for those of the 8Hz trains.

These input sets (A01, A02, A03) were generated for all 4 target frequencies (8Hz, 12Hz, 16Hz, 20Hz). Spike train sets were generated using MATLAB.

3.3 IMPLEMENTATION OF MODELS AND PARALLEL SIMULATIONS

The models used in this study are implemented in the NEURON simulation environment, from the data previously published by Quadroni and Knopfel[7]. These models were implemented in the

7 Implemented by Tom Morse at Yale.Edu.

NEURON environment and were available through the SenseLab Model Database. The models used in the current work were largely unchanged from this model, aside from the inclusion of a 'dummy' current in certain of the mechanisms used, in order to avoid problems with numerical integration that were encountered early in the work.

We also make use of NEURON's inbuilt parallel functions to implement a parallelised Bulletin-Board (or BlackBoard) system (BBS). This BBS can be seen as analogous to the LINDA model of coordination and communication. This allowed the efficient and (relatively) speedy simulation of the large number of populations simulated, as well as the large number of conditions modelled, used both for testing and for the results presented.

LINDA is a coordination language, a model of coordination and communication among several parallel processes, that implements the 'tuple space' paradigm [18] [19]. In turn the 'tuple space' paradigm is an implementation of the associative memory paradigm for parallel or distributed processing [18] [19]. Essentially, it's a simple model for the implementation of trivial or embarrassingly parallel problems, ideal for our work as there is no dependency between the parallel tasks performed in our simulations.

The LINDA coordination language embodies the 'tuple space' model of parallel programming, consisting of a small number of operations for interaction with the tuple space, and a shared memory that composes the tuple space [19]. The LINDA system differs from other parallel approaches, and bears little resemblance to models which deal with message-passing, concurrent logic or concurrent object orientation [19]. In addition, it is a much simpler language/implementation than many others available [18] which has always contributed to its attractiveness [133], in addition to its orthogonality [19].

The LINDA system is based on generative communication – processes communicate with each other through the creation of data objects (tuples) by the data producing process, which are added to tuple space and then accessed by the receiver process [19]. Similarly, to create new processes, a currently running process (that requires some concurrent process) adds a 'live tuple' to tuple space, which will, in turn, spawn the new process.

Originally LINDA was intended for the implementation of BlackBoard systems (where tuple space is iteratively updated by a collection of diverse specialist knowledge sources, or experts, starting with a problem specification and ending with a solution, with each host updating with partial solutions) [18] [19]. However, our implementation would be better described as a

BulletinBoard system, as we do not implement a diverse collection of experts, and are not working through from specification to solution with partial solutions.

Our implementation involved each host that is being used being implemented with the necessary context to run a simulation with the required model (for the given stage of simulations). At initialisation, the BulletinBoard or tuple space is populated with calls to run a simulation, equal in number to the number of simulations required in the batch and containing any required parameters (such as seeds for random streams, initial voltage, spontaneous discharge rates). While there are still calls for simulations to be run, a host (if not already running a simulation) will remove a call from the tuple space and begin execution of that simulation, with its specific parameters. When a simulation is completed, the host 'packs' the results, and adds a new object to tuple space, signifying the results and a call to collect and collate these. This second task (collection of data) is special, in that it can only be executed by hosto, and only when it is not currently running a simulation. What this means is, at initialisation, tasks are added to the BulletinBoard, and then removed and executed by the hosts. When a simulation completes, a host returns the output data to the tuple space, and then removes another task, and continues with simulation. Whenever hosto finishes a simulation, it checks the tuple space for data that is ready to be collected, collects it if available, and then, if no more data is ready for collection, chooses another simulation task, and continues with simulation. When there are no tasks left to be completed (either simulations, or data collection), the final data set is organised and written to a file, and the batch is completed.

This separation, or disconnection, between data submission and data collection (with data being submitted to tuple space, rather than to a host) allows hosts to continue with simulation very shortly after completion of a previous task, rather than having hosts wait to submit data to hosto (or any other central or specific host). That is, our hosts do not have to wait to submit their data after a completed simulation, which could lead to inefficiency and wasted time (as hosts would not be executing simulations while waiting to submit data), and can instead begin with a new simulation, while data waits in tuple space to be collected.

From this, it can be seen that our implementation is still, technically, an implementation of a BlackBoard system – the specification added to the tuple space at initialisation is to complete a simulation, which involves running the simulation (part1) and collection of data (part2), so we can still see that running of the simulation is partial completion, and adding data to tuple space is still submission of a partial solution. However, as our implementation lacks a truly diverse

collection of "experts", with hosto the only real expert (all hosts run simulations, hosto is an 'expert' in that it is the only host to collect and collate data). Further, our task cannot really be seen as a collection of partial solutions making up a complete solution, as the only substantial part of the solution is the simulation itself.

3.4 ANALYSIS METHODS

Before we present results, the methods used for analysing the output of the simulations are presented.

3.4.1 *Response Fidelity Measure*

Response fidelity is measured as 1 - the mean difference of the normalised population Peri-Stimulus Time Histogram (PSTH) with the corresponding input histogram. For each member of the population, the output spike train was 'binned' into fixed width bins (5ms) over the simulation duration (ignoring the initial settling period were input was not provided, and the population was allowed to forget initial conditions), with each spike being added to the corresponding bin. Thus, iterating over all members of the population, the population's PSTH is produced, showing the relative intensity of population spike activity for each bin interval. This was then normalised through the use of standardised Z-scores, such that the output response is centred to have a mean of 0, and is scaled to have a standard deviation of 1. Similarly, a set of input bins was also produced, at the corresponding input frequency, and standardised in the same way as the responses, to be centred around a mean of 0, and have a standard deviation of 1.

The response fidelity score, for a population, was taken to be equal to 1 minus the mean of the square-roots of the squares of (or absolute difference between) the input bins minus the corresponding output bins. Or, rather, 1 minus the mean error between input and output signals, over the simulation period, with a score of 1 being a perfect match between input and output bins. In this way, we essentially calculate the Pearson Correlation of the Output produced to the Input provided.

This population measure is considered accurate and appropriate for the VOR pathway, as there are no further inter-neuron layers, and so no complex population codes need be encoded [68]. The 5ms bin interval was chosen to reflect typical post-synaptic integration time. The final response fidelity measure was taken to be the mean of the response fidelity of 10 populations.

Example Peri-Stimulus Time Histograms are shown in Figure 3.17. These show the population activity of MVNB neurons receiving an 8Hz signal through synaptic input, with heterogeneity modelled through the K-Slow conductance manipulation method.

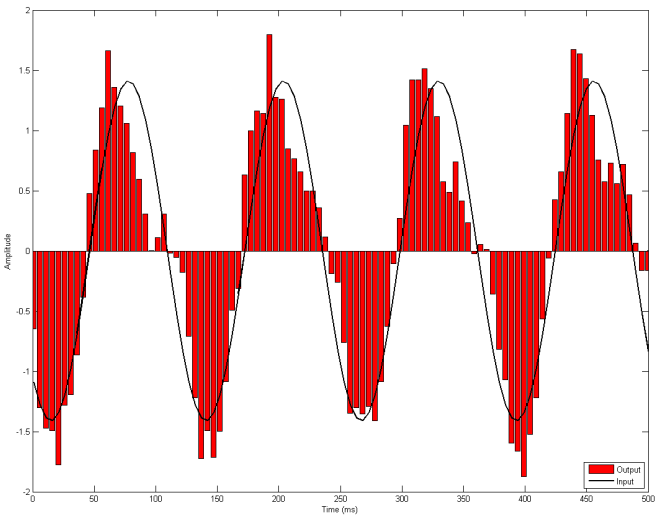

Figure 3.17: Example Peri-Stimulus Time Histogram. Taken from a Heterogeneous population, distributed normally, using the K-Slow conductance manipulation method, receiving an 8Hz current injection input with no noise.

3.4.2 *Measure of Output Frequency Components*

An alternative measure of the sinusoidal signals used for the current work was also implemented, in order to evaluate results in situations were the output signal is out of phase (or has a distorted gain) compared with the input signal. For this measure, a Discrete Fourier Transform (DFT) was performed (sampling frequency = 200Hz, corresponding to bin size chosen for the PSTH from which the output signal is taken) on the output signal of a number of populations, and the (single sided) amplitude spectrum of the output was produced. From this was found the relative amplitude of the population's response to the frequency of the input, along with a visualisation of the other component frequencies. That is, for an 8Hz input signal, we take the amplitude of the output's response for the 8Hz frequency component, and it's amplitude relative to other frequencies present in the output. Figures 3.18 and 3.19 show examples of the obtained amplitude spectrum for populations responding to 8 and 20Hz inputs.

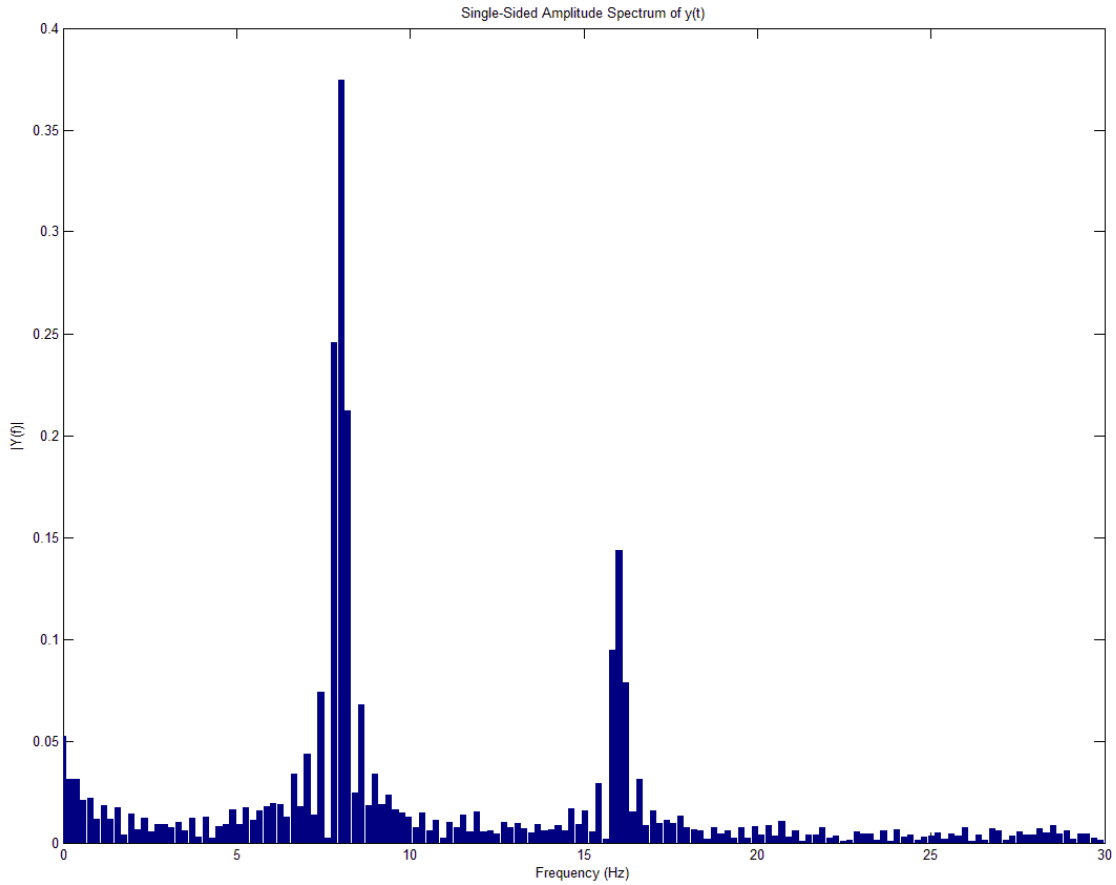

Figure 3.18: Example Amplitude Spectrum of Output to 8Hz Frequency Input. Shows the amplitude of the frequency components of an output signal generated from an 8Hz input. Note the peaks at 8Hz and the harmonic 16Hz. The amplitude value at this target/input frequency is the value we take from this analysis.

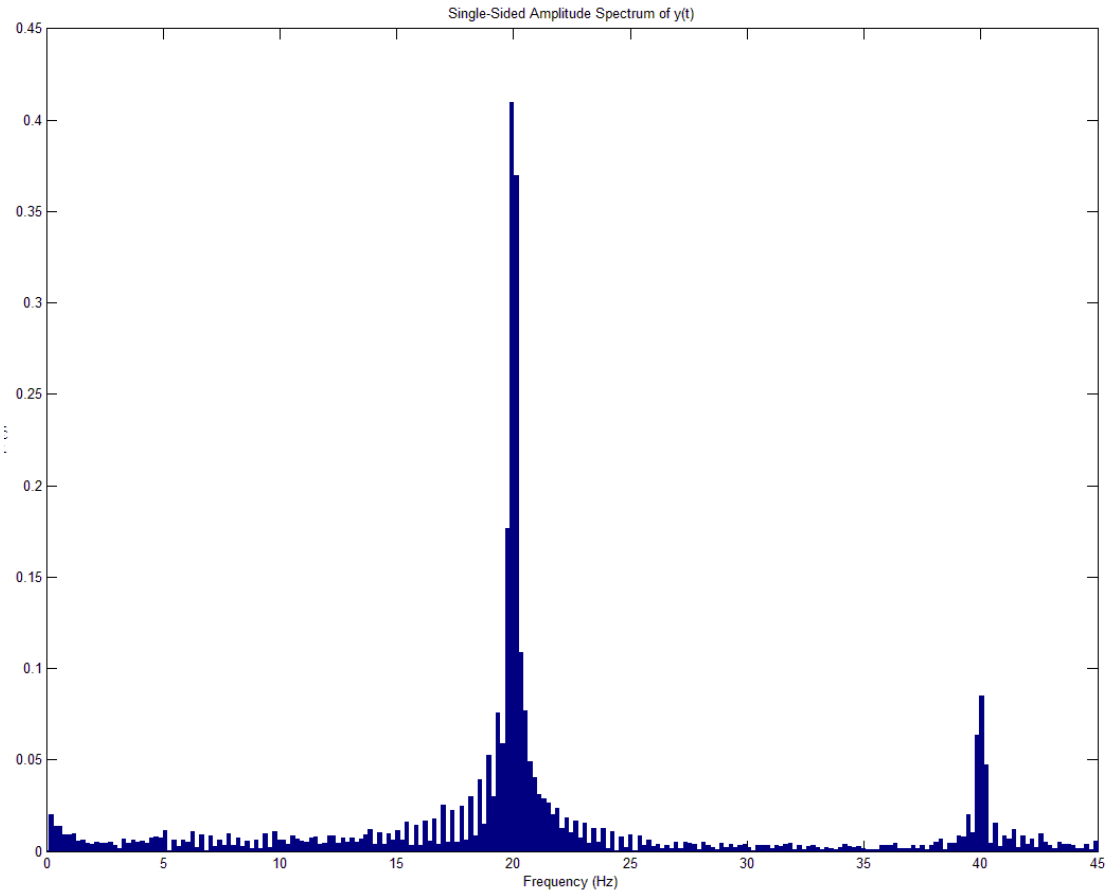

Figure 3.19: Example Amplitude Spectrum of Output to 20Hz Frequency Input. Shows the amplitude of the frequency components of an output signal generated from an 20Hz input. Note the peaks at 20Hz and the harmonic 40Hz. The amplitude value at this target/input frequency is the value we take from this analysis.

We take the amplitude of the input frequency component of the output signal. This measure allows us to obtain a reasonable value (the amplitude of the output's frequency component, corresponding to the input frequency) for comparison of responses when the output is significantly out of phase to the input, as well as providing an additional measure of performance for situations where no phase difference is found between input and output.

Essentially, this method converts the output of the population from the time domain, to the frequency domain, providing information on the periodicity of the output, and the relative strength of the target frequency (i.e., the frequency of the input signal that we wish the population to match) in the population's output. This method is similar to a method suggested for improved response estimation using digital filtering techniques [22].

4

RESULTS

4.1 INTRODUCTION

In this Chapter we present the results of three stages of simulation, using the different methods for input generation and simulating population heterogeneity as outlined in the previous Chapter (Chapter 3, Section 3.2). In the first stage of simulations, inputs to the populations were simulated as current injection to the cell model Soma, and heterogeneity was simulated through the introduction of a bias current into the Soma. In the second stage of simulation, population heterogeneity was modelled through the variance of density of the Calcium activated Potassium channels (K-Slow) present in the Soma and Proximal Dendrites. Input was simulated via current injection for this stage. In the third and final stage, heterogeneity was modelled through the manipulation of K-Slow conductance densities, and input was simulated through the delivery of excitatory synaptic events, following pre-generated spike trains.

In addition, at initialisation each member of the population was given an initial membrane potential from a normal distribution of mean -65 millivolts (mV) (normal resting potential of the model) and a variance of 10mV, such that population members did not begin perfectly in phase with each other. In order to allow the population to settle into this initial condition, along with the other conditions altering the simulation, a period of time at the start of each simulation was provided (based on the length of time required for a model to produce stable ISIs).

In all cases, results were obtained using the NEURON Simulation environment[1] running under UNIX, utilising Parallel NEURON through the Message Passing Interface (MPI) to permit the parallel processing of simulations. Simulations were performed on both the Stirling University Division of Computing Science and Mathematics cluster, and the EPSRC funded 'ARCHIE-WeSt' High Performance Computer.

All simulations were performed using a constant time step method, with a time constant of 0.01 milliseconds, such that there were 100 time steps per millisecond (dT = 0.01, steps per ms = 1/dT). Output generated was the spike times of each member of the population.

1 Versions 7.1, 7.2, & 7.3

Simulations for stage 1 involved inputs modelled as direct current injection of a sinusoid signal at the frequencies 8, 12, 16, and 20Hz, into the Soma of our cell models. That is, input was approximated and simulated as a direct current injection of a sinusoidal wave at one of the given experimental frequencies. Current injection had a mean of 0, and an amplitude of 50pA (picoamps). Noise (in the inputs) was modelled as Gaussian white noise added to the current injection, with a mean of 0, a variance of 60pA, and a time constant of 2ms, matching that used in prior modelling studies of implications of noise in MVN neuron response fidelity [68].

Population heterogeneity was modelled as a bias current, injected into the Soma of our model cells. At this stage, for each member of a heterogeneous population, a firing rate was chosen, from a normal distribution of mean 1, and variance of 0.02778. These values gave us (using the 3 Sigma, or 68-95-99.7 rule, that states that 99.7% of the values chosen from a normal distribution are within 3*Sigma, or square root of the variance, from the mean, or 3 standard deviations from the mean) a normal distribution of biases, (between -50pA and 50pA), values which produce firing rates equal to 0.5* and 1.5* the standard spontaneous firing rate (20.904Hz) of the MVNB models. Thus, heterogeneous populations in this stage had a normally distributed spontaneous firing rate (largely) between 11hz and 33hz, and a mean of 20.881hz (as previously illustrated in Section 3.2.1. This distribution was chosen to approximate the distribution of real MVNB neuron firing rates in electrophysiological studies [77]).

Our 4 experimental conditions for this stage, therefore, were: m0 = Homogeneous population (no bias) & clean input (no noise added); m1 = Homogeneous population & Noisy input; m2 = Heterogeneous population & clean input; and m3 = Heterogeneous population & Noisy input. These conditions were simulated with input signals at each of the 4 input frequencies (8, 12, 16, 20Hz). Figure 4.1 shows the overall setup for this stage of simulations. Noise and bias, applied to the common input signal each cell receives, were optional, depending on the model being simulated.

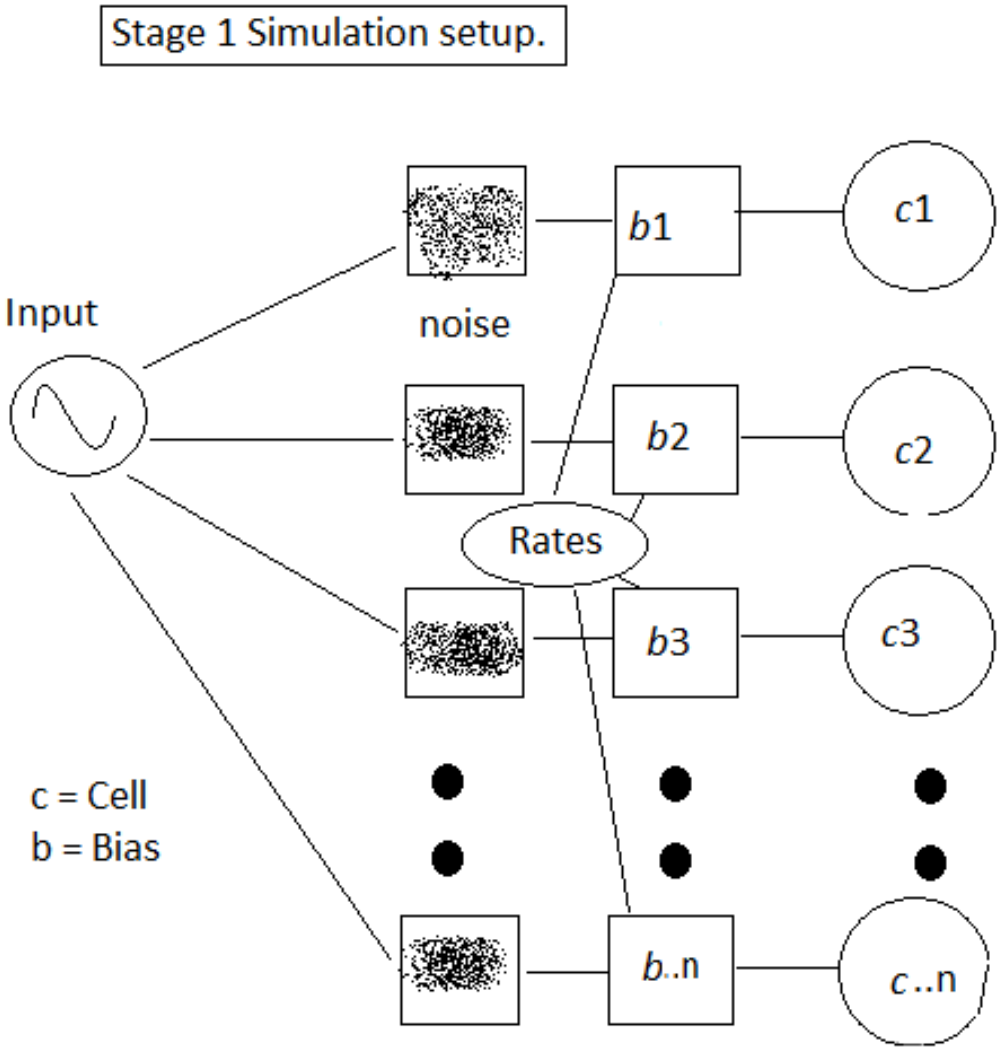

Figure 4.1: Stage 1 Simulation Setup. Common input, in the form of a current injection sinusoidal wave of a given frequency, is provided to each cell of population. Independent noise and bias current (b) was added to the signal, with the bias chosen from the rate distribution, and noise following a time constant of 2ms.

For all conditions and input frequencies, 10 populations of 500 neurons were simulated, thus allowing us to take the mean of the response fidelity of 10 populations for each of the conditions (populations of n=500 were chosen in order to replicate the population sizes used in previous work looking at Heterogeneity in the VOR[68]). The initial delay (prior to current injection input began, but not bias injection[2]) was 500ms, and the stimulation time of the simulations was 3000ms (we therefore simulate 3.5 seconds of activity, but ignore the initial 500ms for analysis purposes).

2 We wish for the model to 'settle in' to the bias current, and for it to achieve stable ISIs at the expected spontaneous firing rate

Figure 4.2 shows the response fidelity scores (mean of 10 populations response fidelity scores) for all 4 experimental conditions, at all 4 input frequencies.

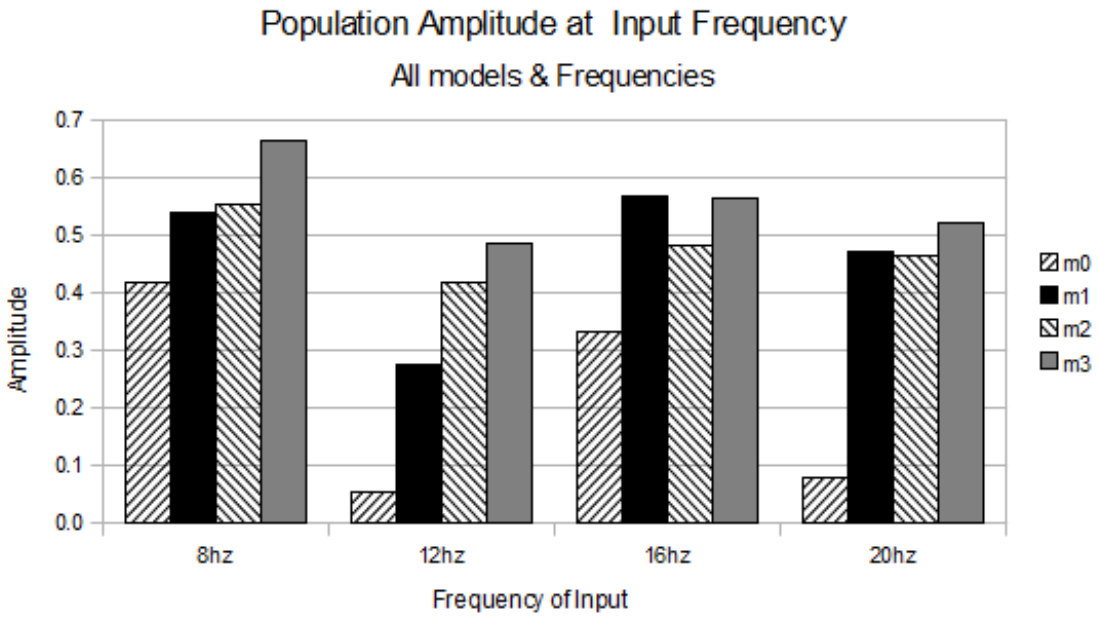

Figure 4.2: Stage 1 Response Fidelity Scores for all experimental conditions, and all input frequencies. mo = Homogeneous population & Clean input, m1 = Homogeneous population & Noisy input, m2 = Heterogeneous population & Clean Input, m3 = Heterogeneous population & Noisy input. Response fidelity is the mean of the fidelity scores of 10 population's responses. Variance was extremely minor (<0.002) and so is not shown in figure

Models m1, m2, and m3 all perform significantly better than model mo. That is, there is a significant increase in response fidelity scores for noisy, heterogeneous, and combined populations, for all input frequencies ($p<0.005$, two-tailed t-test, equal variance assumed).

Population heterogeneity alone (m2) performed significantly better than noisy input alone (m1) for the 8 and 12Hz frequencies ($p<0.05$), but performed significantly worse than the noisy condition at 16Hz ($p<0.05$), and slightly worse at 20Hz (not significantly so, $p = 0.06$).

The combined heterogeneous and noisy condition (m3) performed significantly better ($p<0.05$) than noise alone (m1) for all input frequencies other than 16Hz, at which the homogeneous population with noisy inputs performed significantly better ($p<0.05$). Combining heterogeneity and noise improved response fidelity significantly ($p« 0.05$) over heterogeneity alone for all frequencies.

Figure 4.3 shows the amplitude of the input frequency component of the output, taken from the FFT spectral analysis. From these values, we can see that the amplitude of the target frequency

component, in the output signal, is improved over homogeneous populations by the inclusion of noise, heterogeneity, and combined noise & heterogeneity for all frequencies.

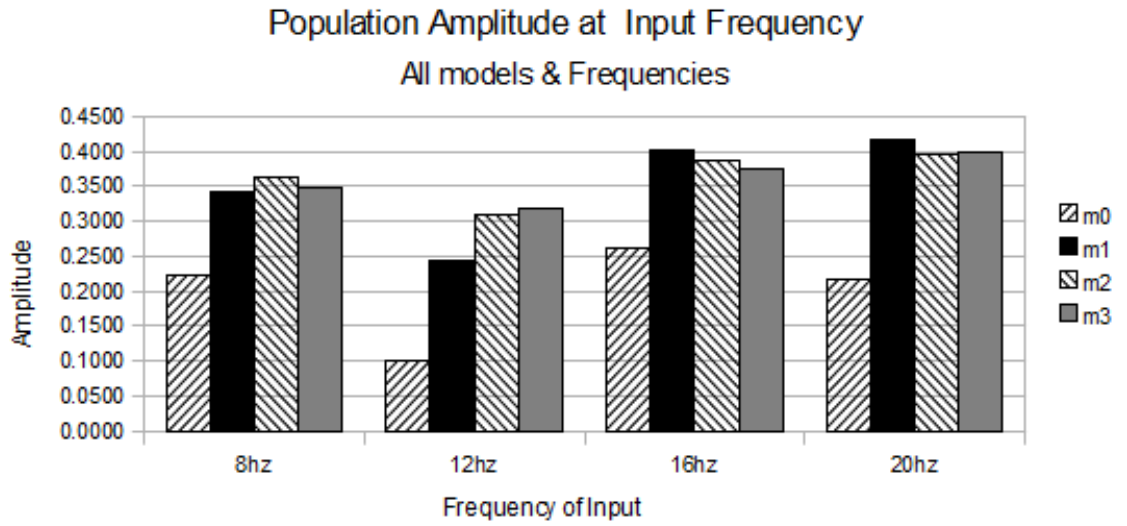

Figure 4.3: Input Component Frequency Values of Output Signals, for all conditions of stage 1. Shows the amplitude of the target frequency (8, 12, 16, or 20Hz) component of the average of the output of 10 population. m0 = Homogeneous population & Clean input, m1 = Homogeneous population & Noisy input, m2 = Heterogeneous population & Clean Input, m3 = Heterogeneous population & Noisy input.

To summarise these results, response fidelity scores show a significant improvement when variation, either as noisy inputs or population heterogeneity, are included in the population simulations. Generally, heterogeneity alone improves response fidelity more significantly than noise alone, while combining the two generally improves response fidelity further. The input frequency component of the population output is improved for all forms of variance, for all frequencies other than 8Hz.

Figure 4.4, 4.5, 4.6, and 4.7 show (a section of) the peri-stimulus time histogram of the response of populations for all 4 models used in stage 1, for an 8Hz input.

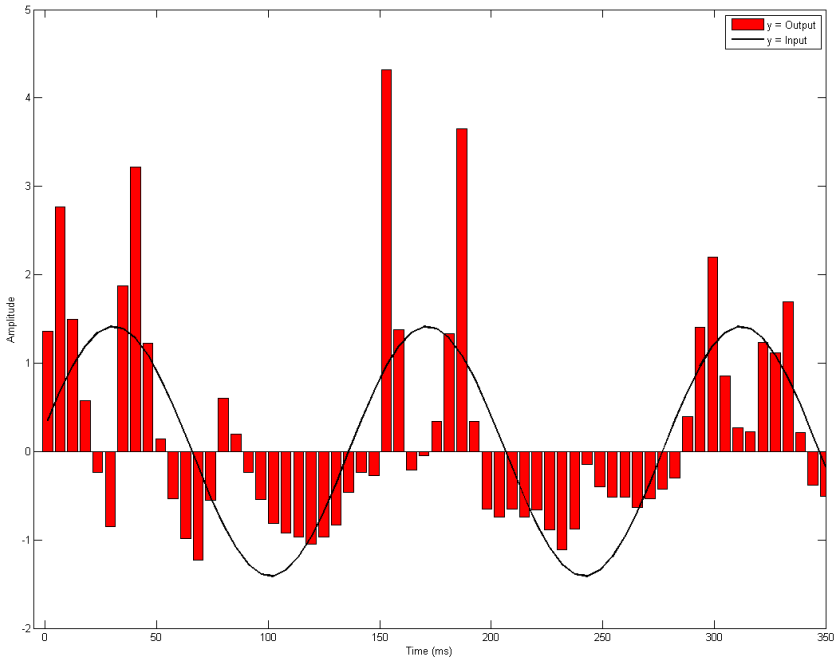

Figure 4.4: Example Peri-Stimulus Time Histogram of Model 0 Response Fidelity. Homogeneous population performance, receiving 8Hz input signal with no noise. Bars represent the amplitude of the population response over time (350ms). The input provided to the population is the line superimposed over the output.

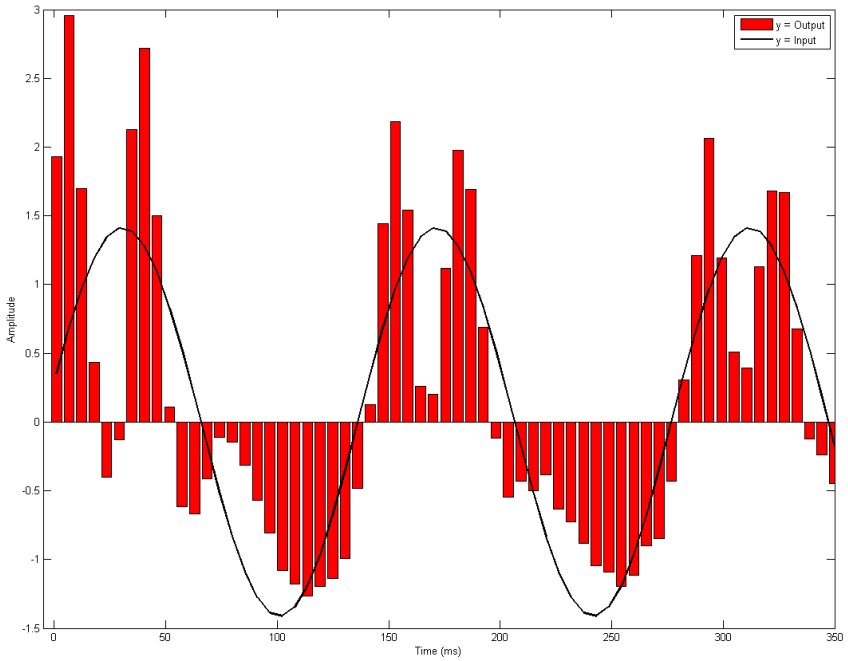

Figure 4.5: Example Peri-Stimulus Time Histogram of Model 1 Response Fidelity. Homogeneous population performance, receiving 8Hz noisy input signal with. Bars represent the amplitude of the population response over time (350ms). The input provided to the population is the line superimposed over the output.

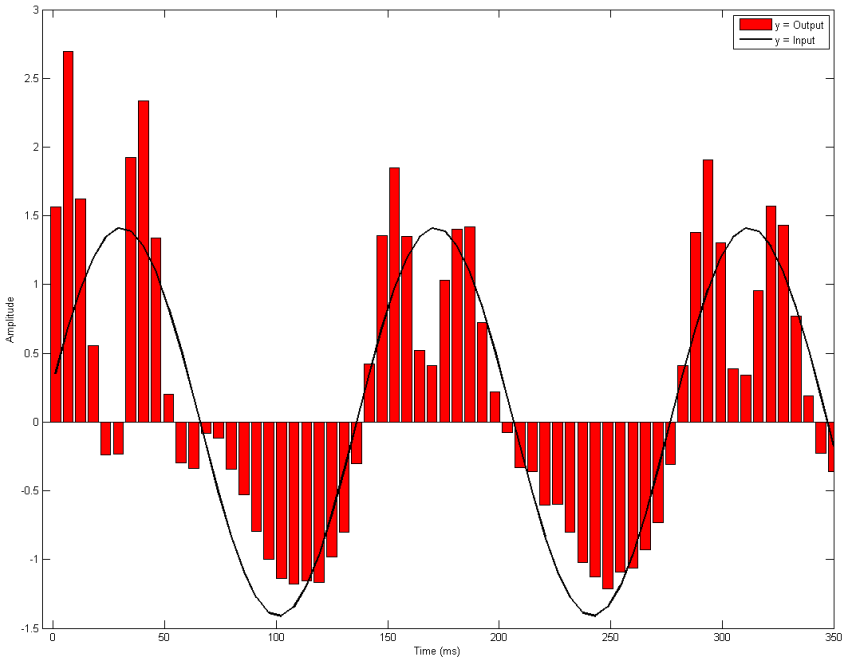

Figure 4.6: Example Peri-Stimulus Time Histogram of Model 2 Response Fidelity. Heterogeneous population performance, receiving 8Hz input signal with no noise.

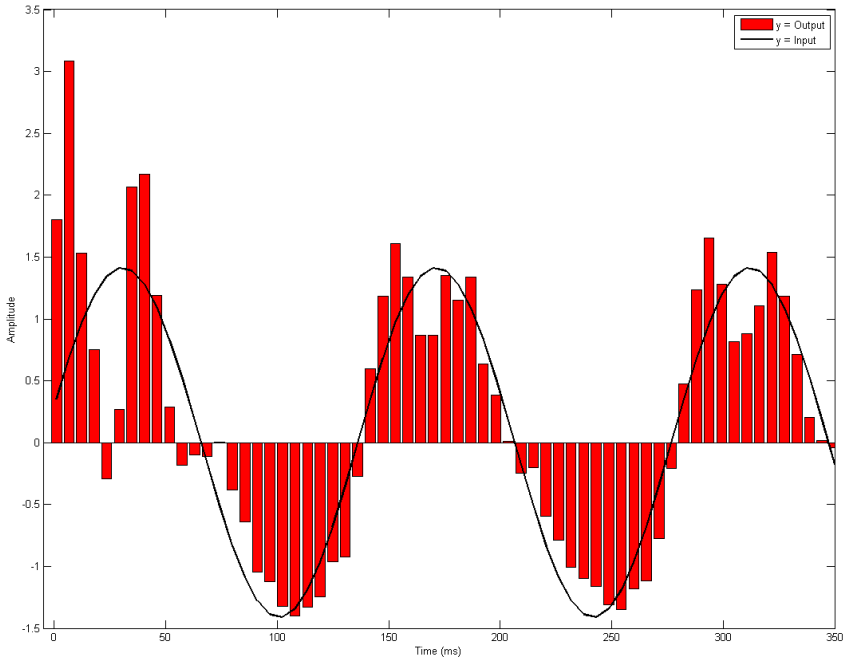

Figure 4.7: Example Peri-Stimulus Time Histogram of Model 3 Response Fidelity. Heterogeneous population performance, receiving 8Hz noisy input signal.

4.3 STAGE 2

In stage 2, the use of a bias current to alter spontaneous firing rate of members of the population was replaced with manipulation of the slowly relaxing voltage activated K^+ (K-Slow) conductance density. Spontaneous firing rate values were chosen from a normal distribution (mean = 0, variance 0.0277) for each population member, the densities of K-Slow required to produce this firing rate were calculated, and these densities were applied to the neuron prior to simulation (as described in Chapter 3, section 3.2.2). Similar to the distribution of firing rates in the previous stage, the values chosen for the normal distribution produced populations with firing rates normally distributed between 0.5 and 1.5* the standard firing rate of the MVNB model (21.059Hz. As already described, populations with this methods were normally distributed around 20.881Hz, largely between 11Hz and 33Hz). This distribution was chosen to approximate the distribution of real MVNB neuron firing rates in electrophysiological studies [77]. No homogeneous populations were simulated at this stage of simulation, and all populations had a normally distributed range of spontaneous firing rates.

Inputs were modelled as direct current injection (as in previous stage). In this stage inputs were simulated at 3 different levels of amplitude and mean. These were: amplitude & mean = 50pA; amplitude & mean = 75pA; amplitude & mean = 100pA. This allows us to evaluate the effect of input strength on the population response fidelity, and other measures. In addition to a clean input condition (m1), two volumes of noise were simulated (variance of 60pA and 20pA) both modelled in the same way as the previous stage of simulations, as Gaussian noise added to the current injection input. Again, as in the previous stage, the Gaussian noise had a time constant of 2ms. Again, inputs were sinusoidal waves at 8, 12, 16 and 20Hz.

Thus, we have 9 conditions in this stage of simulations: 3 input values with different means and amplitudes (50/50, 75/75, 100/100), and 3 models of noise (m1 = no noise, m2 = 'high' noise 60pA variance, m3 = 'low' noise 20pA variance). These 9 conditions were simulated with input frequencies of 8, 12, 16, & 20Hz. Initial delay was set to 1200ms (time required for MVNB model to regain stable ISIs after manipulation of K-Slow density for the range of values possible), and stimulation periods of simulations were 3000ms (total time of 4.2seconds). For all conditions and input frequencies, 10 populations of 500 neurons were simulated. Figure 4.8 shows the overall setup for this stage of simulations. Noise, applied to the common input signal each cell receives, was optional, depending on the model being simulated.

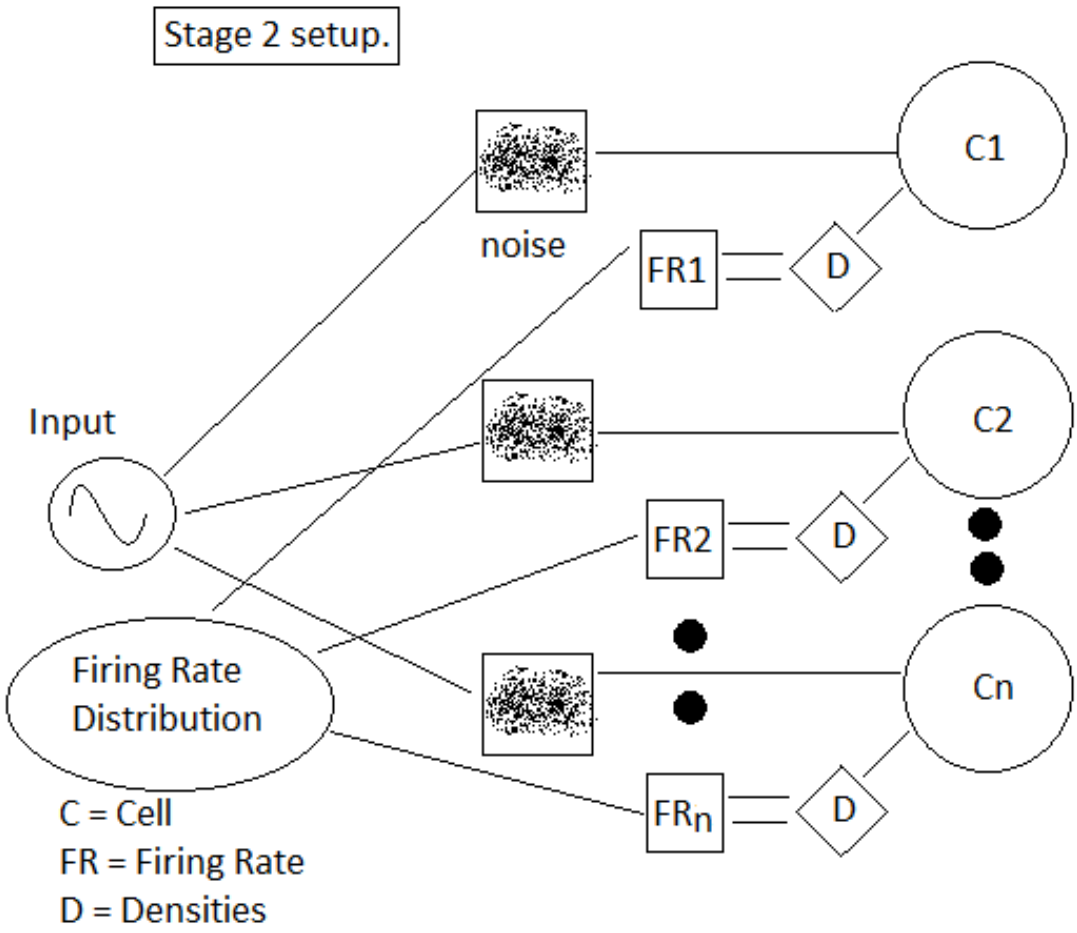

Figure 4.8: Stage 2 Simulation Setup. Common input, in the form of a current injection sinusoidal wave of a given frequency, is provided to each cell of population. Independent noise was added to the signal, following a time constant of 2ms. Firing rates (FR), chosen from a given distribution, were used to determine the required densities of K-Slow conductances (D), which were then applied to the cell, prior to simulation.

Figures 4.9, 4.10, and 4.11 show the effect of noisy inputs on population response fidelity, for all input frequencies and for each of the input amplitude/mean conditions.

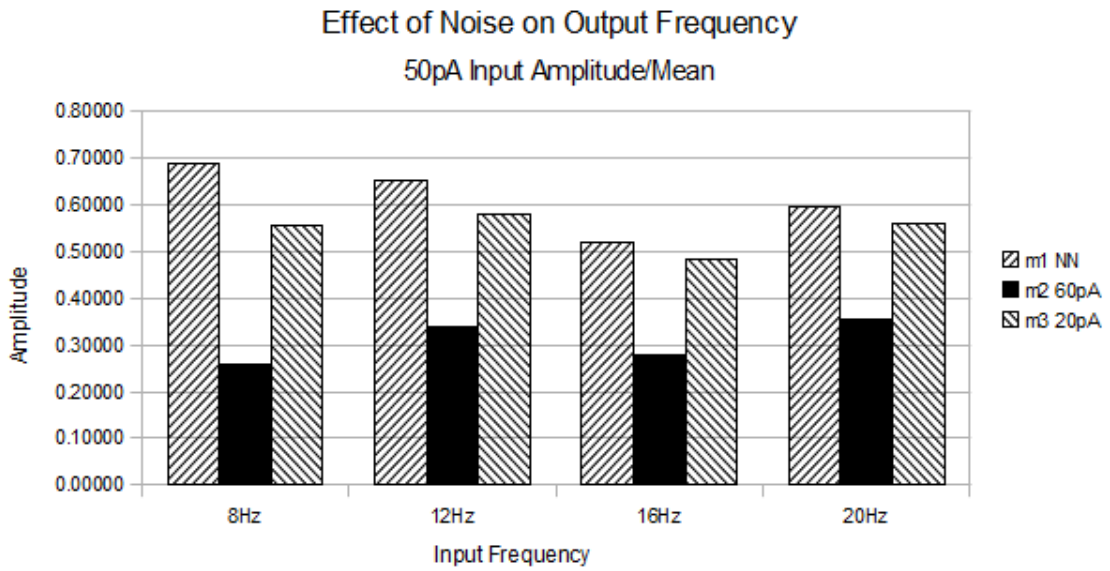

Figure 4.9: Effect of noise on population response fidelity measure, for all input frequencies, and input amplitude of 50pA and mean of 50pA. The low variance (20pA) noise (m3) is on the right of the cluster, the high variance (60pA) noise (m2) are black bars in the middle. Clean input (m1) is on the left. Variance was extremely minor (<0.002) and so is not shown in figure

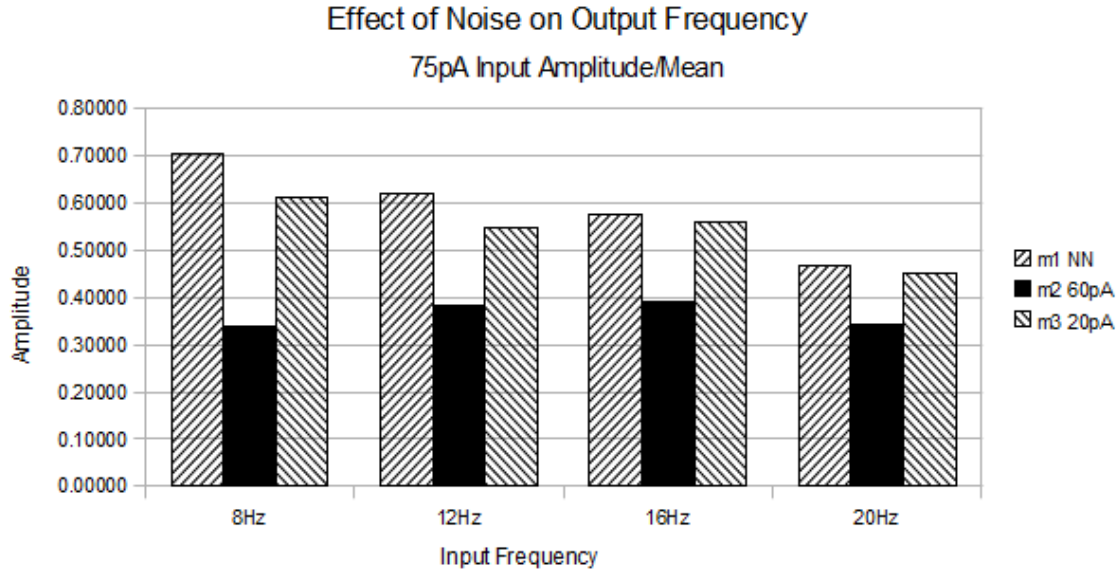

Figure 4.10: Effect of noise on population response fidelity measure, for all input frequencies, and input amplitude of 75pA and mean of 75pA. The low variance (20pA) noise (m3) is on the right of the cluster, the high variance (60pA) noise (m2) are black bars in the middle. Clean input (m1) is on the left. Variance was extremely minor (<0.002) and so is not shown in figure

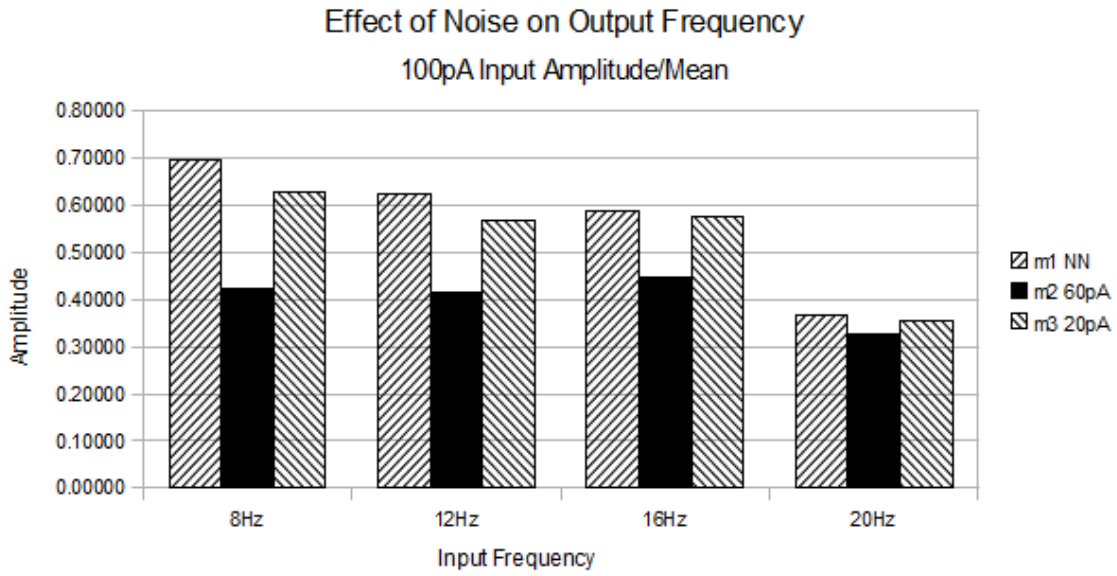

Figure 4.11: Effect of noise on population response fidelity measure, for all input frequencies, and input amplitude of 100pA and mean of 100pA. The low variance (20pA) noise (m3) is on the right of the cluster, the high variance (60pA) noise (m2) are black bars in the middle. Clean input (m1) is on the left. Variance was extremely minor (<0.002) and so is not shown in figure

For all input frequencies and for all input values, noise added to the current injection input had a significant detrimental effect on the population response fidelity measure. That is, the heterogeneous populations receiving clean (no noise) input (m1) performed significantly better for all frequencies, and across all input amplitudes, than both the high and low variance noise models (all $p<0.005$). For 16 and 20Hz input frequencies, the detrimental effect of low volume noise (m3), compared to clean input (m1) was small, but still significant, especially for the 100pA input amplitude and mean conditions (Figure 4.11). Similarly the low variance noise model (m3) performed significantly better than the high variance noise model (m2) for all input parameters and frequencies (all $p<0.005$).

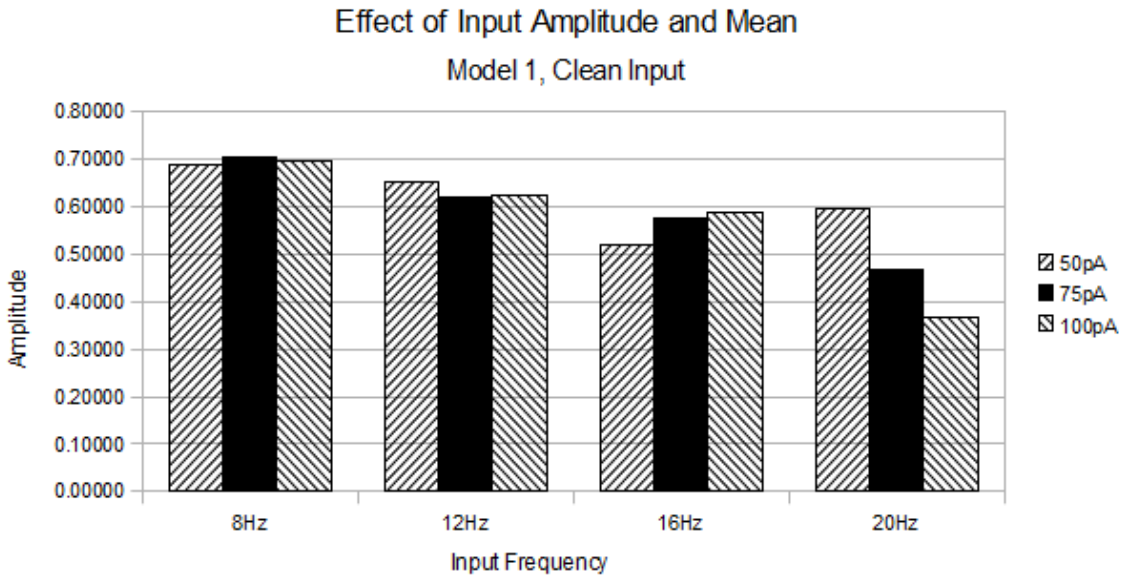

Figure 4.12: Effect of Input Amplitude and Mean on Response Fidelity on model receiving clean input, at all frequencies. Variance was extremely minor (<0.001) and so is not shown in figure

Figure 4.12 shows the effect of the different values of input amplitude and mean on the population response fidelity for heterogeneous populations receiving clean input. Increasing input mean/amplitude, had no significant effect for 8Hz inputs, caused a significant decrease in response fidelity for 12 and 20Hz inputs ($p<0.01$), and caused significant increase in performance for 16Hz ($p<0.01$).

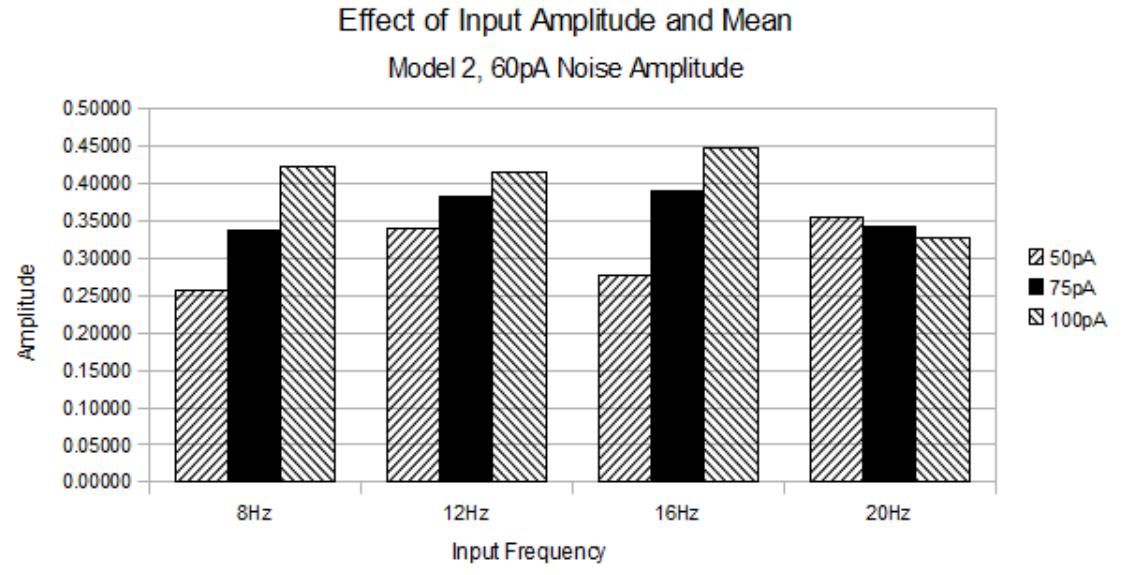

Figure 4.13: Effect of Input Amplitude and Mean on Response Fidelity on model receiving inputs with high variance noise (60pA), at all frequencies. Variance was extremely minor (<0.002) and so is not shown in figure

Figure 4.13 shows the effect of input parameters on the response fidelity of populations receiving inputs with high variance noise. Increasing amplitudes and means of input caused a significant improvement in response fidelity measures for 8Hz, 12Hz and 16Hz inputs. No significant improvements were seen between the 50pA and 75pA inputs at 20Hz, while the 100pA condition performed significantly better than the 50pA condition ($p<0.001$).

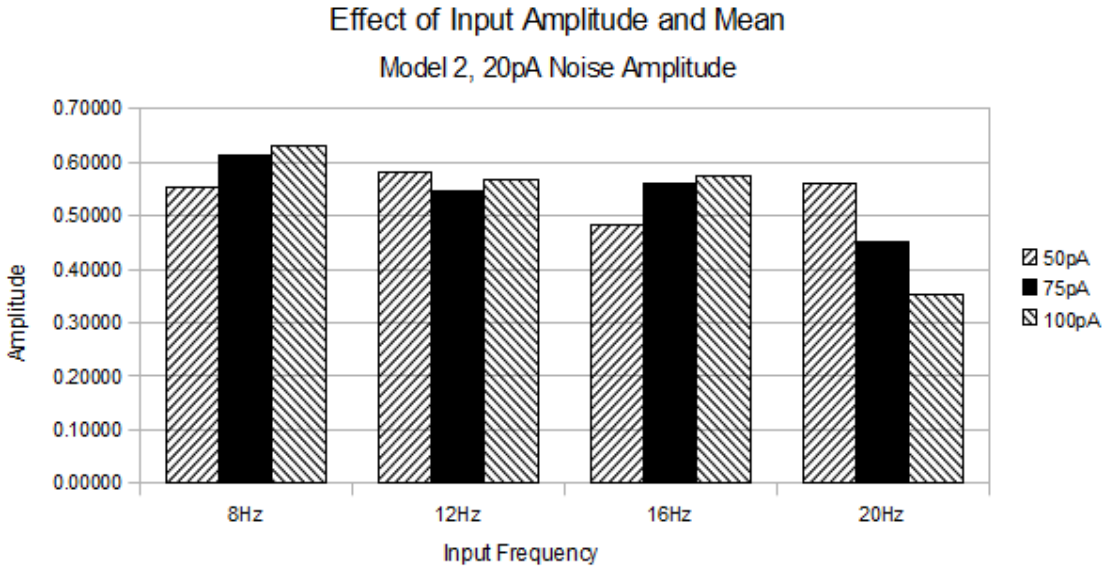

Figure 4.14: Effect of Input Amplitude and Mean on Response Fidelity on model receiving inputs with low variance noise (20pA), at all frequencies. Variance was extremely minor (<0.002) and so is not shown in figure

The effect of input parameters on models receiving low variance noise is shown in Figure 4.14 Increasing input amplitude and mean caused an improvement in response fidelity for 8 and 16Hz input frequencies, and caused a decrease in performance at 20Hz ($p<0.001$). No Significant effect was seen for the 12Hz input.

4.4 STAGE 3

In stage 3, population heterogeneity was modelled through the use of the K-Slow conductance manipulation method used for stage 2. As in the previous stage, spontaneous firing rates of the populations simulated were normally distributed between 0.5 and 1.5* the standard firing rate of the MVNB model (21.059Hz). Along with these heterogeneous populations, homogeneous populations, with no change to the spontaneous firing rates, were also simulated, for all conditions used at this stage.

This stage used the Synaptic Spike Train method, as described in Chapter 3, section 3.2.2, for the generation and simulation of inputs through excitatory exponential synapses. Synapses were distributed uniformly over the dendritic structure (both Proximal and Distal dendrite compartments), and provided a spike train (of input spike times) prior to simulation. During simulation, these spike times were delivered as excitatory inputs using the NEURON environment's NetCon object. These synapse inputs work to produce excitatory post synaptic current events in the dendritic structure of the cell. This method of input, via excitatory synaptic events, provides a more realistic approximation of true synaptic events.

Spike trains at the 4 target frequencies (8, 12, 16, 20Hz) were generated and used, with 3 separate parameter sets, in order to reflect a range of possible Afferent neuron properties. Examples of these are shown in Figure 4.15 and Figure 4.16, for 8Hz and 16Hz target frequencies. Input set A01 had a mean of 50Hz, and amplitude of 25Hz (50+/-25 spikes per second). Input A02 a mean of 75Hz and amplitude of 25Hz (75+/-25). Input A03 a mean of 35Hz and amplitude of 20Hz (35+/-20). As the mean and amplitude frequencies of the input trains reflects the relative intensity of the 'input populations', we thus have "low" (A03), "medium" (A01), and "high" (A02) input intensity conditions, for all 4 target frequencies (8Hz, 12Hz, 16Hz, 20Hz), where it is the target frequency of the input that we intend to be recreated in the output of the MVNB model cells. As the input mean and amplitude represent the velocity of the head rotations compensated for (higher mean/amplitude = higher velocity rotation), this would allow us to investigate any effects of the speed of the head rotations on the model VOR response.

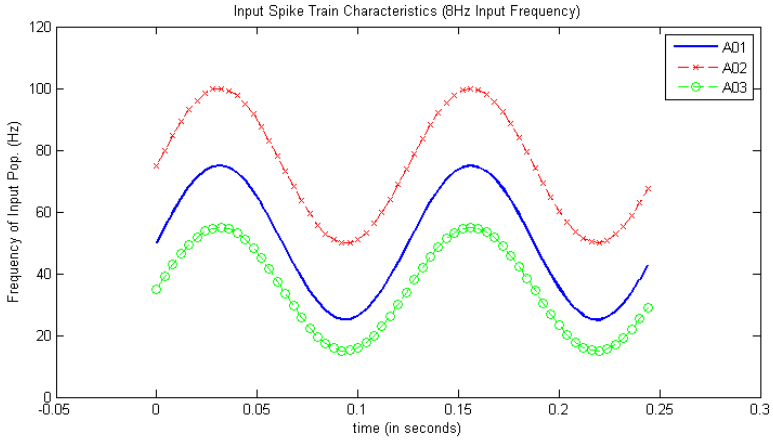

Figure 4.15: Input Train Characteristics for 8Hz Target Frequency. A01 had a mean frequency of 50Hz and Amplitude of 25Hz. A02 a mean of 75Hz and amplitude of 25Hz, and A03 a mean of 35Hz and amplitude of 20Hz.

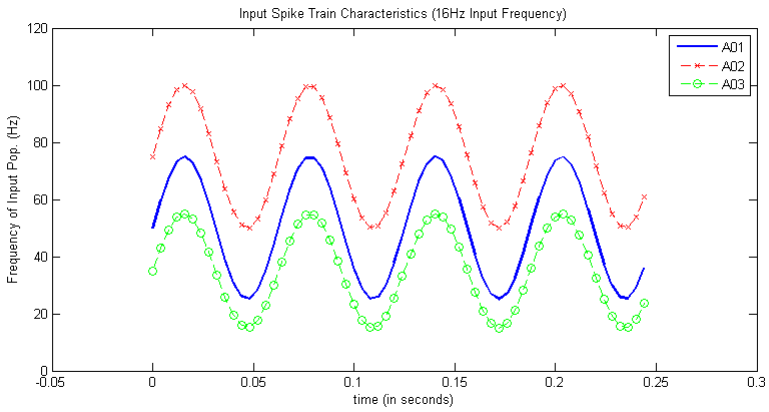

Figure 4.16: Input Train Characteristics 8Hz

Figures 4.17 and 4.18 show examples of the input spike trains used to drive synaptic input, normalised and compared to the sine waves (8Hz (500ms) and 16Hz (250ms)) which were used to generate them.

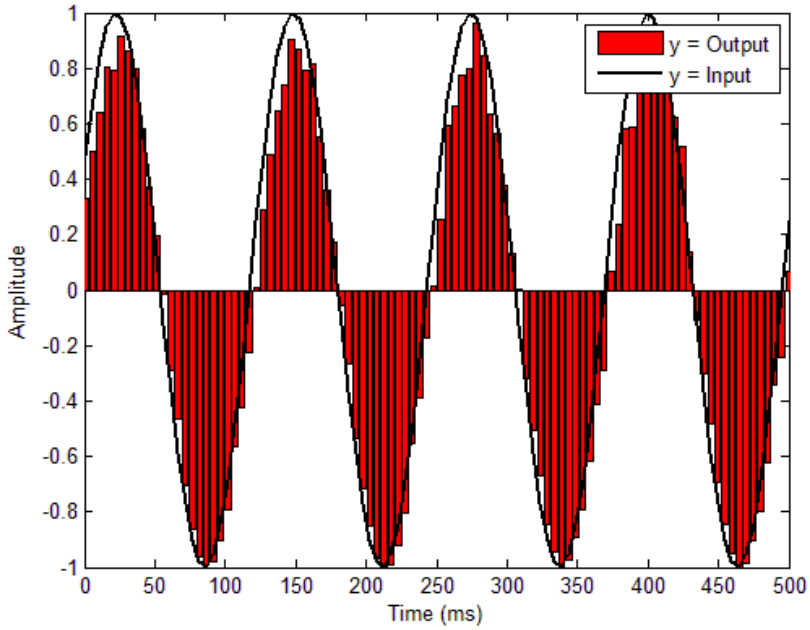

Figure 4.17: Example of Collected Input Spike Train Activity for 8Hz input. 500ms of input spike trains, at 8Hz, normalised and compared to the sine wave they follow

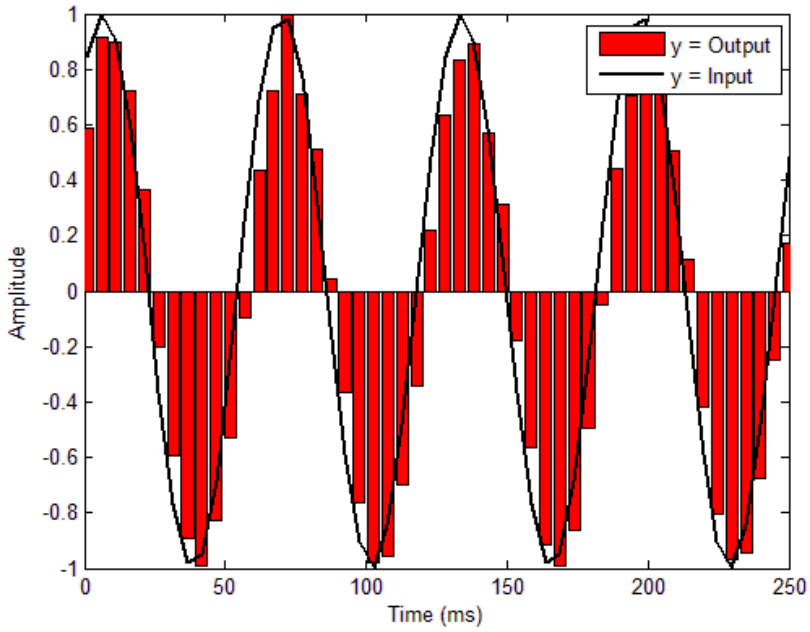

Figure 4.18: Example of Collected Input Spike Train Activity for 16Hz input. 250ms of input spike trains, at 16Hz, normalised and compared to the sine wave they follow

These three input parameter sets, for all 4 target frequencies, were used to simulate populations of 500 MVNB neurons (with 10 populations being used to give an indication of average performance), with varying numbers of synapses distributed uniformly across the dendritic structure (nsyn = 20, 40, 60), at various synaptic weights (w = 0.1, 0.5, 1.0), for both Heterogeneous and Homogeneous populations. The overall simulation setup for this stage is illustrated in Figure 4.19.

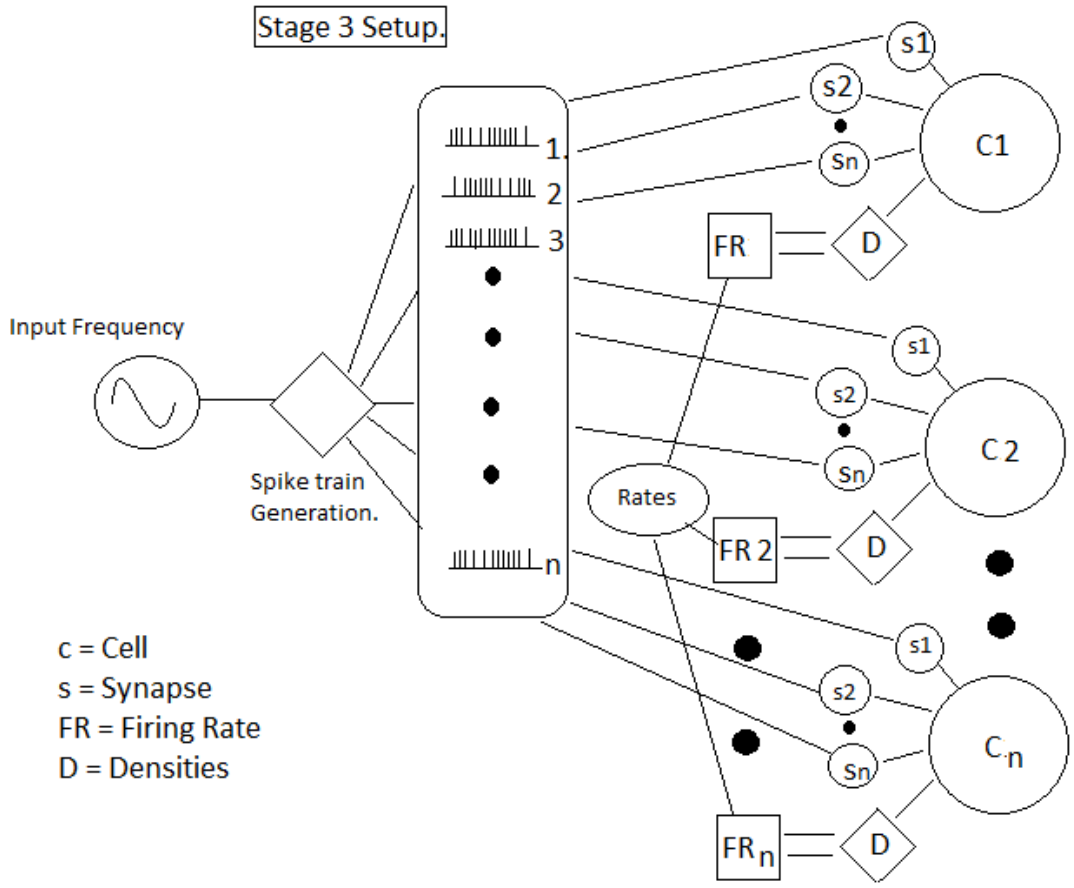

Figure 4.19: General Overview of Simulation Setup for Stage 3. Inputs are pre-generated into large sets. Each synapse, of each member of the population, is provided input spike time events, chosen randomly from the pre-generated set. These spike times trigger excitatory synaptic inputs at the corresponding times. Population heterogeneity is simulated via the setting of K-Slow densities in order to achieve the required firing rate chosen from the required distribution.

Initial response fidelity scores obtained from the outputs produced by heterogeneous populations were somewhat poor for certain conditions, performing not much better than the homogeneous populations receiving the same input, and with the same input parameters. However, this poor performance seen in some Heterogeneous populations was found to be due the introduction of slight "phase lead" in the output of these Heterogeneous populations. That is, the output of the populations leads the input signal provided, thus the fidelity response measure became distorted, and did not accurately represent the ability of the Heterogeneous populations to reproduce the input signal.

Phase lead is an observed phenomenon in the real VOR, seen in the output of both the Central Vestibular neurons [32] [70], and the Vestibular afferents [69], as well as being predicted in modelling of Central Vestibular neurons [117]. As such, measures were implemented to estimate

and correct for the phase lead of Heterogeneous populations, in order to obtain more useful response fidelity measures. Figure 4.20 and 4.21 show an example of the original phase lead in the population, and the response fidelity when phase lead was measured and accommodated for in a Heterogeneous population receiving an 16Hz input signal.

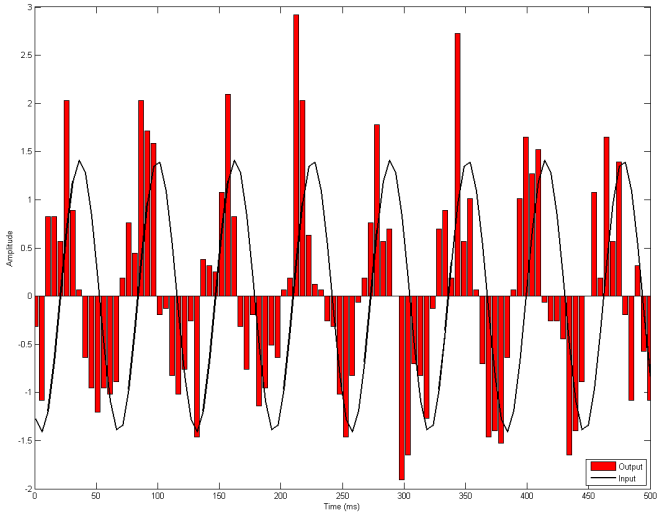

Figure 4.20: Uncorrected Population Output Showing Phase Lead of Heterogeneous Population for 16Hz Input, with Input Parameters A02, number of synapses = 60, synpase weight = 1.0. Shows a Phase lead of 10ms compared to the Input signal

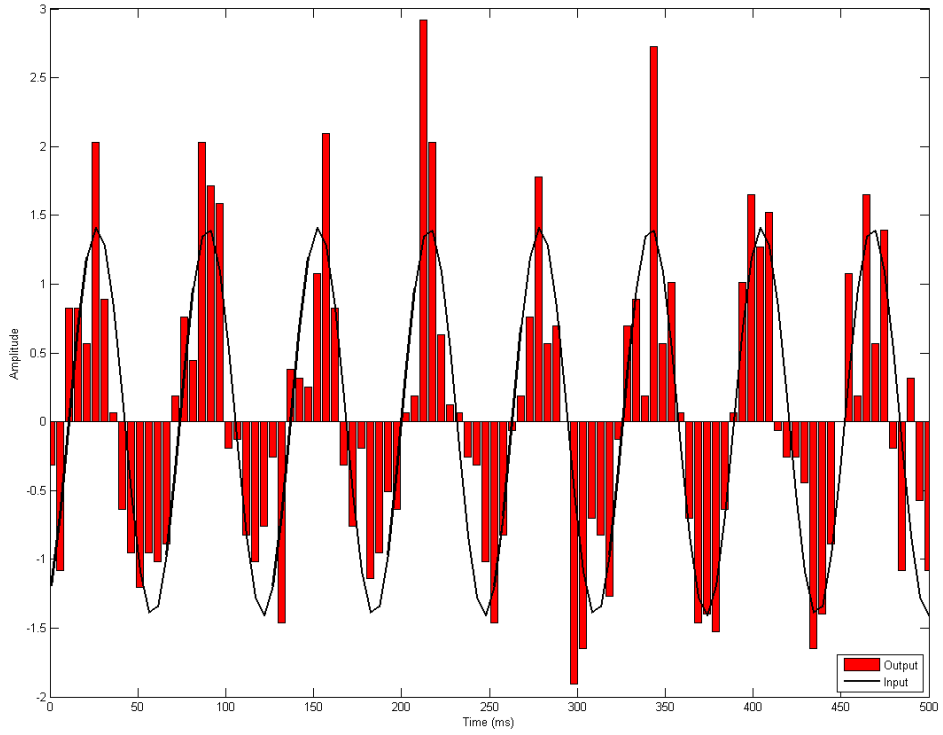

Figure 4.21: Corrected Population Output Showing Phase Lead of Heterogeneous Population for 16Hz Input, with Input Parameters A02, number of synapses = 60, synpase weight = 1.0. Phase lead of 10ms was corrected from the original response.

Figures 4.22 and 4.23 show a further example of the original output, uncorrected for phase lead, and the corrected output accommodating for the estimated phase lead, in a Heterogeneous population receiving an 8Hz input signal.

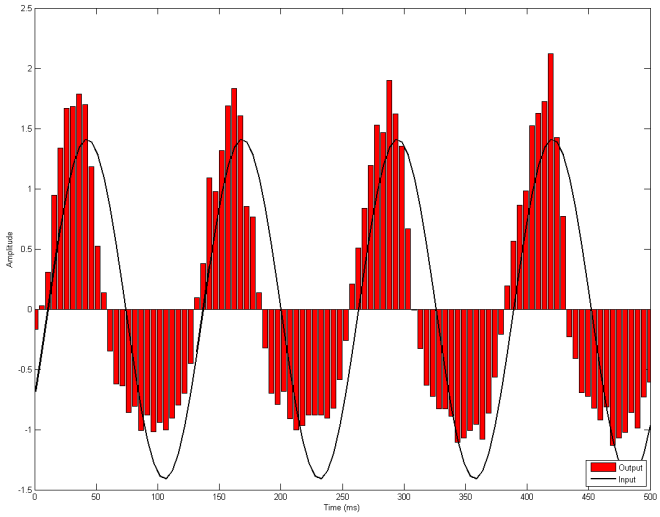

Figure 4.22: Uncorrected Population Output Showing Phase Lead of Heterogeneous Population for 16Hz Input, with Input Parameters A01, number of synapses = 60, synpase weight = 0.1. Shows a Phase lead of 5ms compared to the Input signal

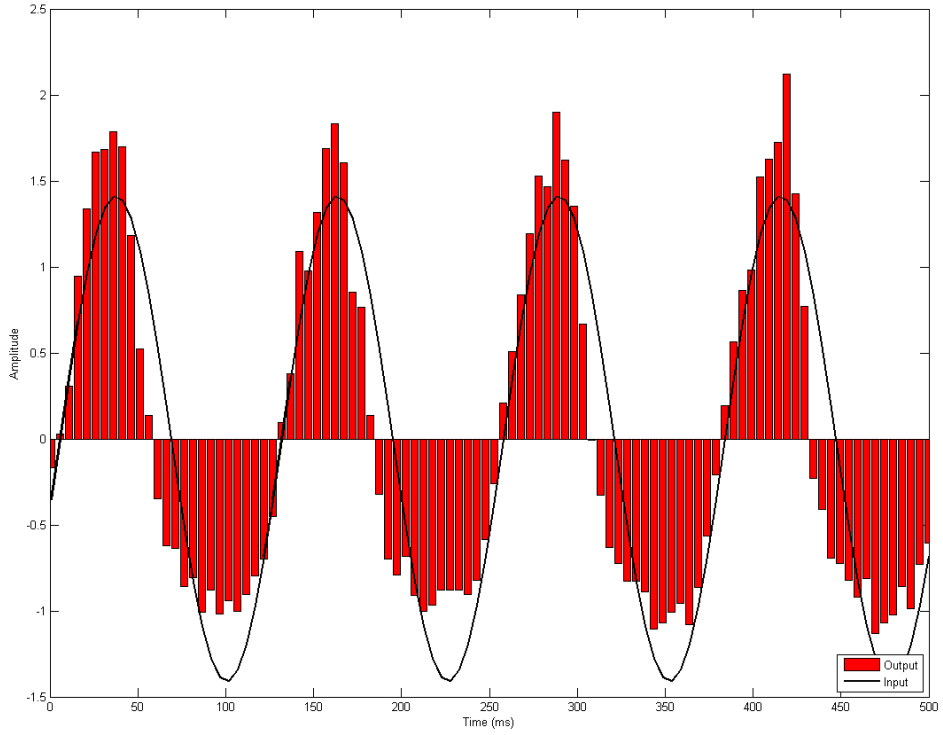

Figure 4.23: Corrected Population Output Showing Phase Lead of Heterogeneous Population for 8Hz Input, with Input Parameters A01, number of synapses = 60, synpase weight = 0.1. Phase lead of 5ms was corrected from the original response.

Phase lead was estimated and accommodated for through the best-fit alignment of the population outputs with the input signal, the time difference between the two (original and best fit) being taken as the estimate of phase lead present. Phase leads, when present, were found to be constant across the entire simulation duration. Estimated phase leads, for the Heterogeneous populations, are shown in Figure 4.24. Phase leads increase as the velocity of the inputs increases (thus A03 shows the smallest phase leads, and A02 the largest), and increase as the number of synapses and synapse weight increase. No such phase accommodation could be performed on the Homogeneous population responses.

Phase Lead Estimates for All Heterogeneous Populations.

nSyn	w	8Hz A03	8Hz A01	8Hz A02	12Hz A03	12Hz A01	12Hz A02
20	0.1	0	0	0	0	0	0
20	0.5	0	0	0	0	0	0
20	1	0	0	0	0	0	0
40	0.1	0	0	5	0	0	0
40	0.5	0	0	5	0	0	0
40	1	0	0	5	0	0	5
60	0.1	0	5	10	0	5	5
60	0.5	5	5	10	0	5	10
60	1	5	10	10	5	10	10

nSyn	w	16Hz A03	16Hz A01	16Hz A02	20Hz A03	20Hz A01	20Hz A02
20	0.1	0	0	0	0	0	0
20	0.5	0	0	0	0	0	0
20	1	0	0	0	0	0	0
40	0.1	0	0	0	0	0	0
40	0.5	0	0	0	0	0	0
40	1	0	0	5	0	0	0
60	0.1	0	0	5	0	0	5
60	0.5	0	0	5	0	0	5
60	1	0	5	10	0	5	5

Figure 4.24: Phase Leads Estimated for All Heterogeneous Populations. Note that input sets are placed in order of their amplitudes/means, to show the general trend for increased phase lead as the amplitude/mean of the input increases. nSyn is synapse number, w is weight of synapses.

Once phase lead was estimated and accommodated for, response fidelity scores for Heterogeneous populations was significantly better than comparable Homogeneous populations, across all frequencies, and for all input parameters (all $p < 0.05$, two-tailed t-test, equal variance assumed). Comparisons of these scores are shown in Figures 4.25, 4.26, 4.27, and 4.28, for input parameters A01 (mean 50Hz, amplitude 25Hz). Those for input parameters A02 and A03 are shown in Appendix A. Variance of population response fidelities was universally small (variance <0.002) and so are not shown.

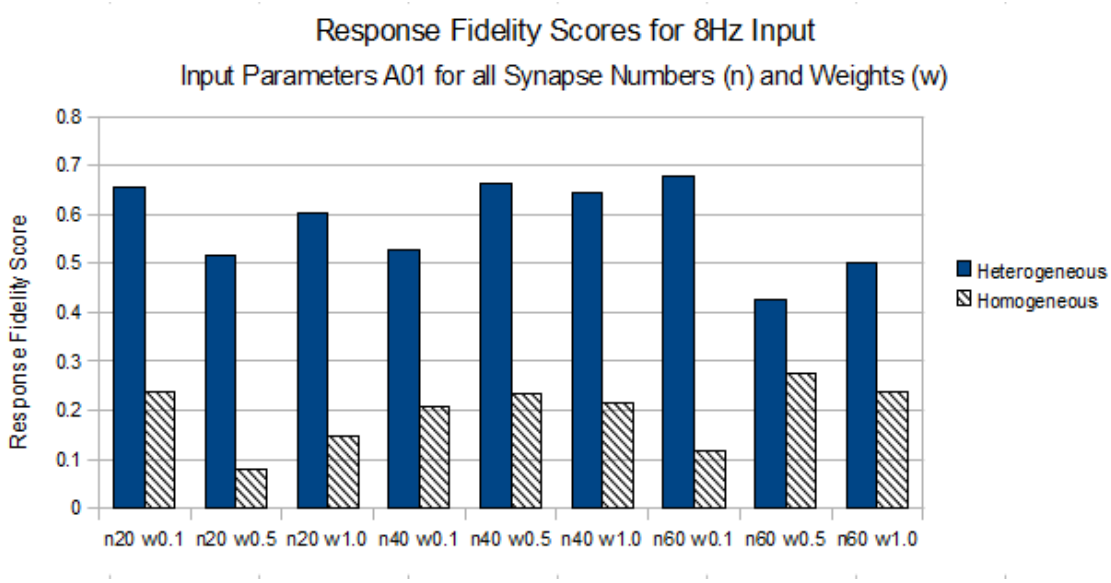

Figure 4.25: Stage 3 Response Fidelity Comparison for 8Hz Input, Heterogeneous vs Homogeneous Populations. For A01 Input set, across all synapse numbers and weights. Variance was extremely minor (<0.002) and so is not shown in figure

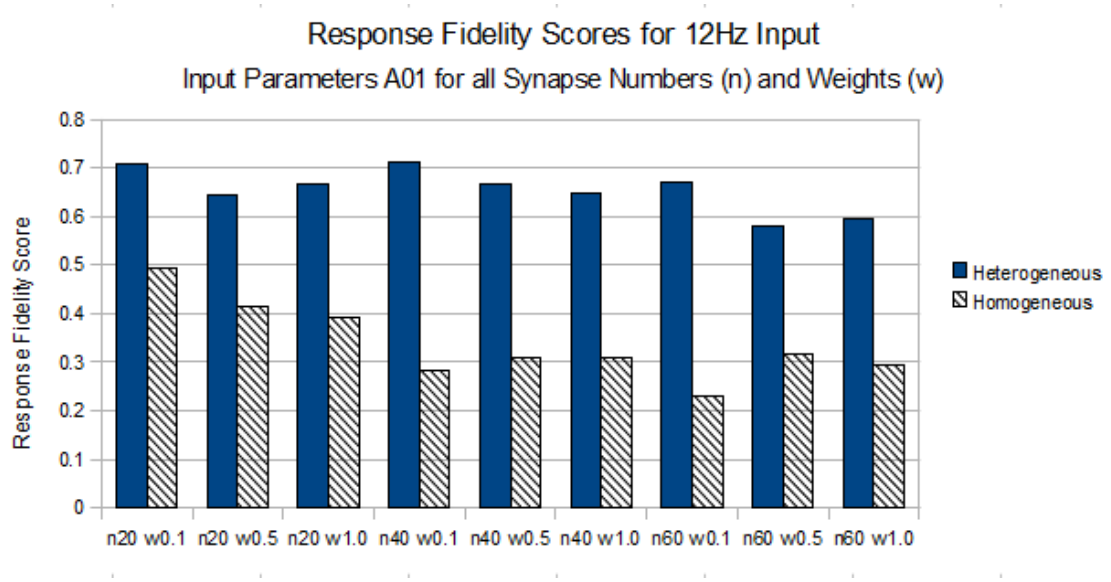

Figure 4.26: Stage 3 Response Fidelity Comparison for 12Hz Input, Heterogeneous vs Homogeneous Populations. For A01 Input set, across all synapse numbers and weights. Variance was extremely minor (<0.002) and so is not shown in figure

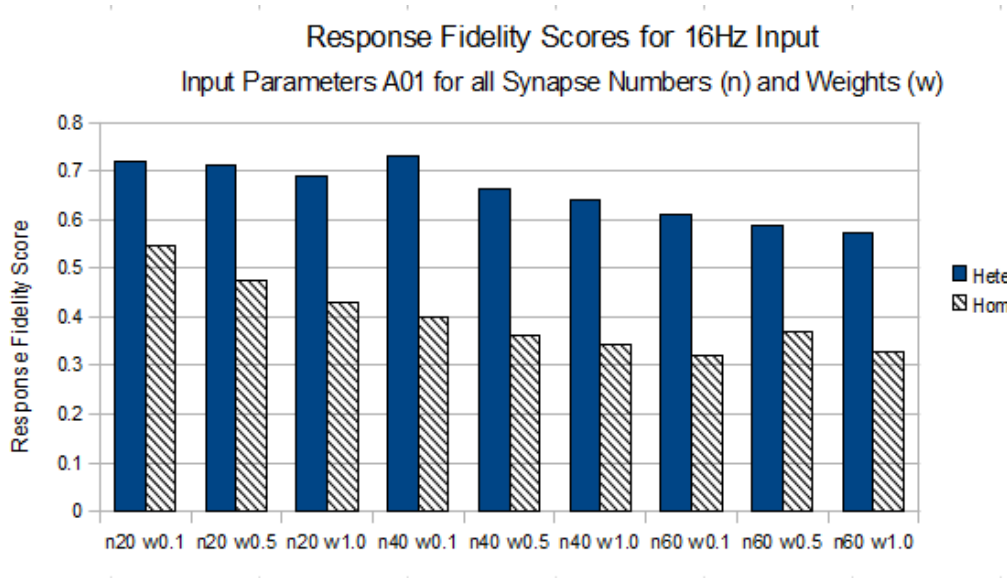

Figure 4.27: Stage 3 Response Fidelity Comparison for 16Hz Input, Heterogeneous vs Homogeneous Populations. For A01 Input set, across all synapse numbers and weights. Variance was extremely minor (<0.002) and so is not shown in figure

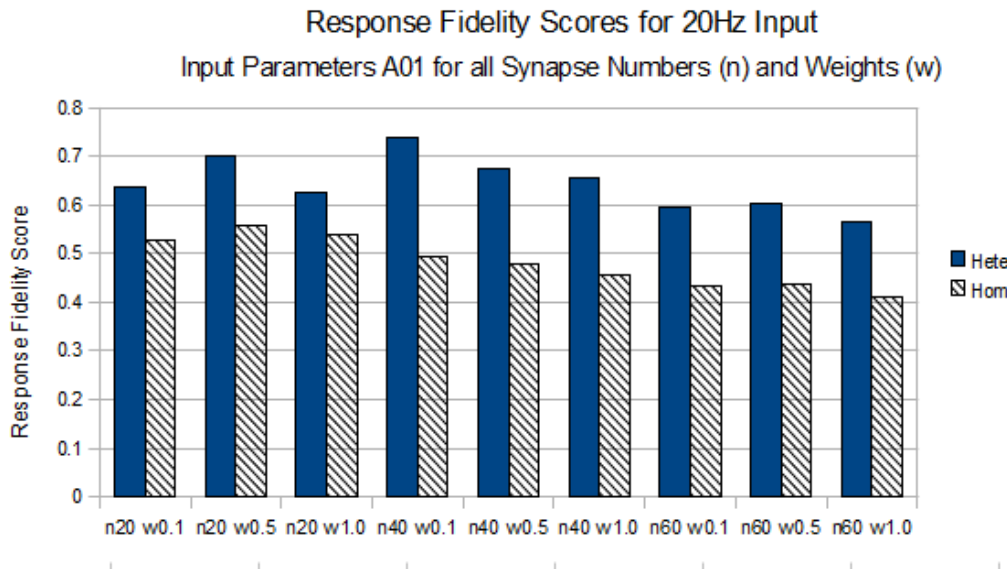

Figure 4.28: Stage 3 Response Fidelity Comparison for 20Hz Input, Heterogeneous vs Homogeneous Populations. For A01 Input set, across all synapse numbers and weights. Variance was extremely minor (<0.002) and so is not shown in figure

Comparison of responses to 8Hz inputs for all synapse parameters, for the 3 input sets are shown in Figure 4.29. A general trend, for inputs A01 and A03, of reduced scores as synapse number increases can be seen. As well, for conditions with 20 and 60 synapses, we generally see a

decrease in performance as synapse weight increases for input sets A01 and A03, but an increase in performance for input set A02.

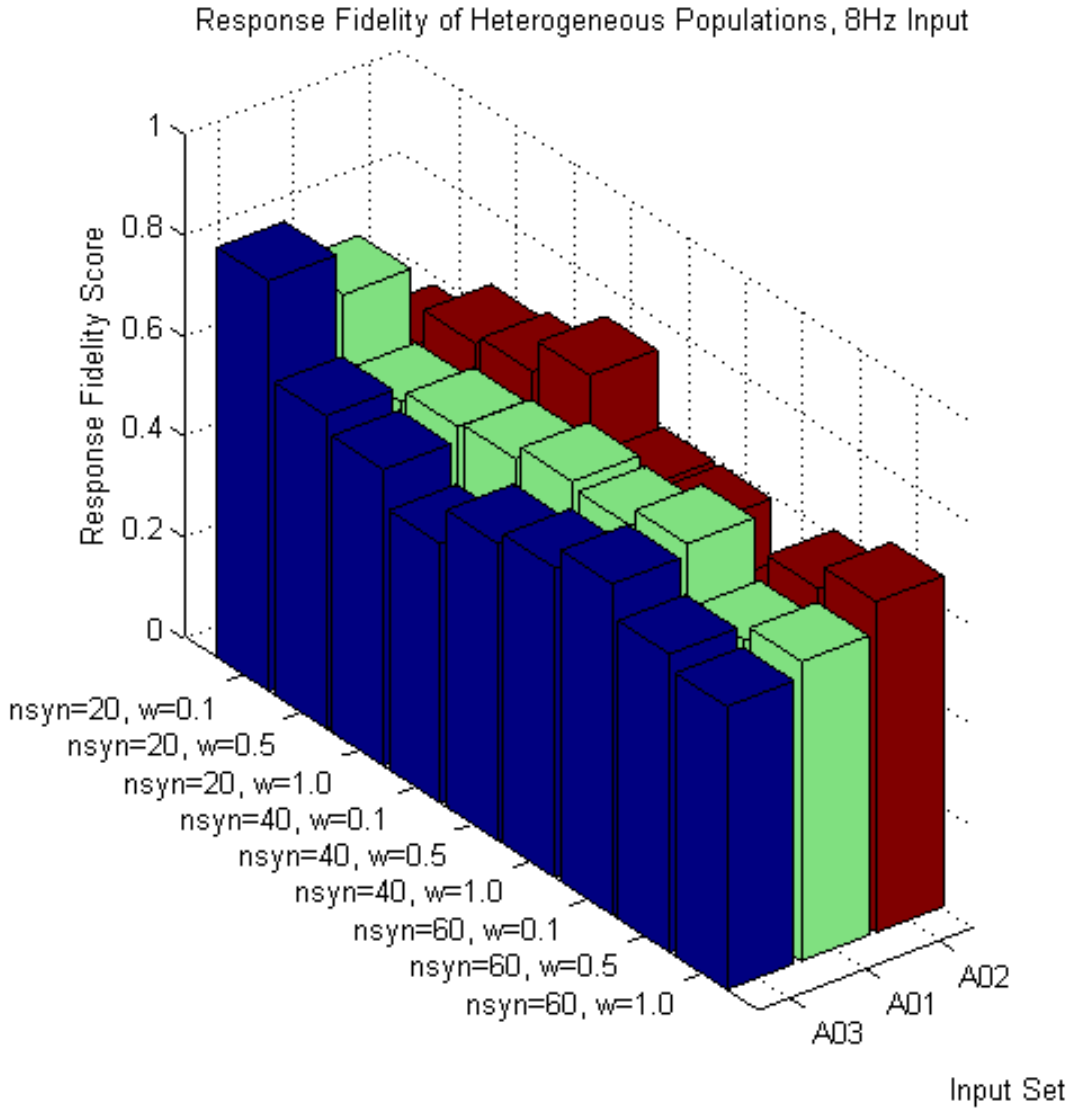

Figure 4.29: Heterogeneous Population Response Fidelity Scores for 8Hz Inputs Across all Input Sets and Synapse Paramaters.

Figure 4.30 shows a comparison of response fidelity scores for Heterogeneous populations receiving 12Hz inputs, across all input sets and synapse parameters. Again, the general trend of decreased response fidelity as both synapse numbers and synapse weights increase can be seen.

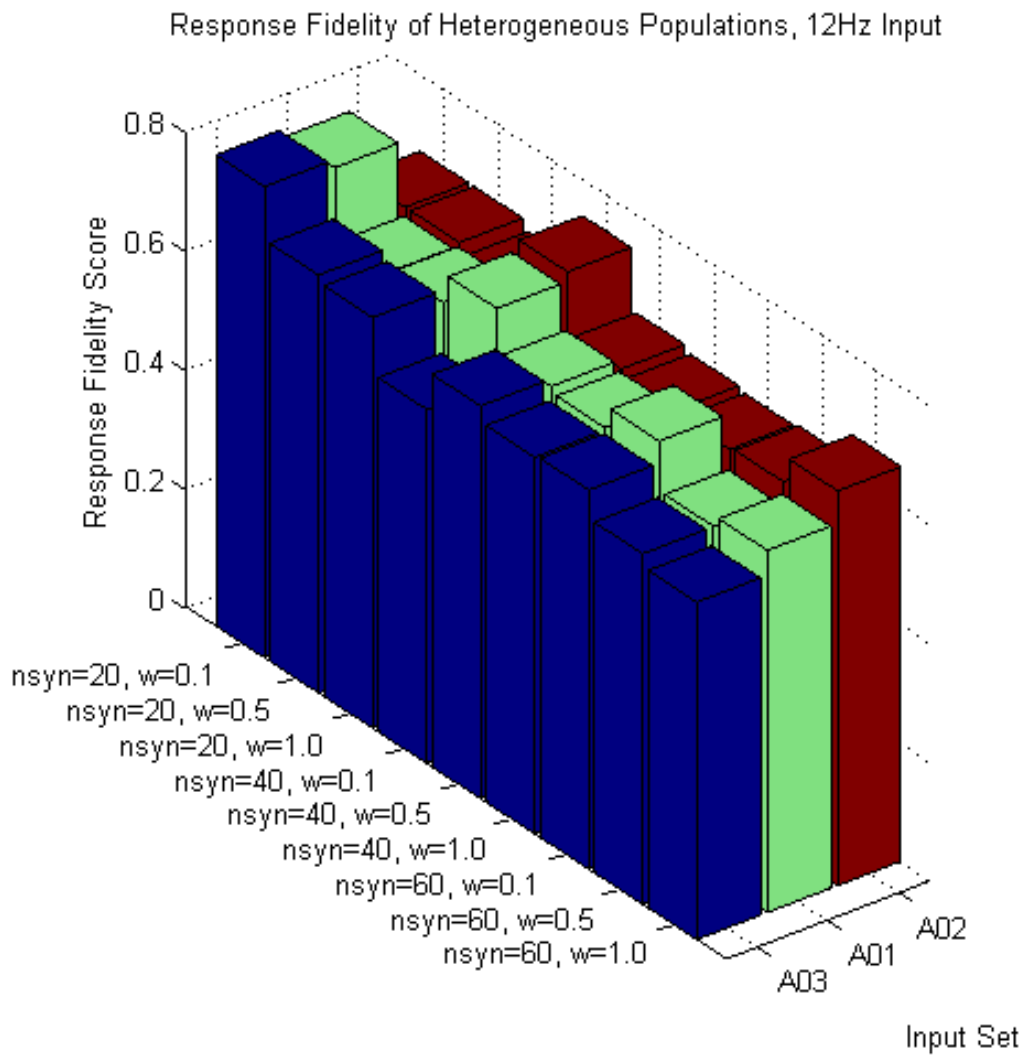

Figure 4.30: Heterogeneous Population Response Fidelity Scores for 12Hz Inputs Across all Input Sets and Synapse Paramaters.

Figure 4.31 shows comparison of fidelity scores for Heterogeneous populations receiving 16Hz inputs, across all conditions. Again, although not a universal trend for all conditions, increases in synapse numbers and synapse weights reduces the response fidelity scores for the population.

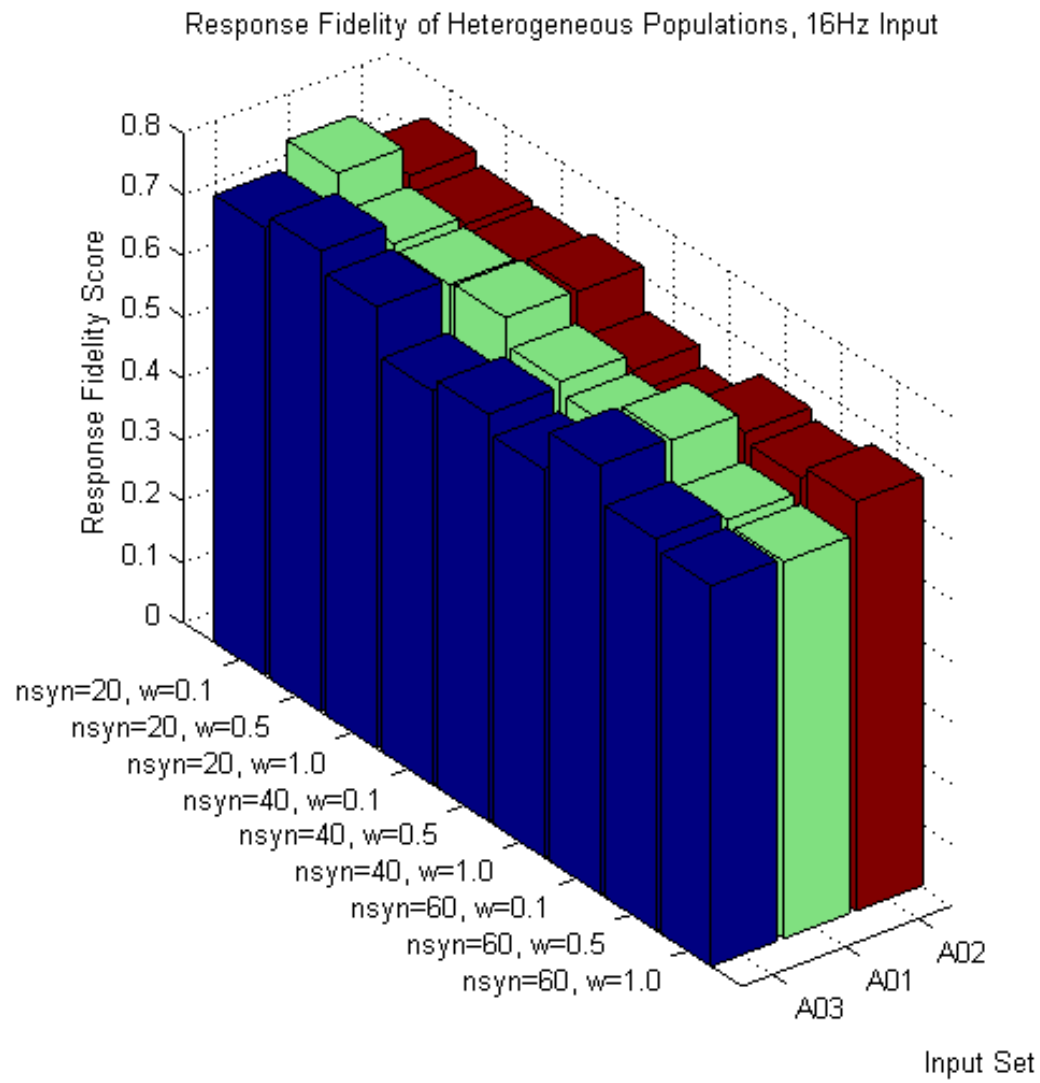

Figure 4.31: Heterogeneous Population Response Fidelity Scores for 16Hz Inputs Across all Input Sets and Synapse Paramaters.

Comparison of response fidelity scores for 20Hz inputs are shown in Figure 4.32. The trend of increasing synapse numbers and synapse weight reducing the response fidelity scores is perhaps most clearly shown in this comparison. Aside from input sets A01 and A03 (with the nSyn = 20 w = 0.1 parameters), increasing synapse numbers and weight decreases response fidelity significantly.

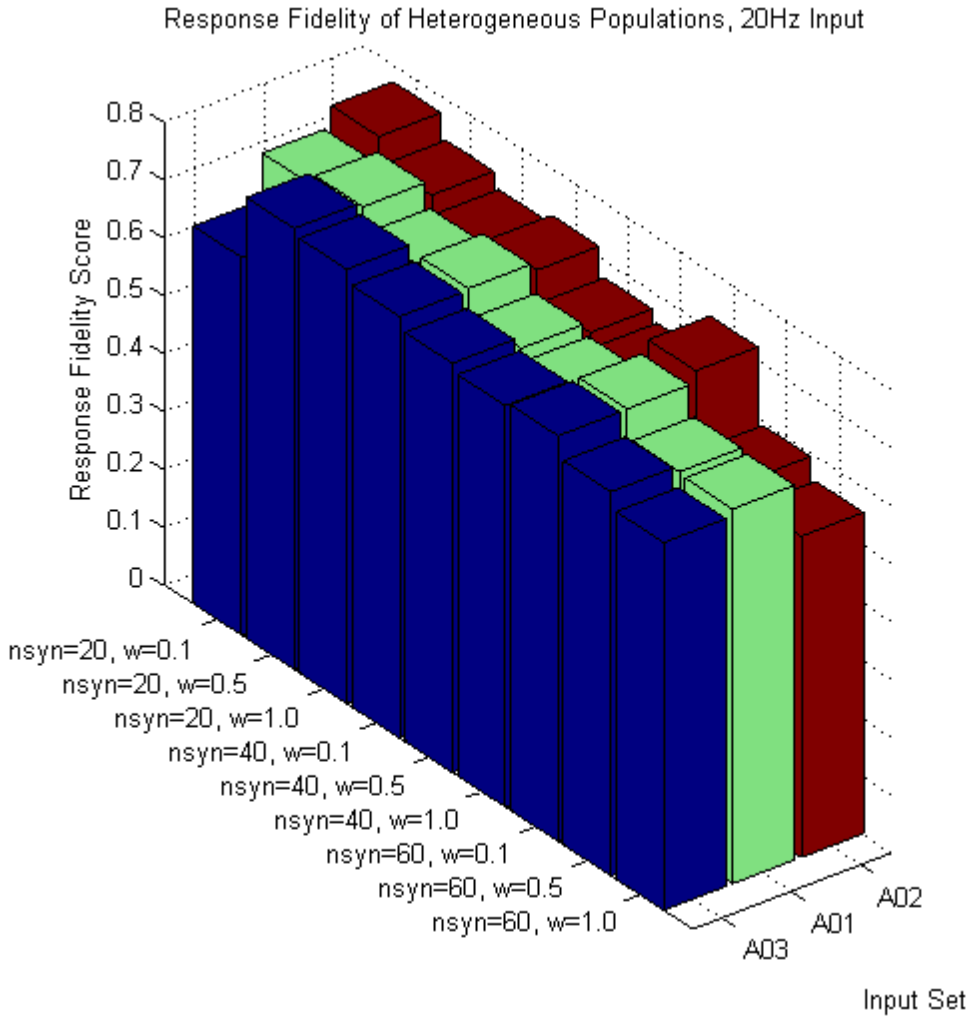

Figure 4.32: Heterogeneous Population Response Fidelity Scores for 20Hz Inputs Across all Input Sets and Synapse Paramaters.

Generally then, we see reduced response fidelity scores for increased synapse parameters, with performance decreasing as synapse numbers and weights increase independently, as well as in combination. However, this trend is not universal, especially for the 8Hz target frequency inputs.

In addition to the response fidelity scores, Heterogeneous populations produced outputs with significantly larger target frequency components than Homogeneous populations when the frequency spectrum of the outputs was analysed. Comparisons of these target frequency component amplitudes are shown in !Figures 4.33, 4.34, and 4.35 for the A01 input set, across all Synapse numbers and weights for all frequencies.

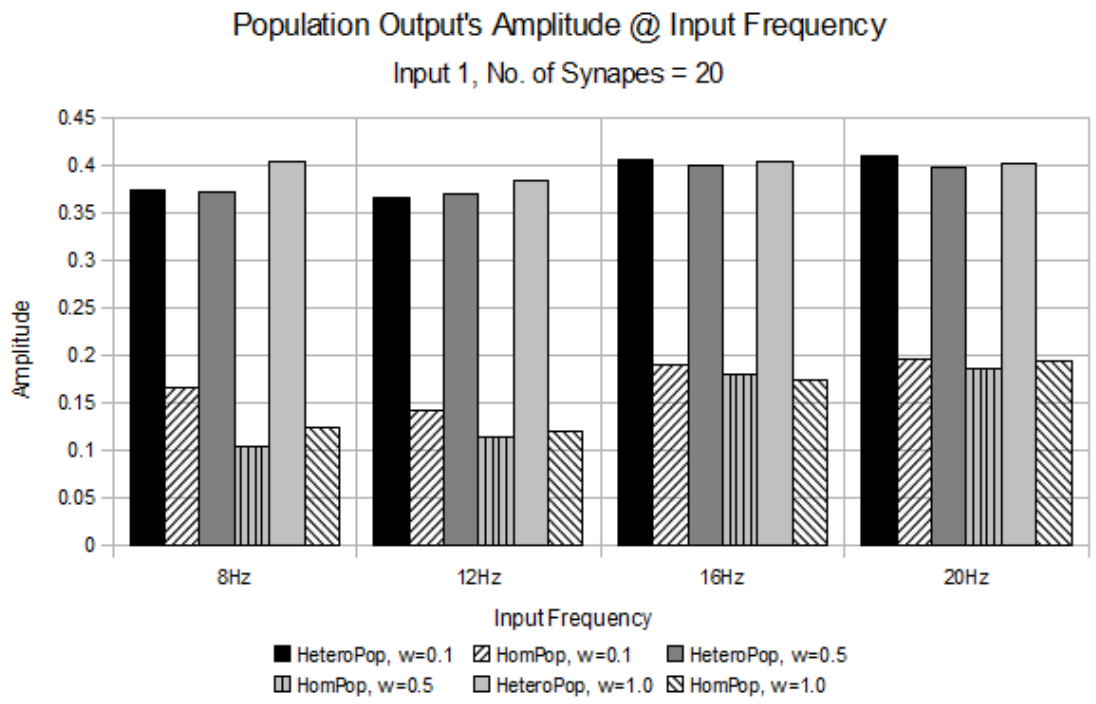

Figure 4.33: Amplitude of Target Frequency Component in Population Output for 20 Synapse Conditions.

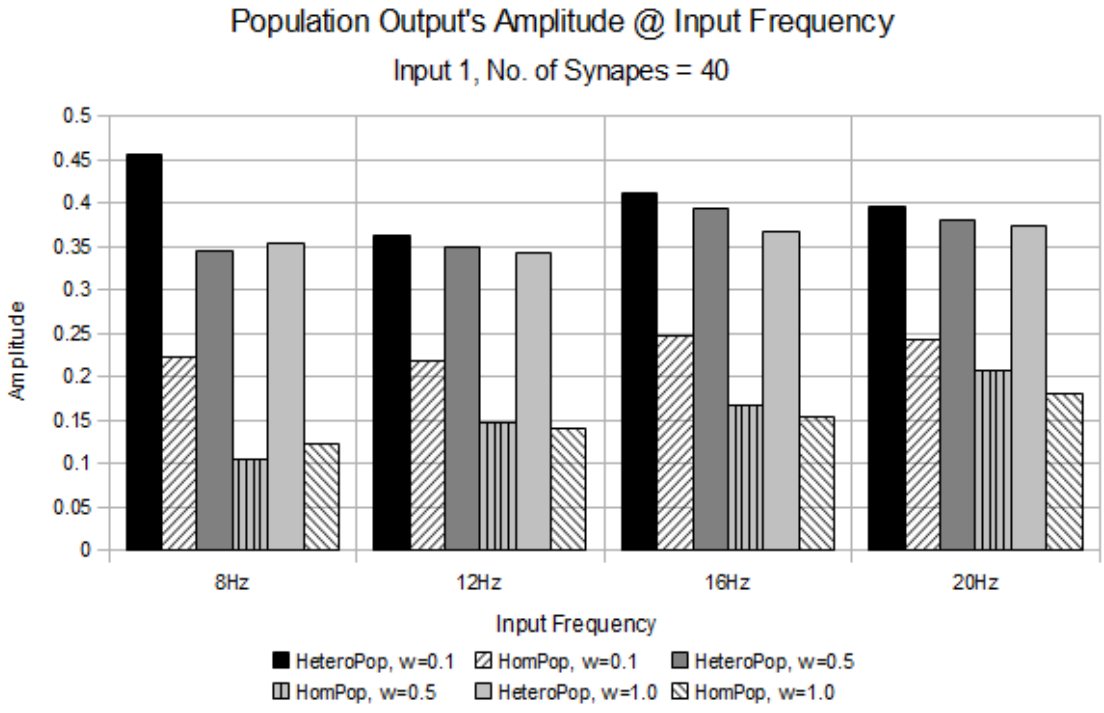

Figure 4.34: Amplitude of Target Frequency Component in Population Output for 20 Synapse Conditions.

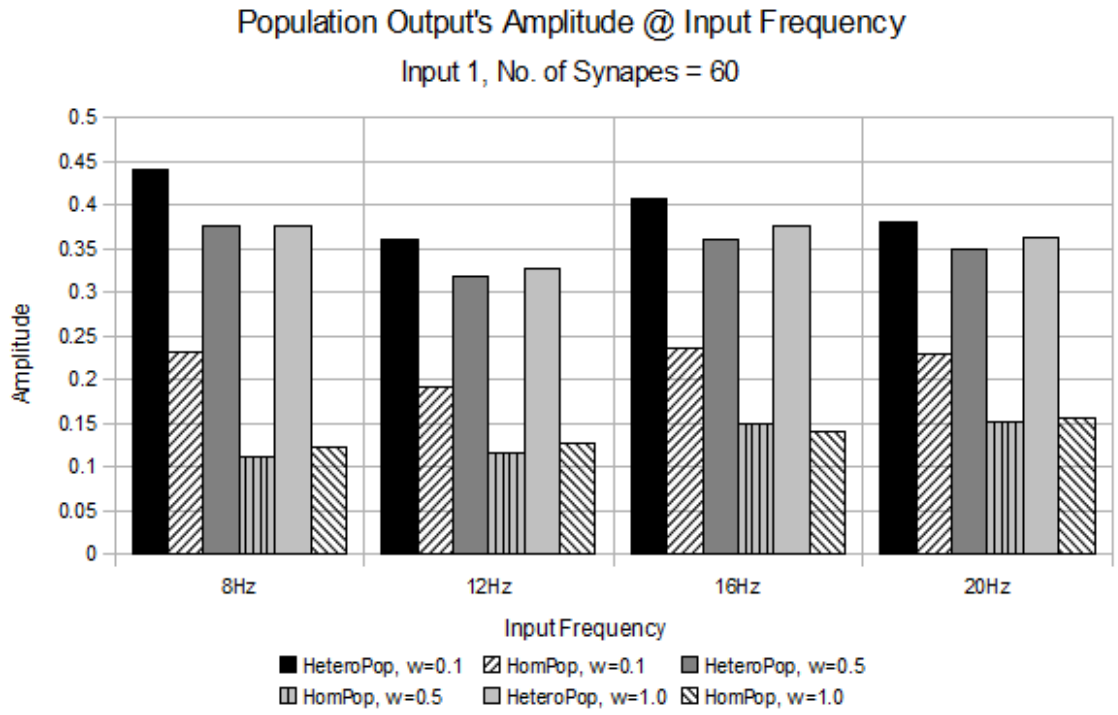

Figure 4.35: Amplitude of Target Frequency Component in Population Output for 20 Synapse Conditions.

4.5 ANALYSIS

4.5.1 *Effect of Population Heterogeneity on Response Fidelity*

Results from stages 1 and 3 allow us to compare the performance of Heterogeneous populations of model MVNB neurons against the performance of Homogeneous populations, receiving the same high frequency inputs. Across all conditions and in both stages, Heterogeneity of the population improved the response fidelity of the output significantly. This was the case when the Heterogeneity was modelled as distributed spontaneous firing rates of the population arising from the introduction of a bias current (stage 1) or through the altered distribution of slow Potassium conductances (K-Slow conductances, stage 3). Performance was improved significantly for all four target frequencies used for the inputs (8Hz, 12Hz, 16Hz, 20Hz) and for numerous input parameters.

Comparing the Peri-stimulus Time Histograms (PSTH) from two populations, one Heterogeneous and the other Homogeneous, can illustrate how this improved response fidelity has been achieved. Figures 4.26 and 4.37 show sample PSTH's for Heterogeneous (response fidelity = 0.739) and Homogeneous (response fidelity = 0.51) populations from stage 3 of the simulations, receiving an 8Hz input signal (A01, 20 synapses of weight 0.1). The Heterogeneous population follows the

periodicity of the input signal impressively, and shows adequate gain (how well the amplitude of the output matches the amplitude of the input). The Homogeneous population, in comparison, shows a poorer periodicity, with output amplitude crossing the mean (0 amplitude) repeatedly in a given cycle, and reduced gain throughout the sample. The Heterogeneous population smoothly matches the shape and frequency of the input signal, although not matching gain exactly throughout, while the Homogeneous population produces of distorted output, not matching the input wave smoothly (there are periods where amplitude drops significantly towards the mean of 0 between bins, when it should be smoothly away from the mean, and increasing in amplitude), regardless of gain, especially in the upper half of the PSTH.

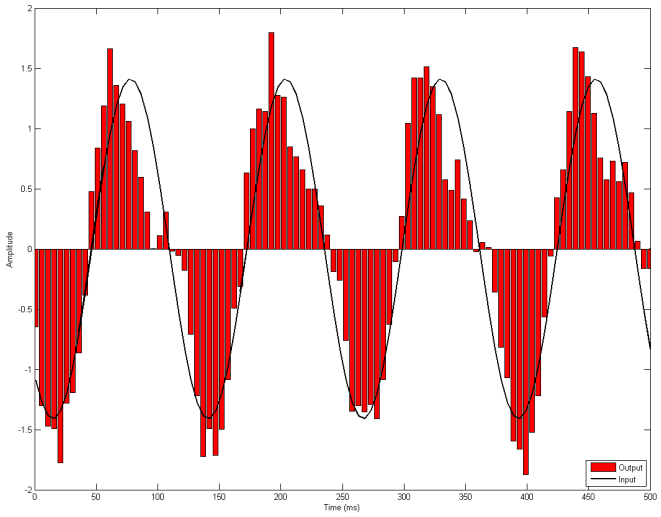

Figure 4.36: Response Fidelity of Heterogeneous Population Receiving 8Hz Input, from Stage 3, using Input Set A01, with 20 Synapses of weight 0.1. Input signal is the black line overlayed atop the output response bars.

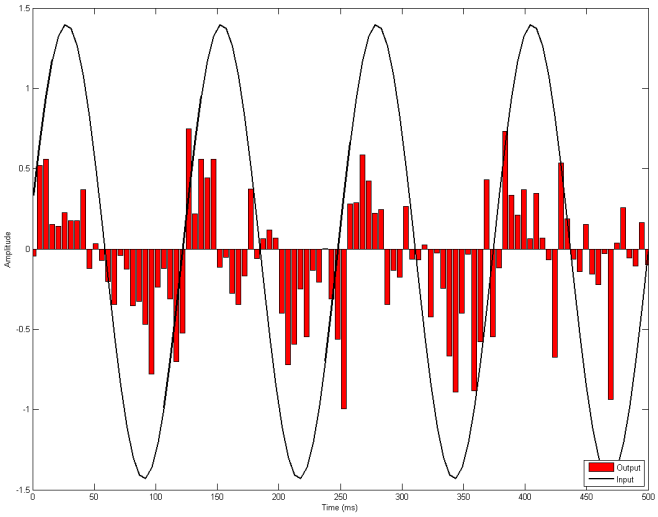

Figure 4.37: Response Fidelity of Homogeneous Population Receiving 8Hz Input, from Stage 3, using Input Set A01, with 20 Synapses of weight 0.1. Input signal is the black line overlayed atop the output response bars.

Figures 4.38 and 4.39 show a similar comparison for Heterogeneous (response fidelity = 0.776) and Homogeneous (response fidelity = 0.55) populations receiving 16Hz inputs (input A01, 20 Synapses of weight 0.1). Again, the Heterogeneous population shows impressive periodicity, in line with that of the input signal, along with adequate gain matching between the output and the input throughout each cycle, while the Homogeneous population shows a poorer match between input and output gain, and a poorer match for the periodicity of the input signal.

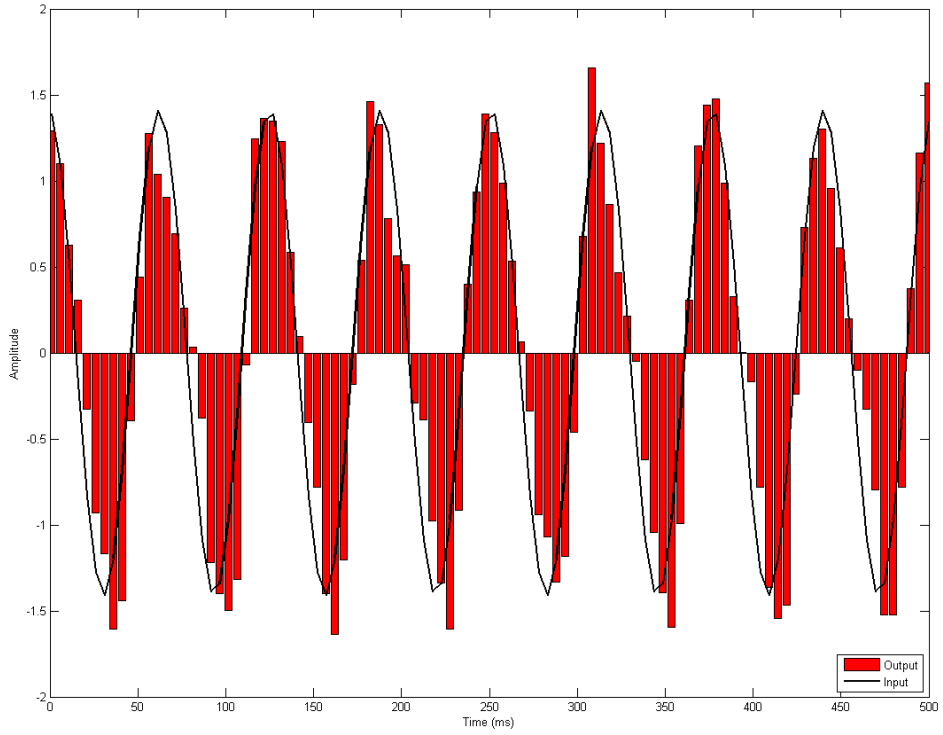

Figure 4.38: Response Fidelity of Heterogeneous Population Receiving 16Hz Input, from Stage 3, using Input Set A01, with 20 Synapses of weight 0.1. Input signal is the black line overlayed atop the output response bars.

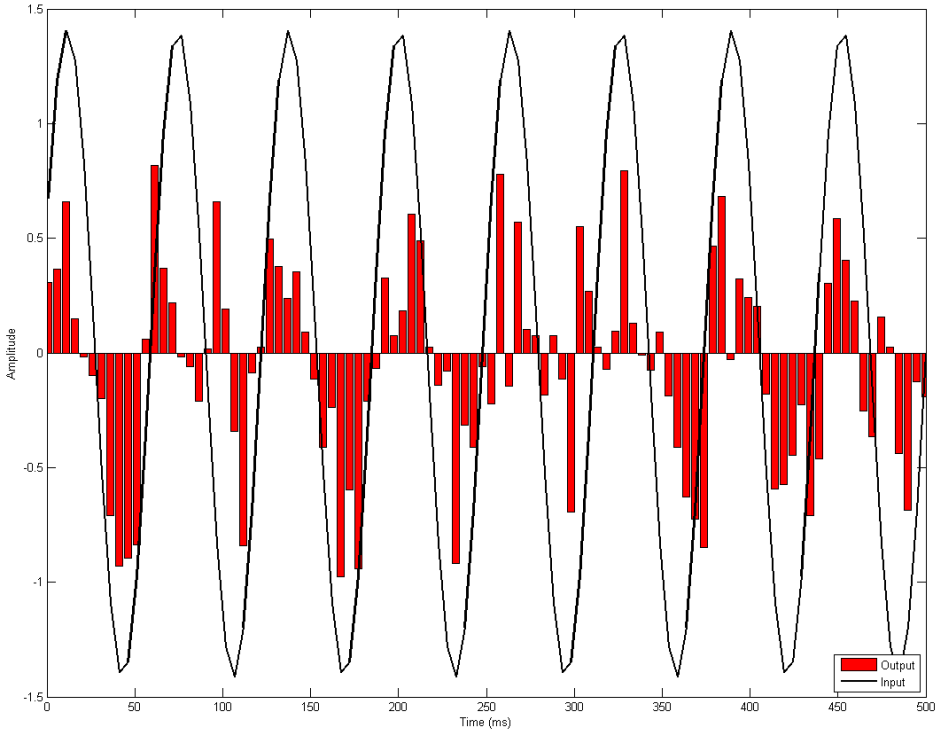

Figure 4.39: Response Fidelity of Homogeneous Population Receiving 16Hz Input, from Stage 3, using Input Set A01, with 20 Synapses of weight 0.1. Input signal is the black line overlayed atop the output response bars.

Heterogeneity allows the population to more smoothly and accurately match the input signal, maintaining a consistent periodicity and adequate gain against the input signal, even for the high frequency inputs, improving response fidelity score and the amplitude of the target frequency in the frequency spectrum of the output signal.

4.5.2 *Desynchronisation of Output Populations*

One readily apparent means by which Heterogeneity improves population response fidelity, is through the desynchronisation of the population response to the common input provided. Desynchronisation across a population of neurons provides them with a better temporal basis for the representation of the signals they deal with, as each neuron is able to fire independently and code for a different temporal component of the signal. In synchronised populations the temporal basis for representation is reduced for that population, becoming a single "cluster" state of neurons, were the firing patterns of the neurons become identical [54] [58], due to the

synchronising effect of the common input received by the neurons, and the effects subthreshold input has on the the timing of neuronal firing, driving a population towards near threshold, before an input sufficient to elicit a spike arrives [72]. Even minor commonality of input in Homogeneous populations impedes those population's ability to representation information [139].

Although no specific measure of population synchrony was used in the current work, the extent to which Homogeneous populations become synchronised, and the impact of this synchrony on the population response can be seen by comparing the response of Homogeneous populations receiving an input with no noise, with the response of populations with Heterogeneity or those receiving noisy input. Figure 4.40 shows the response of a Homogeneous population receiving a current injection input with no noise added, at 12Hz target frequency (mo output from stage 1. The amplitude of the output and the input has been normalised using standardisation through Z-Scores (as previously described), but with a mean of 1, rather than 0, in order to illustrate the synchronisation more clearly). Large peaks in the output response are seen during the cycles, followed by periods of response with gain matching the input poorly, showing large numbers of individual neurons of the population firing within the same 5ms of each other.

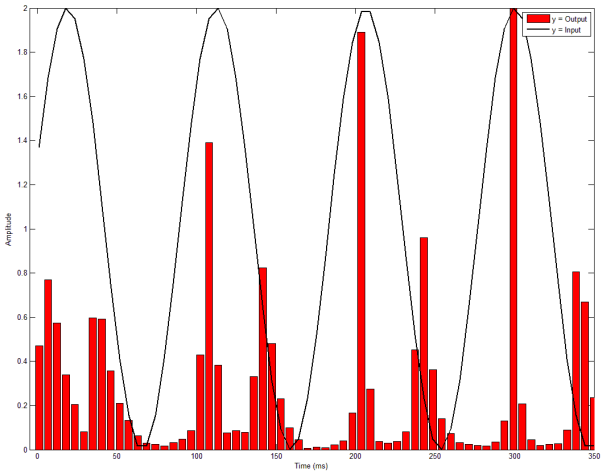

Figure 4.40: Illustration of Synchronisation in Homogeneous Population Receiving 12Hz Current Injection Input (No Noise). Example of PSTH normalised with mean 1, for 350ms of simulation.

In comparison to the above, Figures 4.41 and 4.42 show the responses of a Homogeneous population receiving a noisy input (12Hz, m1 from stage 1), and a Heterogeneous population receiving a input with no noise (12Hz, m2 from stage 1). The diversity of response (elicited either through the added Gaussian noise of the input, or the diverse spontaneous firing rates of the population members) leads to an increased desynchronisation in the response of the population.

Peaks are still apparent in the response, but they are not as severe as those seen in the more synchronised population above. The populations do not produce spikes within the same 5ms, and instead their spikes are spread out to the adjacent bins, reducing the relative magnitude of the peaks, and improving the gain of the response for each cycle. That is, the population is not synchronised to the common input signal, with the desynchronisation produced by noise or heterogeneity allowing a smoother response, matched more closely to the input signal.

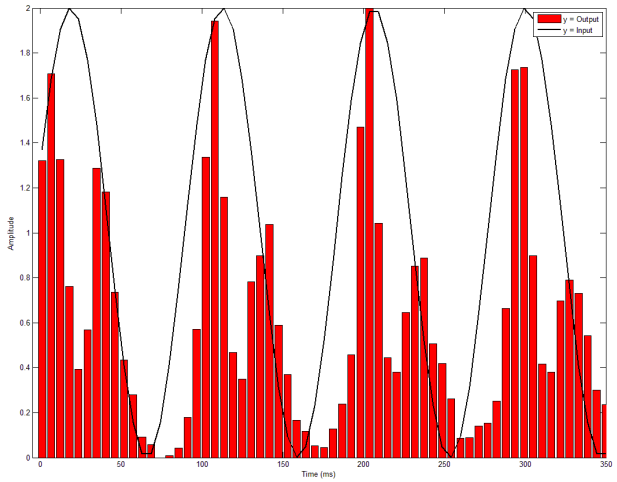

Figure 4.41: Illustration of Synchronisation in Homogeneous Population Receiving 12Hz Current Injection Input, with Added Gaussian Noise. Example of PSTH normalised with mean 1, for 350ms of simulation.

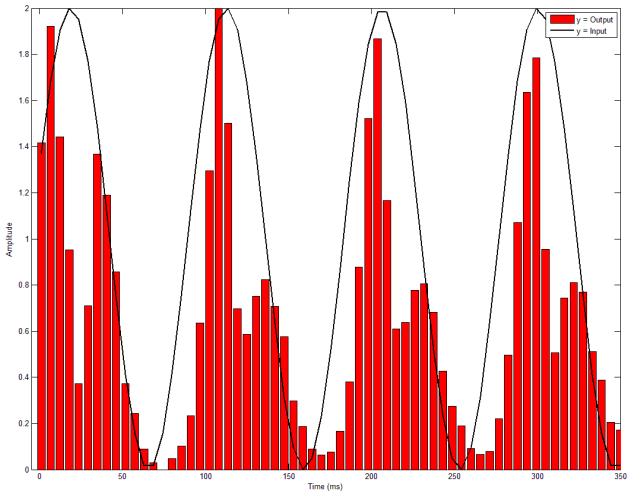

Figure 4.42: Illustration of Synchronisation in Heterogeneous Population Receiving 12Hz Current Injection Input (No Noise). Example of PSTH normalised with mean of 1, for 350ms of simulation.

Figure 4.43 shows the response of a population of model MVNB neurons with both Heterogeneity and receiving a noisy input (12Hz). The population shows very little synchrony (aside from the single peak in each cycle that would be expected from a close reproduction of the input signal) with the response of the population spread out across the duration of each cycle. Again, this smooths the population response, allowing it to more closely match the input signal provided.

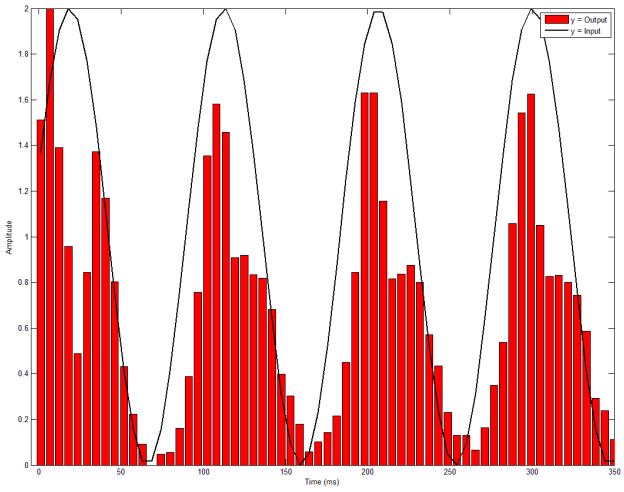

Figure 4.43: Illustration of Synchronisation in Heterogeneous Population Receiving 12Hz Current Injection Input, with Added Gaussian Noise. Example of PSTH normalised with mean of 1, for 350ms of simulation.

The desynchronisation of Heterogeneous populations is repeated in those simulated in stage 3 (and stage 2, although no Homogeneous populations were simulated in this stage), although the synchronisation of Homogeneous populations is not as apparent in these simulations, most likely due to the inhomogeneous input spike trains that were used in this stage of simulations. That is, the common input signal received by each member of the Homogeneous population is slightly varied, due to the variance present in each spike train adding variance to the population response. However, this variance was not enough to remove the synchronisation of the population entirely, as we still see large peaks of response amplitude surrounded by lower amplitude response bins, showing a lack of smooth response to the input signal.

4.5.3 *Effect of Noise on Response Fidelity*

Results from stage 1 of simulations showed that, when population heterogeneity was simulated through the addition of a bias current to individual cells, thus varying their spontaneous firing rates, the addition of noise to the input signal (current injection) led to a significant improvement

of response fidelity scores over those of Heterogeneous populations receiving an input signal with no added noise. However, in the second stage of simulations, in which population heterogeneity was modelled through the manipulation of K-Slow conductances, the addition of Gaussian noise to the input current injection led to a significant decrease in response fidelity, for both high and low volume noise. This significant decrease in response fidelity was seen across all input amplitude/means used in this stage, and all target frequencies used by the inputs.

Due a lack of direct control in the noise inherent in the spike train inputs used in stage 3 (and the lack of inputs with absolutely no 'noise'), no benefit or detriment from noise in those results can be seen. However, as the Heterogeneous and Homogeneous populations shared the same input generation methods, and effectively used the same input spike trains to drive their synaptic inputs, we can assume that any differences seen in the performance between Heterogeneous and Homogeneous populations were not due to any noise introduced by the inputs (that is, any noise in the input trains is shared between the two conditions).

Why the introduction of noise into the inputs of Heterogeneous populations may lead to a significant decrease in response fidelity, when previous studies on model MVN neurons have shown an improvement from combined noise and heterogeneity [68] may be due to the competing effects of noise and heterogeneity [72], or the specific means by which Heterogeneity has been modelled in our simulations.

In support of the idea that competing benefits of noise and heterogeneity may be at play, it has been found (using leaky integrate-and-fire and FitzHugh-Nagamo models of neurons) that the addition of noise to a Heterogeneous population of neurons reduces the information capacity of that population, degrading the performance of that population [72]. This is possibly due to the shared mechanisms by which the benefits of Noise and Heterogeneity arise.

Alternatively, the detriment to response fidelity from noise may be due to the volume of the noise used in stage 2 of simulations, compared to the strength of the input currents used at this stage. Lower volume noise caused less of a performance decrease to the population outputs (as measured by response fidelity) than high volume noise. Or, rather, the higher the volume of noise, the greater the impact on response fidelity from the populations. Further to this, if we compare the effect of noise to response fidelity by the magnitudes of the input currents used in this stage, we see that, as the input magnitude (amplitude/mean) increases (and the ratio between the noise added and the signal increases), the detriment to response fidelity reduces. These comparisons are shown in Figures 4.44 and 4.45. For all input frequencies used (except 20Hz with 20pA noise

condition), as the input magnitude increases, while noise volume remains constant, performance increases significantly ($p < 0.05$) except for the 50pA and 75pA input conditions (increase in response fidelity is seen, but not significantly so). This could reflect the fact that we have chosen non-optimal volumes of noise, compared to the magnitude of the input currents used, and that perhaps lower volumes of noise than 20pA, maybe improve response fidelity over simulations with no noise included in the input currents.

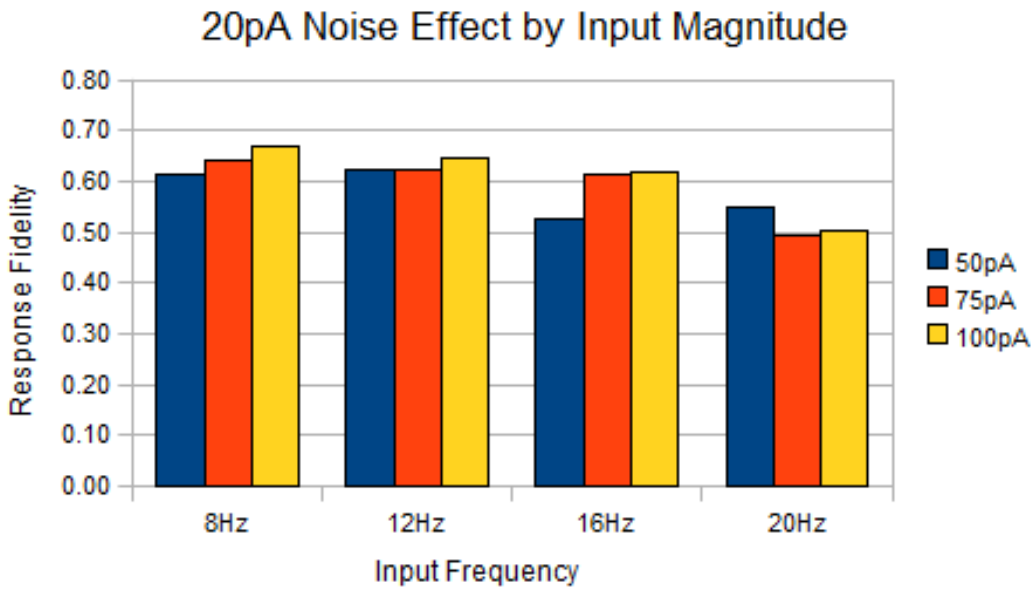

Figure 4.44: Comparison of the Effect of 20pA Noise on Response Fidelity with Input Magnitude. Variance was extremely minor (<0.001) and so is not shown in figure

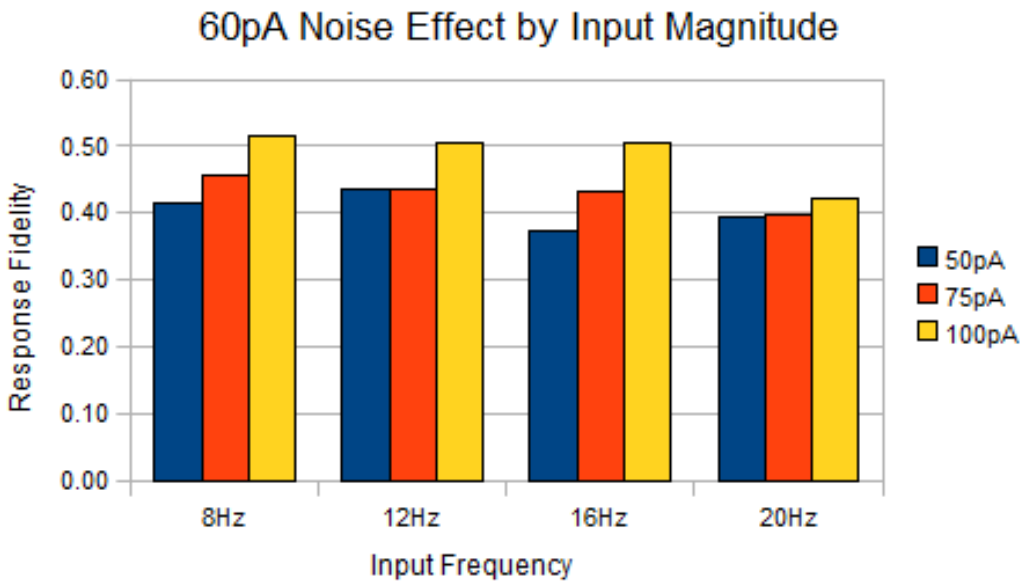

Figure 4.45: Comparison of the Effect of 20pA Noise on Response Fidelity with Input Magnitude. Variance was extremely minor (<0.001) and so is not shown in figure

4.5.4 *Phase Leads in Stage 3 Heterogeneous Populations*

Although initially the response fidelity scores of some Heterogeneous populations in stage 3 were found to be significantly lower than those for comparable Homogeneous populations, once the presence of phase lead in these Heterogeneous populations was estimated and accounted for, the response fidelity of these populations was seen to be significantly greater than the Homogeneous populations. The presence of phase leads in all stages of the Vestibulo-Ocular Reflex is proposed from the literature, both in the real system [98] [32] [69] [70] [74] [106], and in model VOR systems [117], especially in response to High frequency inputs, such as those that have been investigated in the current work. Investigation of the phase lead present in the VOR is important not only to understanding of the normal VOR function, but also to the clinical investigation of the deficient VOR [66].

Firstly, during high frequency rotations (up to 15Hz) some phase lag would be expected from the response, due to an estimated 7ms delay in the response from the three neuron arc which produces it [98]. However, for these rotations it was found that phase lag was reduced from the expected values, thus suggesting the presence of phase lead effects in the individual stages of neural processing to compensate for the lag that would arise naturally from the delay [98]. This was supported in further studies of VOR response dynamics, showing a near phase response for

high frequency rotations, up to 15Hz [74]. Thus, the phase lag arising from the inevitable delay involved in the neural processing of the VOR response is almost certainly compensated for by the involvement of phase lead somewhere in the individual stages involved in the processing.

Recordings of MVN neurons in response to rotations (up to 4Hz) in the alert monkey, showed a significant phase lead in their responses, of up to 30 degrees relative to head velocity [32]. This phase lead aspect reflected a similar phase lead seen in irregular vestibular afferents [32]. However, a lack of correspondence between the input signals used in our work, and the actual head velocities they would represent, does not allow us to compare the magnitudes of lead seen in our models, with that present in the real system. Integrate-and-Fire modelling studies of irregular Central Vestibular Nucleus neurons reproduced this observed phase lead [117]. Interestingly, it was suggested from these modelling studies, that the phase lead of the model CVN neurons was due to the heterogeneity of modelled neuron's firing dynamics, arising from their intrinsic membrane properties.

Similarly to the phase lead present in Central Vestibular neurons, phase lead has been observed in the other stages of the VOR's neural circuitry. Regular afferents showed increasing phase lead for rotational frequencies up to 20Hz [69]. However, while we see reduction of phase lead as input frequency increases, this likely reflects our modelling of the irregular MVN neurons, and some differences between the pathways of the VOR which the two types of neurons (irregular/regular) are involved (linear/non-adaptive vs non-linear/adaptive). Recordings of Vestibular afferents and neurons of the Abducens Nuclei (the third stage of the VOR, after the Central Vestibular Nucleus neurons) showed equal phase for low frequencies (<4Hz), with significant and increasing phase leads as rotation frequency increased (up to 50Hz) [106].

Accommodation of phase lead is therefore justifiable for the results presented here. Phase lead must be present in the individual components, to account for the phase lag introduced by delay of the neural components of the circuit involved. Our finding of phase lead in some simulation conditions in response to inputs representing high frequency rotations is in line with experimental findings, as well as predictions from alternative modelling of the neurons involved. In addition, although we have not concretely tied the velocity of head rotations represented by our input signals, increased mean and amplitude of the spike trains does, broadly, represent increased velocity of these rotations (thus input set A03 represents the lowest velocity of the rotational movements, and A02 the highest velocity), and as such we see more phase lead present with the A02 input set, and less with the A03 input set. Recordings of Vestibular afferent neurons

involved in the rotational VOR of the Chinchilla showed phase leads for high frequency rotations, with increasing phase lead as rotational velocity increased [70]. Our results generally match this relation, with the inputs representing higher velocity rotations causing increased phase lead, compared to the inputs representing lower velocities.

That the observed phase shift (when observed) is a genuine phase lead, and not a phase lag, is shown in Figure 4.46 below, which shows the initial response of a Heterogeneous population, from the very first cycle of the input, for an 8Hz input using input set A01 with 60 synapses of weight 1.0. This population showed a phase lead of 10ms occurring with the first cycle of the input, and continuing throughout the duration of the simulation.

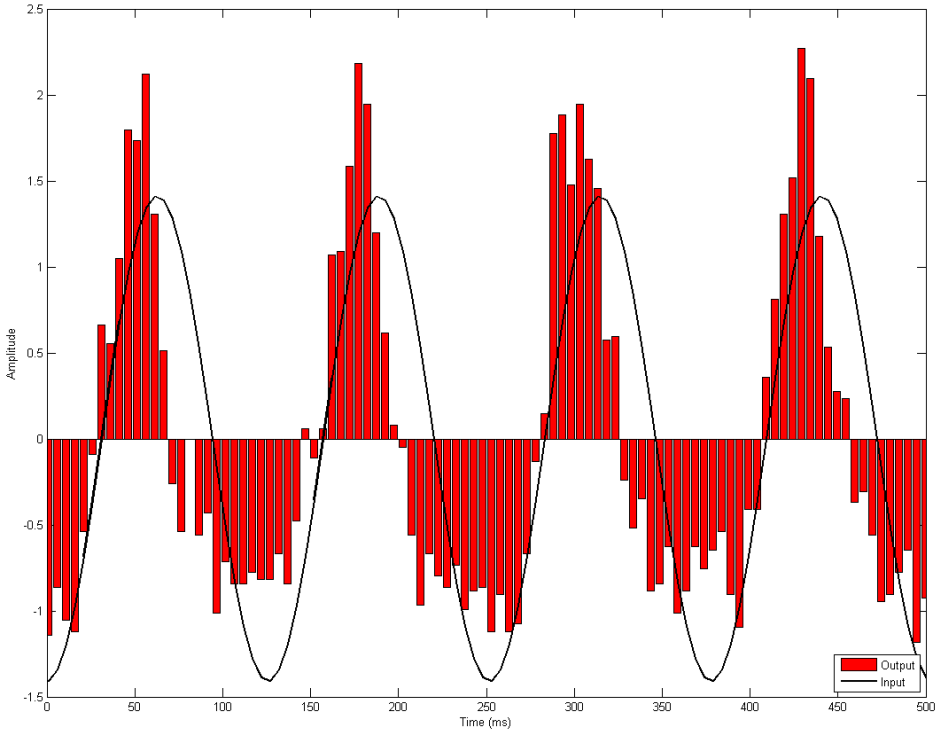

Figure 4.46: Initial response of a Heterogeneous population to the first cycle of an 8Hz input. This illustrates that the initial response shows a phase lead which continues for the duration of the simulation, and not a phase lag.

The cause of the apparent phase lead seen in the results presented here is largely down to the population response rising in volume slightly faster than the corresponding synaptic input provided for the latter half of the up-cycle, reaching its peak earlier than the corresponding input, and decreasing earlier and significantly faster in the first half of the down-cycle than the input. In

effect, this shifts the peak volume of the output to an earlier time than the corresponding input, essentially causing the output wave to lead the input wave, and to appear narrower for the upper half of the cycle. This is shown in Figure 4.47, which shows the corrected response (10ms) for a Heterogeneous population receiving an 8Hz input. Apparent is the slightly steeper increase in response for the latter half of the up-cycle (output increases slightly faster than input above the mean of 0) and the significantly steeper decrease of the output compared to the input for the first half of the down-cycle (large gaps between the output and input above the mean of 0). This faster increase, and earlier and faster decrease in response for the upper half essentially skews the uncorrected response to the left, causing an apparent phase lead from the population.

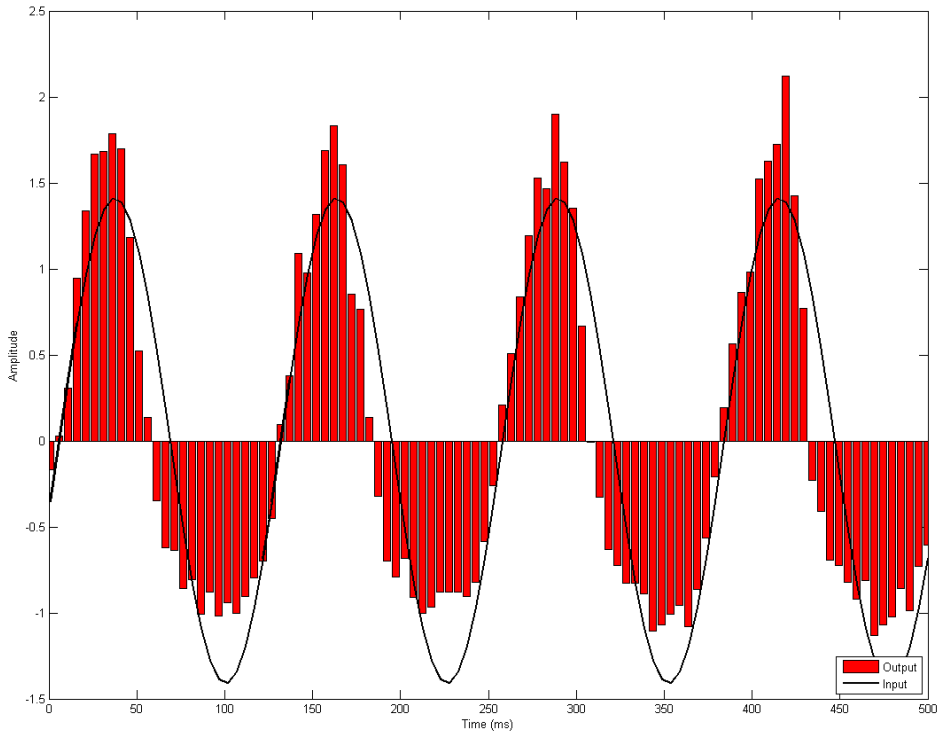

Figure 4.47: Phase corrected response of Heterogeneous population receiving 8Hz input. Corrected for 10ms phase lead. This illustrates the slightly faster increase, and significantly faster decrease of population output response compared to the input, for the upper half (above mean 0) of the population response.

The skewing caused by the non-linear response is more apparent in Figure 4.48, which shows the uncorrected response of the same population as in Figure 4.47 above. The faster, non-linear

rise and decline in population output essentially shifts the response to the left, causing it to lead the input provided.

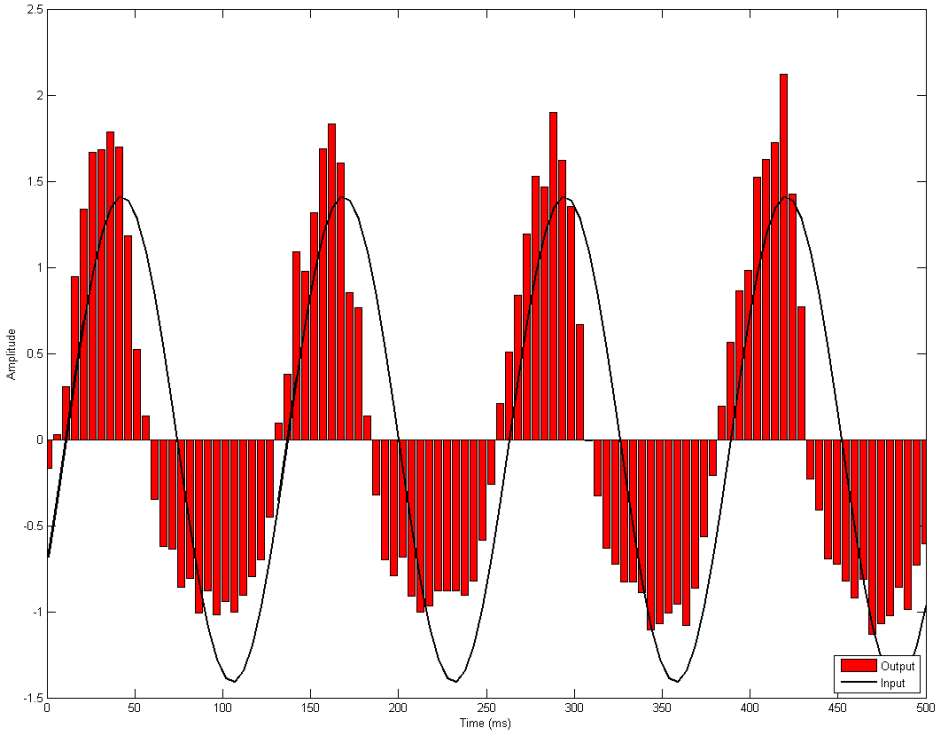

Figure 4.48: Uncorrected response of Heterogeneous population receiving 8Hz input. This illustrates the slightly faster increase, and significantly faster decrease of population output response compared to the input, for the upper half (above mean 0) of the population response.

This slightly non-linear increase and decrease in output response is largely due to the nature of the synaptic mechanisms implemented in the simulations, with increased input leading to saturation of the population, and the corresponding non-linear decrease in population output. This would explain why, with larger input amplitudes (i.e. input set A02) and with increased synapse numbers and weight, we see more and larger phase leads.

Interestingly, the phase leads apparent in these results are not present in the input trains driving the population response, possibly suggesting that it arises from the intrinsic properties of the neurons simulated, rather than the properties of the inputs driving them. Finally, it should be noted that the precision of the phase lead estimates we have made is hampered by the resolution of our analysis, in that we only estimate the phase lead within 5ms, tied to the bin size chosen for our response fidelity analysis.

4.5.5 *Accounting for Random Errors*

Although the results presented thus far have been the mean response fidelity scores of 10 populations of 500 neurons each (n=500), in order to ascertain any possible effects of Random Error (introduced from the random selection of neuron firing rates across a population), and to isolate those Random Errors from any Systematic Errors present (introduced by the simulation methods used), further simulations were conducted such that average response fidelities could be calculated over larger number of neurons.

For this, response fidelities were calculated for 10 populations of 1000 and 5000 MVNB neurons, using the Stage 3 experimental setup, across all conditions present in Stage 3. That is, Stage 3 simulations were replicated with these increased population sizes (n=1000 and n=5000). Any Random Error, if it were present, would thus be reduced in the larger populations. This process, of investigating the presence of Random Error in populations of different size, is somewhat similar to the process used in previous work examining performance of feedback networks of Artificial Neuron models, using delta-rule learning, between populations of size n=100 and n=1000 [107].

However, in the work presented here, the response fidelity scores, and the variance across the 10 populations, for populations of 1000 and 5000 neurons were found to be almost identical to those found for populations of 500 neurons. That is, both the average response fidelity scores of 10 populations, and the variance of scores across these 10 populations were found to be near identical to those found in Stage 3 previously. Where a difference was found (as in the case of Figure 4.48 below) the difference was negligible, and far from being significant. As with previous results, only minor variance (<0.001) was observed in the response fidelity scores across the 10 populations. Figures 4.49, 4.50, and 4.51 show the response fidelity scores for all input frequencies, using input parameters A01, A02, and A03, with synapse weight 0.1 and 20 synapses. Other parameter sets showed similar results, in that there was no significant change in response fidelity or variance found.

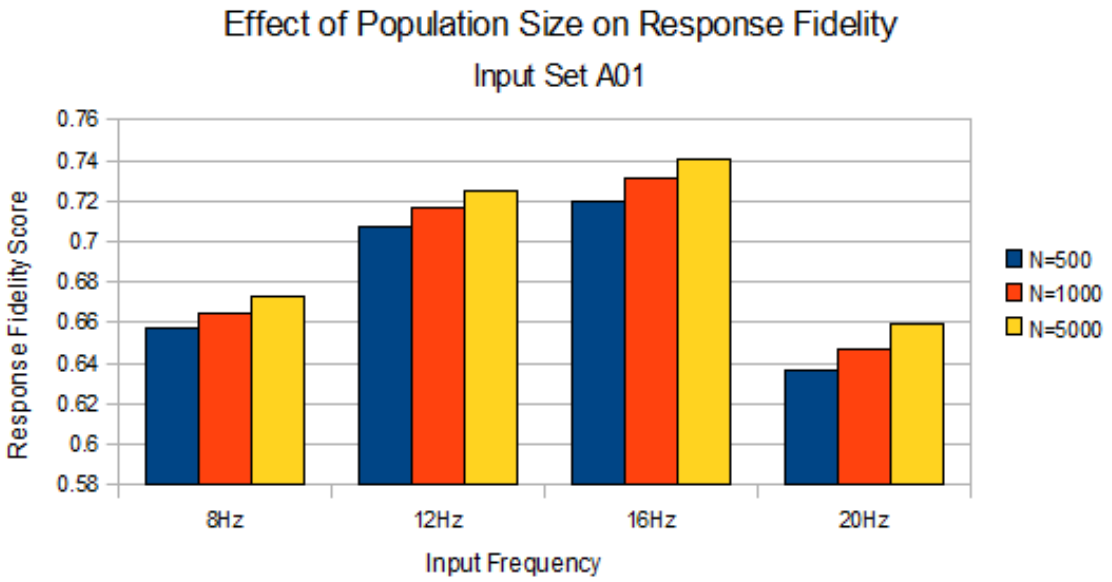

Figure 4.49: Comparison of the Effect of Population Size on the Response Fidelity of Stage 3 simulations. Average response fidelity scores for populations of 500, 1000, and 5000 MVNB Neurons simulated with the Stage 3 experimental setup, for input set A01, with synapse weight 0.1 and 20 synapses. No significant differences were found for the increased population sizes. Variance was extremely minor (<0.001) and so is not shown in figure

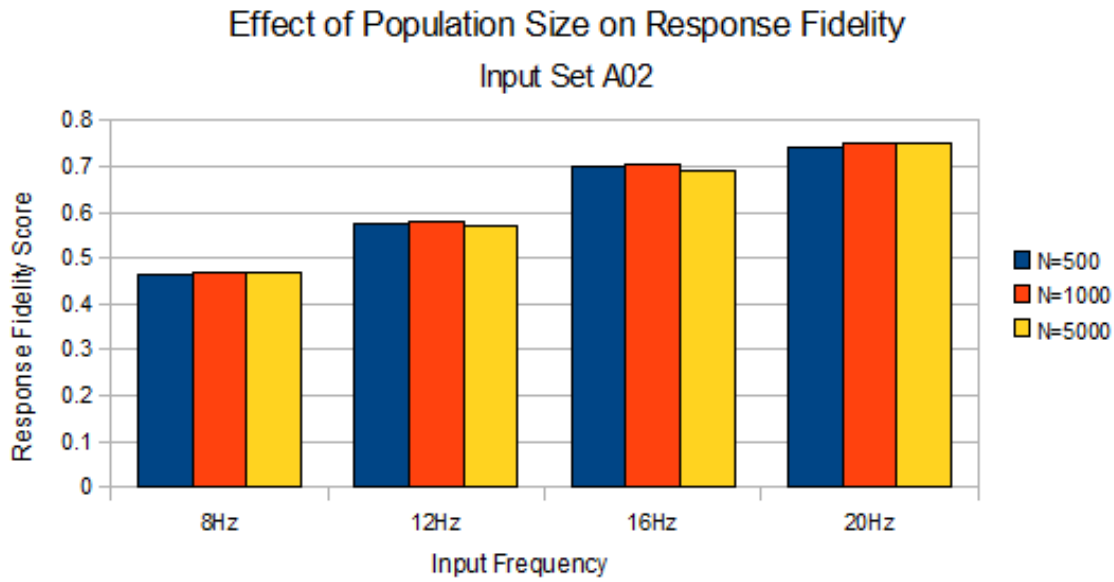

Figure 4.50: Comparison of the Effect of Population Size on the Response Fidelity of Stage 3 simulations. Average response fidelity scores for populations of 500, 1000, and 5000 MVNB Neurons simulated with the Stage 3 experimental setup, for input set A02, with synapse weight 0.1 and 20 synapses. No differences were found for the increased population sizes. Variance was extremely minor (<0.001) and so is not shown if figure

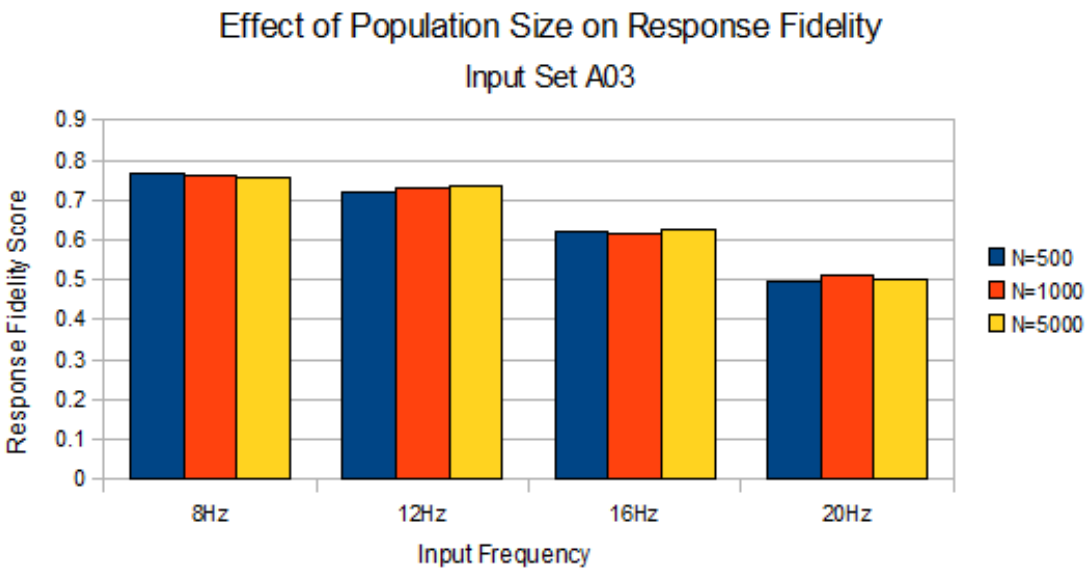

Figure 4.51: Comparison of the Effect of Population Size on the Response Fidelity of Stage 3 simulations. Average response fidelity scores for populations of 500, 1000, and 5000 MVNB Neurons simulated with the Stage 3 experimental setup, for input set A03, with synapse weight 0.1 and 20 synapses. No differences were found for the increased population sizes. Variance was extremely minor (<0.001) and so is not shown if figure

Therefore, as no significant difference in either response fidelity scores, or the variance of response fidelity scores across 10 populations, was seen with increased population sizes, it can be concluded that any Random Error present in the simulations performed are already eliminated or mitigated by the population size (n=500) and number of populations (10) used throughout the work presented. This would be in line with previous work on the implications of Heterogeneity in the Vestibulo-Ocular Reflex (using leaky integrate-and-fire models, work which we have largely replicated using the more biophysically complete Compartmental neuron models), which found that a population of size n=500 was sufficient to convey the population response to sinusoidal inputs of varying frequency, over a subset of these populations (n=10)[68].

4.5.6 *Performance to Arbitrary Input Amplitudes and Frequencies*

The results presented thus far have been obtained through the simulation of populations to each input frequency and amplitude independently. In order to ascertain the performance of a population with the same settings of parameters (K-Slow densities and initial membrane voltages across the population) to input of arbitrary amplitude and frequency, further simulations were performed and analysed, using arbitrarily chosen input conditions, in which the setup parameters

of the populations were maintained across simulations. In effect, this simulated the performance of the same population in transmitting arbitrarily chosen input frequencies and amplitudes.

Initially two recurring populations (Population 1 and Population 2) were simulated across all four input frequencies (8, 12, 16, and 20Hz), maintaining the parameters of the two populations across each of the simulations (in effect simulating the performance of the same population to all four, or arbitrary, input frequencies) with arbitrarily chosen synapse weights and numbers[3] using the A01 input set (input mean of 50Hz and amplitude of 25Hz). As the input set used was constant across the simulations, this only investigated the ability of a given population to transmit an input of arbitrary frequency, but not amplitude.

The performance of these two populations was compared against the results for the given input parameters from Stage 3, to ascertain if there was any difference in performance between the two sets of results (that is, does a single population perform the same, and transmit the same arbitrary signal frequency, as the independent populations). Performance (response fidelity score) was near identical to performance seen in the main Stage 3 results (that is, there were no significant differences in response fidelity scores for the single recurring, or constant, populations compared to the independent populations. Differences in response fidelity score were, at most, 0.01). The results for populations 1 and 2, compared to the performance of the Stage 3 populations are shown in Figures 4.52 and 4.53 below. From this, it can be concluded that the same population (with the same setup parameters of K-Slow densities and initial membrane voltage) can transmit inputs of arbitrary frequency.

3 Synapse weights and numbers for the 2 sets of simulations were as follows: Population 1 - 8Hz number of synapses = 20, weight = 1.0; 12Hz, nsyn=40, w=0.5; 16Hz, nsyn=40, w=0.5; 20Hz, nsyn=20, w=0.1. Population 2 - 8Hz, nsyn=60, w=0.5; 16Hz, nsyn=40, w=0.1; 20Hz, nsyn=20, w=0.5.

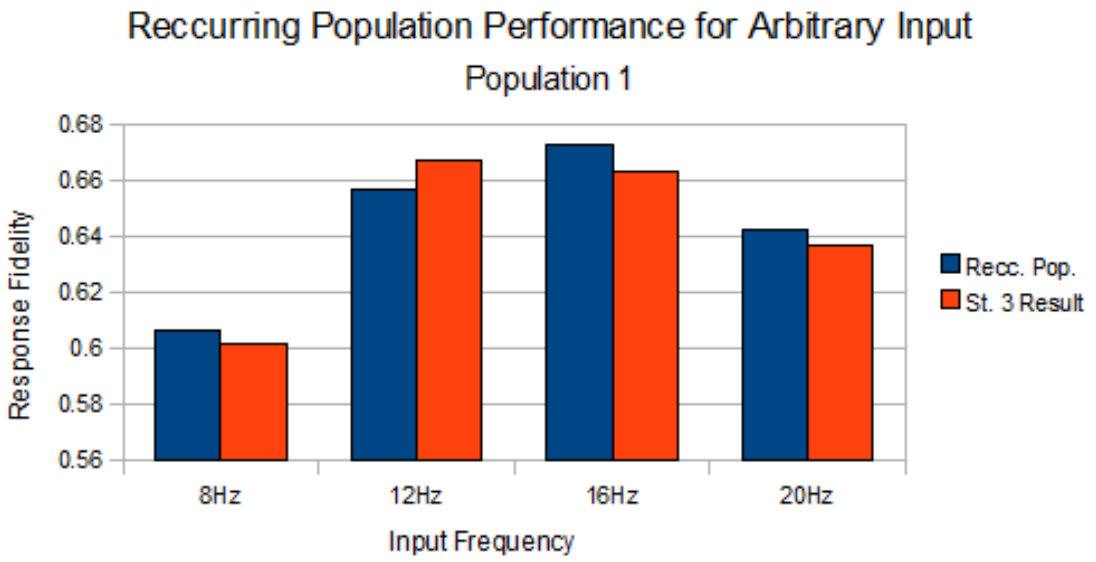

Figure 4.52: Comparison of performance for recurring Population 1 against performance from the independently chosen populations used in Stage 3. No significant differences in performance were found.

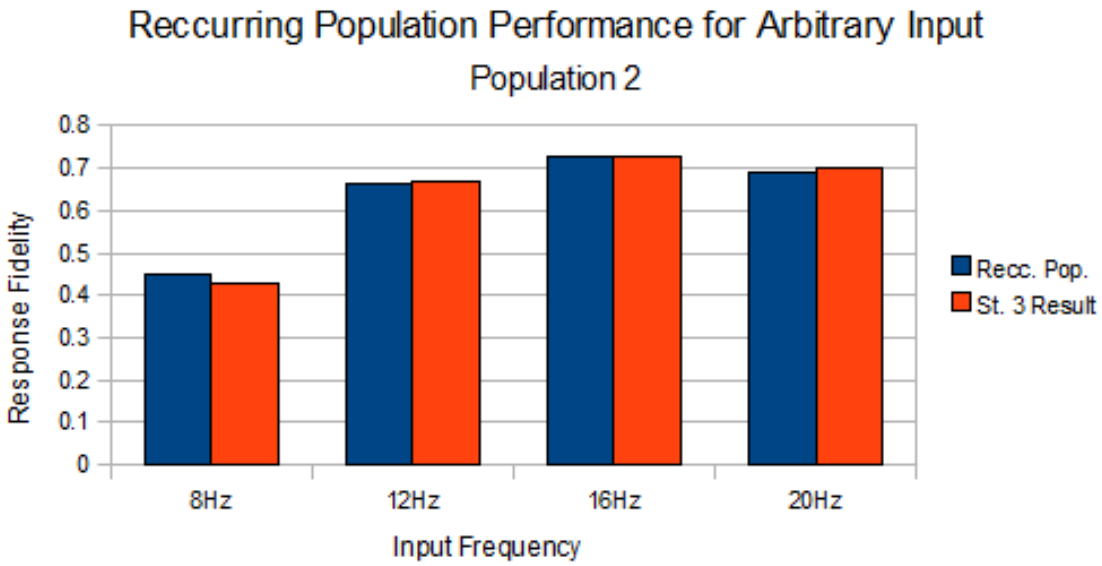

Figure 4.53: Comparison of performance for recurring Population 2 against performance from the independently chosen populations used in Stage 3. No significant differences in performance were found.

Further to these, in order to determine the ability of a recurring population to transmit an input of both arbitrary input frequency and amplitude, a third population was simulated (Population 3) across all 4 input frequencies, and across all 3 input sets (therefore, all 4 input frequencies across all 3 input amplitudes and means. In effect simulating the performance of the same population to

all four, or arbitrary, input frequencies, and all 3, or arbitrary input amplitudes) with arbitrarily chosen synapse numbers and weights[4]. As the same recurring population was simulated with both different input frequencies and input amplitudes, this investigated the ability of a given population to transmit an input of arbitrary frequency and amplitude.

The performance of this recurring population was compared against that of independent populations simulated in Stage 3 of the work presented. Performance of the recurring population was found to be near identical to the performance of the independent populations. The results for Population 3, compared with those of the independent populations of Stage 3 are shown, for each input set, are shown in Figures 4.54, 4.55, and 4.56 below. From this, it can be concluded that the same population (with the same setup parameters of K-Slow densities and initial membrane voltage) can sufficiently transmit inputs of arbitrary frequency and amplitude.

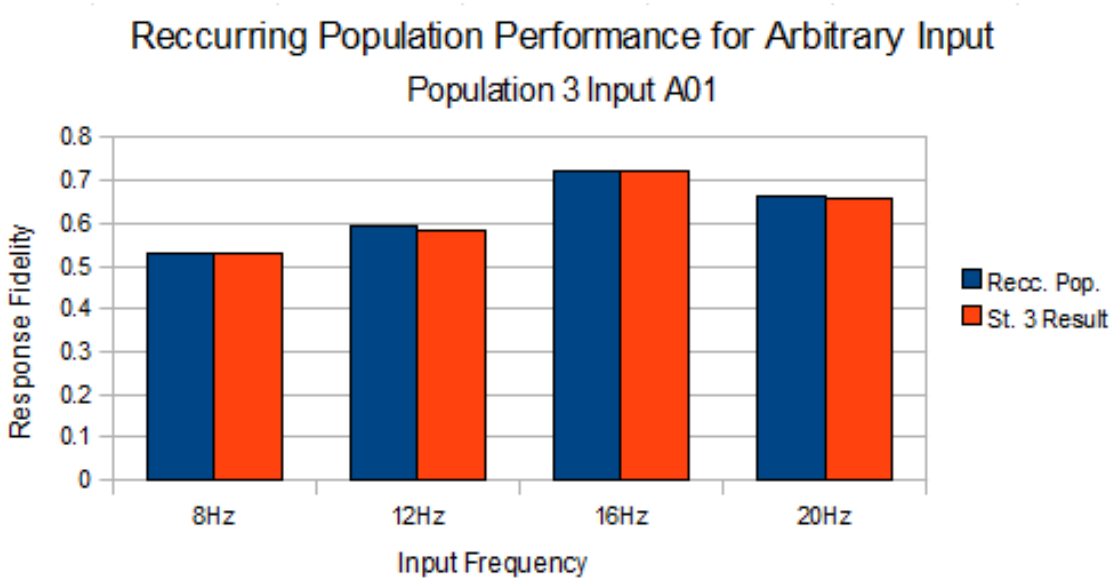

Figure 4.54: Comparison of performance for recurring Population 3 against performance from the independently chosen populations used in Stage 3, for input set A01 (mean of 50Hz, amplitude of 25Hz). No significant differences in performance were found.

4 Synapse numbers and weights were as follows: Population 3 - 8Hz, nsyn=40, w=0.1; 12Hz, nsyn=60, w=0.5; 16Hz, nsyn=20, w=0.1; 20Hz, nsyn=40, w=1.0.

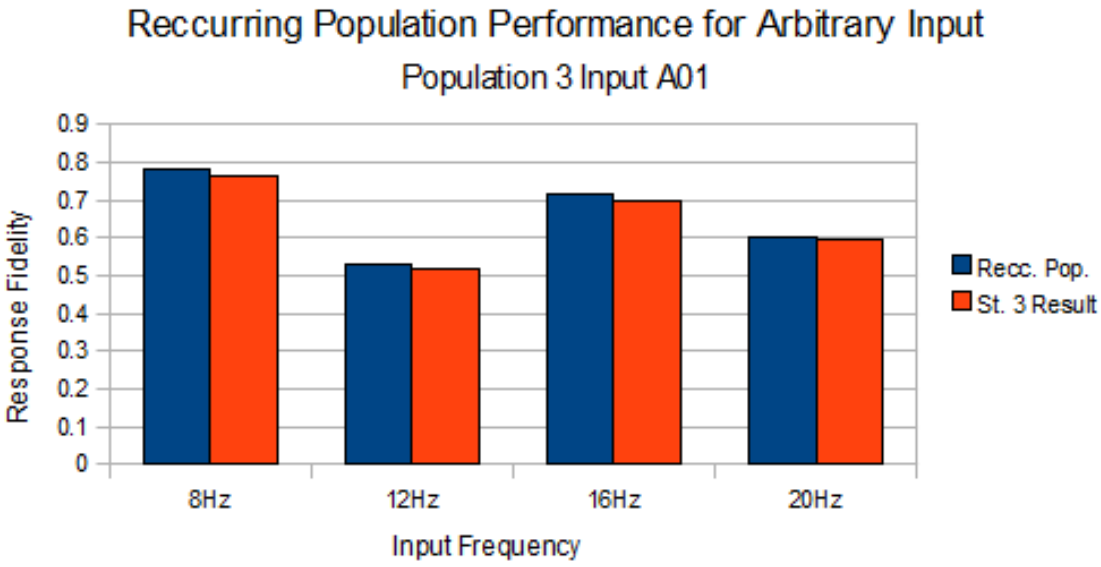

Figure 4.55: Comparison of performance for recurring Population 3 against performance from the independently chosen populations used in Stage 3, for input set A02 (mean of 75Hz, amplitude of 25Hz). No significant differences in performance were found.

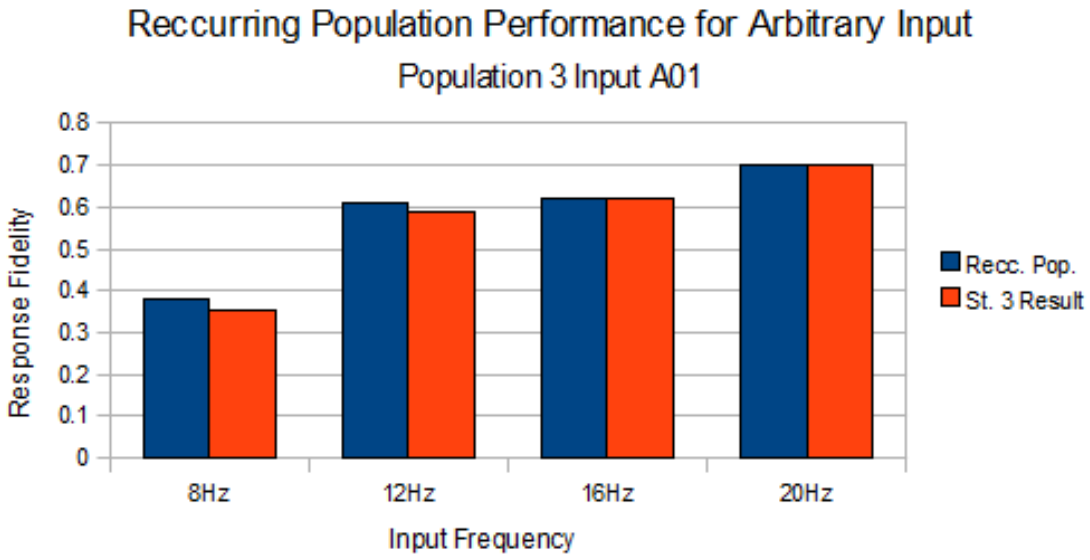

Figure 4.56: Comparison of performance for recurring Population 3 against performance from the independently chosen populations used in Stage 3, for input set A03 (mean of 35Hz, amplitude of 20Hz). No significant differences in performance were found.

5

DISCUSSION

5.1 DISCUSSION

Here we have presented work investigating the functional role of population heterogeneity in the fidelity of response from neuron populations. That is, we have investigated the functional role of population heterogeneity, in the form of diverse spontaneous firing rates, on the ability of that population to faithfully transmit high frequency inputs, using bio-physical models of MVN neurons involved in the linear Horizontal Vestibulo-Ocular reflex (hVOR) response. We have compared the performance of Heterogeneous populations with that of Homogeneous populations of the same (model) neurons, to the same inputs, to judge the effect of the Heterogeneity on a given response fidelity measure. Thus, we have investigated the role of the intrinsic membrane properties on the ability of neurons to produce a wide and dynamic range responses, rather than the circuit properties of the population. More so, we have investigated the specific means of diversity by which this population heterogeneity may arise, in the form of varied density of certain Ion channels of the neurons involved. Specifically, we have asked whether population heterogeneity in the form of the diversity of slow Voltage activated Potassium channel conductances across a population of MVN Type B neurons, creating a population of neurons with a distributed rate of spontaneous firing, leads to improved response fidelity of these Heterogeneous populations to high frequency inputs, over Homogeneous populations.

We have approached this through the simulating of the response of populations of model MVN Type B neurons involved in the hVOR, to high frequency inputs, across a range of input frequencies incorporating the high physical range of head rotations that these neurons are known to respond to faithfully and accurately to produce compensatory eye movement. We have measured the response fidelity of Heterogeneous and Homogeneous populations, to frequencies ranging from 8 to 20Hz, for input parameters representing various head velocities, and using various methods of both modelling the Heterogeneity of the populations, and the inputs provided to the populations. In this way we have evaluated the importance of the diverse intrinsic membrane properties

(conductance densities) in producing Heterogeneity (spontaneous firing rate) of model MVNB neurons, rather than the circuit properties (inputs).

The results presented in this work consistently show that Heterogeneous populations of model MVN Type B neurons, when that Heterogeneity takes the form of diverse spontaneous firing rates across the population, reproduce high frequency input signals significantly and consistently better than comparable Homogeneous populations. More, we have shown that, when the diversity of firing rates arises from Heterogeneous slow Potassium conductances across the population, the performance of Heterogeneous populations is significantly better than that of Homogeneous populations, suggesting that Heterogeneity of these Potassium conductances provides a specific means by which these populations are Heterogeneous, and a functional role for this Heterogeneity. Therefore, the results here indicate that population Heterogeneity in the form of the diversity of slow Voltage activated Potassium channel conductances across a population of MVN Type B neurons, creating a population of neurons with a distributed rate of spontaneous firing, does indeed lead to improved response fidelity of these Heterogeneous populations, over Homogeneous populations.

We have shown that the improvement to response fidelity from Heterogeneity is robust across a range of frequencies representing the high physical range the real VOR deals with, and that the improvement is consistent for a range of input magnitudes. More, the comparison of Homogeneous and Heterogeneous populations have shown that the circuit properties alone of the population cannot adequately explain the high frequency response of the MVN B populations, and that the intrinsic membrane properties of the neurons play an important role in their functioning. Further, we have shown that populations simulated here are capable of conveying inputs of arbitrary input frequency and amplitude, as well as demonstrating that the population size chosen for simulation are robust in regards to the mitigation or elimination of random errors.

Previous work has suggested a functional role for population Heterogeneity [72] [92], and shown a role for this Heterogeneity specifically in the high frequency response of the VOR [68] [5]. The work presented has confirmed the role of Heterogeneity in MVN B neurons for their processing high frequency responses, as well as suggesting a specific biological means by which the Heterogeneity of these populations is embodied, in the diversity of slow Potassium conductances. In addition, we have obtained these results using bio-physical, compartmental models of MVNB neurons, with a high-predictive value [104]. This is, to the author's knowledge, the first time a specific biological means for the functional population Heterogeneity of MVNB

neurons has been shown, and the first time this has been shown using bio-physical, compartmental models of MVNB neurons.

Neural Heterogeneity is a fact, with individual neurons, even within the same class, showing a wide range of diverse responses to the same stimuli [21]. Evidence has shown that diversity of ion channel expression, and the conductances arising from these channels, are responsible for Heterogeneity in the populations involved [37], and that this Heterogeneity is responsible for the diversity of responses seen in the neurons involved in the hVOR [109] [83] [20]. The work here is in line with these findings, showing that the diversity of response, and accuracy of population responses, may be achieved through the diversity of specific Potassium conductances in MVNB neurons.

Experimental [2] and theoretical work has shown a functional role of Heterogeneity in neural processing, both for general populations [72] [92], and in the neural processing of the VOR specifically [68] [5]. Particularly, the effect of desynchronisation on a population has been suggested as a functional role for Heterogeneity [54] [58]. Again, the results presented here support the idea of Heterogeneity (and the desynchronisation arising from this) as a means by which accurate population response fidelity is achieved in the MVNB neurons of the VOR, with Homogeneous populations showing highly synchronised responses, leading to poor response fidelity, and Heterogeneous populations showing less synchronisation and significantly improved response fidelity.

As discussed, the likely mechanism by which the population Heterogeneity modelled here improves the response fidelity of our populations is through the desynchronisation of the population response, producing a greater temporal basis over which the individual members of the population are able to respond [72]. Heterogeneous populations show little of the clustering of response (said clustering indicating synchrony) that is seen in comparable Homogeneous populations [54] [58], and show improved fidelity in their reproduction of high frequency inputs.

Interestingly, we found somewhat mixed results for a possible role of Noise in the improvement of response fidelity in our models. A beneficial role for noise has long been suggested in neural systems [17] [90] [91], in sensory-motor systems (such as the VOR) [125], and has specifically been suggested as a means by which VOR response fidelity may be improved [68]. Although we found a beneficial impact for noise in Homogeneous populations, the results of our simulations have shown a detrimental impact on Heterogeneous population's response fidelity when noise is introduced into the signals they process. Although the reason for this detrimental effect was

not investigated, it is suggested that this may be due to the competing benefits to processing provided by noise and Heterogeneity [72]. That is, both noise and Heterogeneity benefit neural processing through the same mechanisms (i.e., desynchronisation), and that, through combining the two, the benefits of both may be lost. Indeed, theoretical studies have shown a detriment to response performance when noise is added to Heterogeneous populations [72].

Another finding of interest from the results presented, is the emergence of phase lead in the population responses of Heterogeneous neurons for certain experimental conditions. The presence of phase leads (where the response shows a lead in time against the stimuli producing the response) in all stages of the Vestibulo-Ocular Reflex is apparent from the literature, both in the real system [98] [32] [69] [70] [74] [106], and in model VOR systems [117], especially in response to high frequency inputs, such as those that have been investigated in the current work. In order for the VOR to provide a fast and accurate compensatory movement to head movements, phase lead must be introduced in the response in order to counter the inevitable delay that arises from the neural processing across the three stages of the response arc. Although phase lead was not observed across all experimental conditions, we have shown the emergence of phase lead in the responses of model MVNB neurons to certain conditions, primarily increased input volume and synapse numbers and weight. Further, the phase lead evident in our results emerged not from the inputs driving the response (as there is no phase lead in the input), and may instead emerge from the intrinsic membrane properties of the population.

Although our results have shown a significant improvement to response fidelity from population Heterogeneity (and thus a significant role of Potassium channel diversity in that response), it has not shown that the Heterogeneity modelled here is the complete story, as far as the population response is concerned. Heterogeneous populations have shown a consistent improvement over Homogeneous populations, but have not shown a perfect translation of inputs in our population outputs (response fidelity scores approaching 0.9, comparable to findings that the VOR compensates for between 90% [98] and 80% [7] of head rotations in the dark).

This deficiency may arise from the response fidelity measure that has been implemented. Although robust in comparing the performance of Heterogeneous populations with Homogeneous populations, we may lose some of the true response accuracy present in the outputs of our populations, due to assumptions made in choosing the bin size for our analysis, and in the gain representation due to the normalisation of our population responses. The PSTH method used makes assumptions regarding bin size, disregards variations in firing within bin periods, and

shows possible errors in the localisation of spikes near bin edges [22]. However, the implementation of our second measure, looking at the magnitude of the target frequency component in the output of our populations, similar to methods suggested as an alternative to the PSTH method [22], and the results from this measure, go a long way to supporting the findings stated, and the satisfactory nature of the PSTH measure.

Another possibility for the deficiency in population response that we see may be the assumptions that we have made in regards to aspects other than the Heterogeneity of slow Potassium conductances in our models. It is unlikely that functional Heterogeneity in populations of MVNB neurons is limited to diversity of slow Potassium conductances alone, and differences in cell morphology (Soma size, dendritic structure and shape, number of dendritic branches) or Heterogeneity in other conductances may play a role in producing the real MVNB population response. In addition, the distribution of firing rates that we have used for our Heterogeneous populations may not match the distribution of real populations, which may be optimised for a more accurate reproduction of the signals they receive.

As such, one possible avenue for further research into the MVNB population response could be to look at different distributions of firing rates across the population, and their effect on response fidelity. Alternatively, the inclusion of known MVNB subtypes, exhibiting low voltage activated spike bursting arising from increased density of the low Voltage activated Calcium channels [118] [119] may be a possible means for improving the population response further.

Another possibility for future research could be the investigation of, and quantification of, the synchrony of our simulated populations, thus confirming the mechanism of desynchronisation in the improved response of the populations. Methods for the analysis and quantification are available in the literature [15], and could be applied, with some modification, to the models simulated in the present study.

Finally, the role of the inhibitory aspects of the hVOR response could be investigated, looking at the response of MVN populations in the context of the commissural inhibitory system [55] and the effects of the push-pull combination of Horizontal Semi-Circular Canals.

APPENDIX A

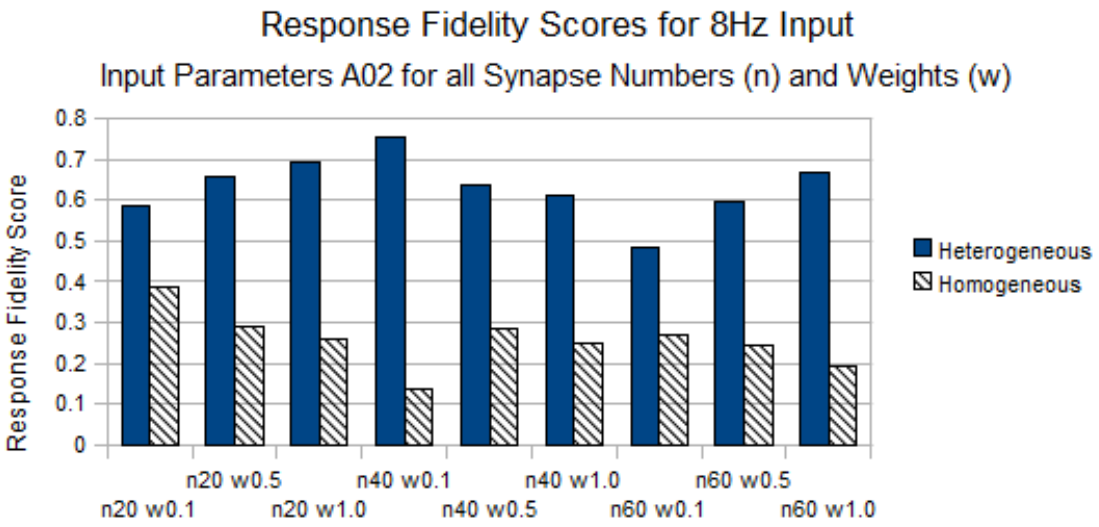

Figure A.1: Stage 3 Response Fidelity Comparison for 8Hz Input, Heterogeneous vs Homogeneous Populations. For A02 Input set, across all synapse numbers and weights

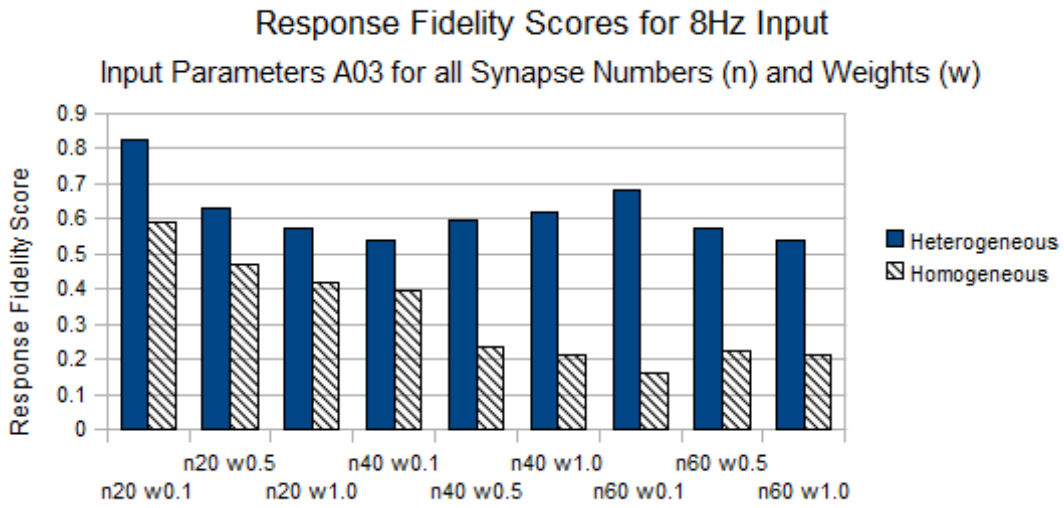

Figure A.2: Stage 3 Response Fidelity Comparison for 8Hz Input, Heterogeneous vs Homogeneous Populations. For A03 Input set, across all synapse numbers and weights

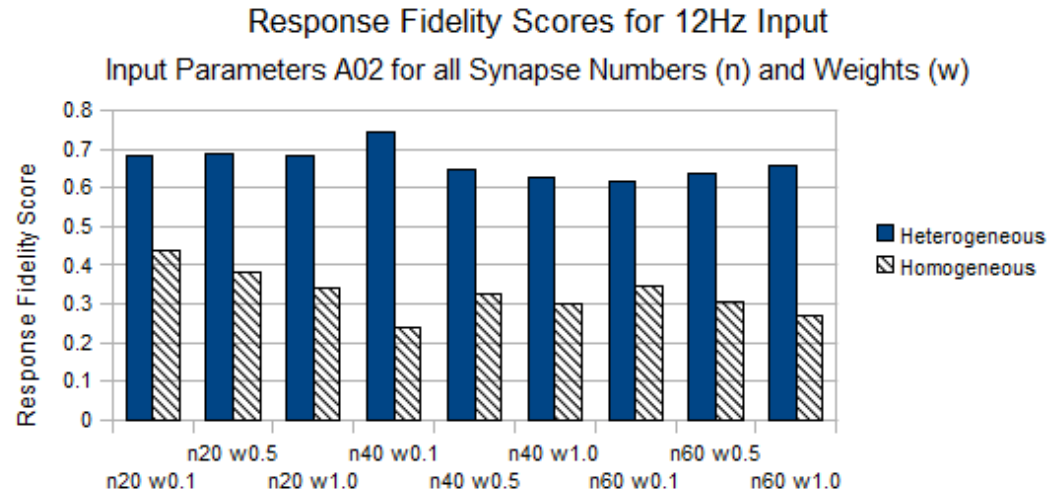

Figure A.3: Stage 3 Response Fidelity Comparison for 12Hz Input, Heterogeneous vs Homogeneous Populations. For A02 Input set, across all synapse numbers and weights

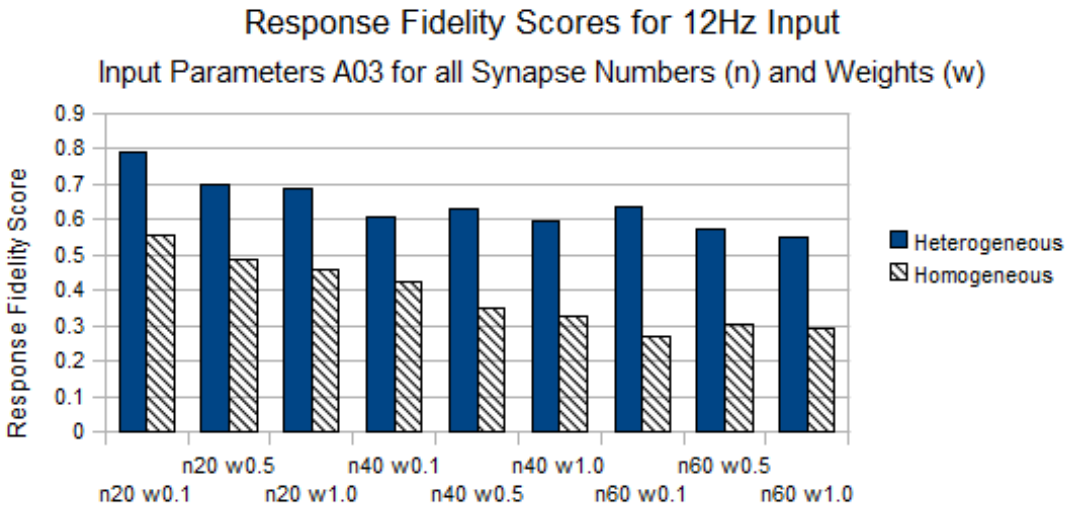

Figure A.4: Stage 3 Response Fidelity Comparison for 12Hz Input, Heterogeneous vs Homogeneous Populations. For A03 Input set, across all synapse numbers and weights

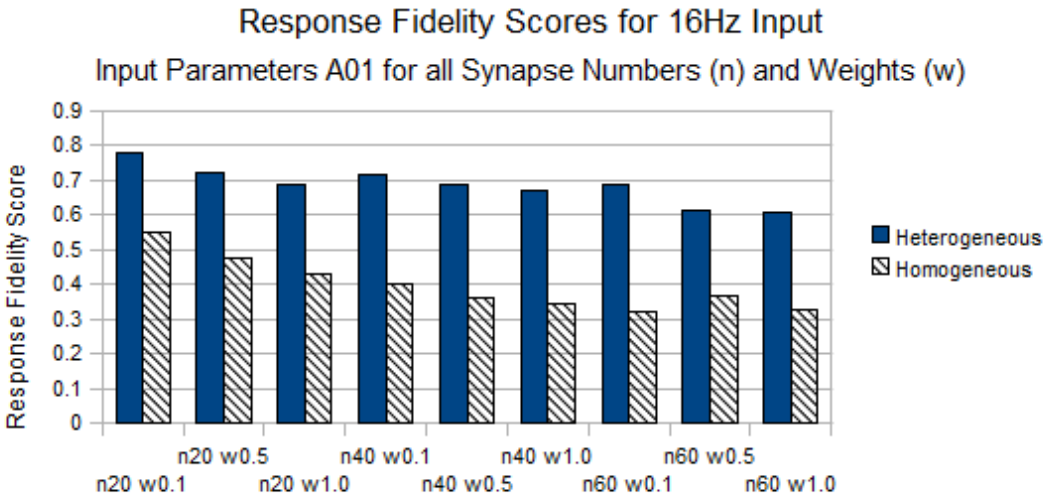

Figure A.5: Stage 3 Response Fidelity Comparison for 16Hz Input, Heterogeneous vs Homogeneous Populations. For A02 Input set, across all synapse numbers and weights

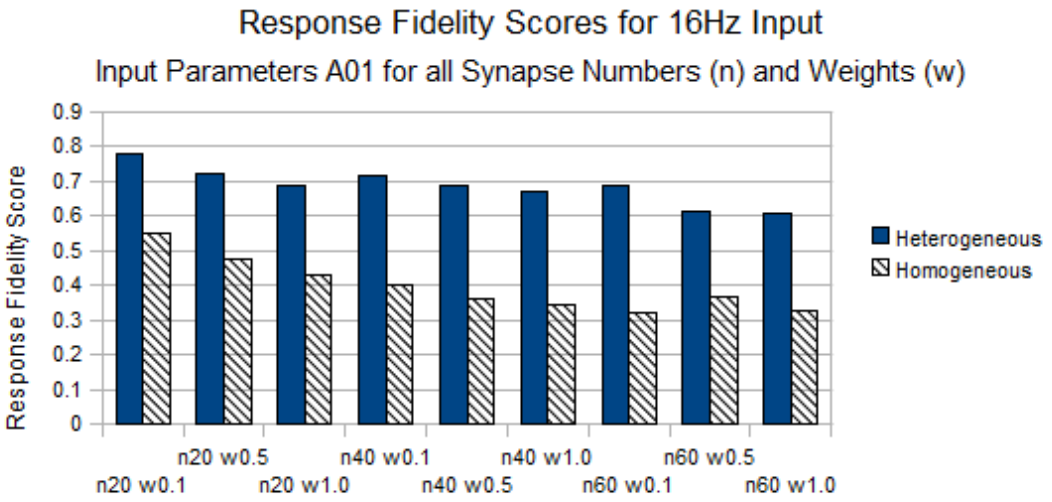

Figure A.6: Stage 3 Response Fidelity Comparison for 16Hz Input, Heterogeneous vs Homogeneous Populations. For A03 Input set, across all synapse numbers and weights

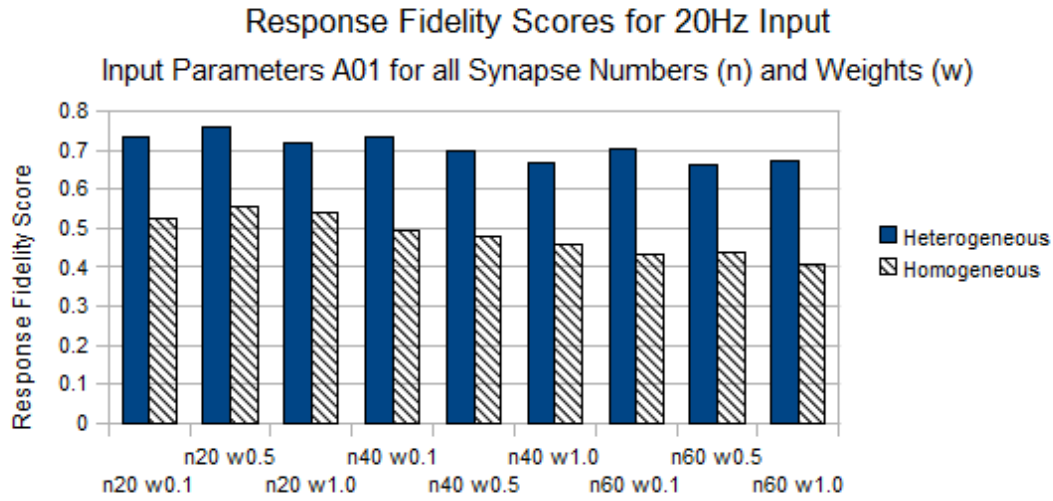

Figure A.7: Stage 3 Response Fidelity Comparison for 20Hz Input, Heterogeneous vs Homogeneous Populations. For A02 Input set, across all synapse numbers and weights

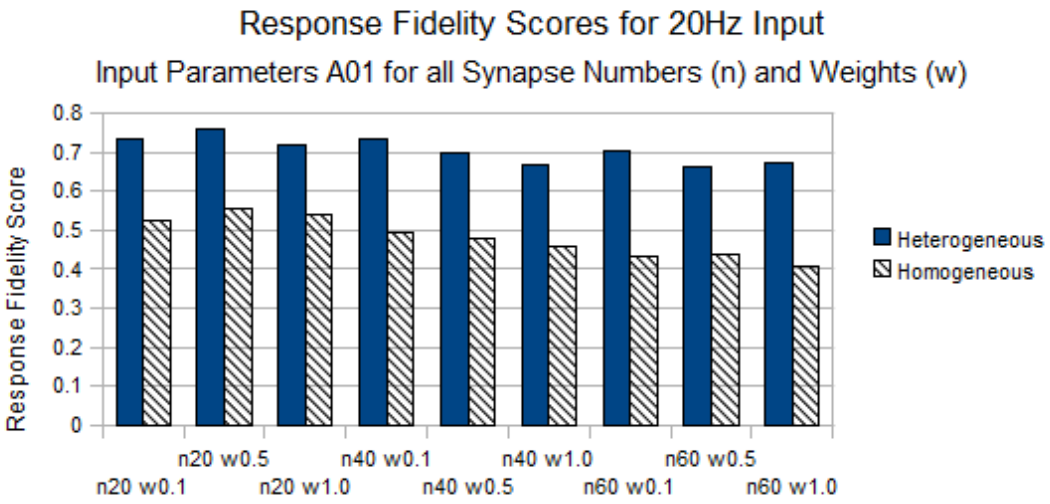

Figure A.8: Stage 3 Response Fidelity Comparison for 20Hz Input, Heterogeneous vs Homogeneous Populations. For A03 Input set, across all synapse numbers and weights

BIBLIOGRAPHY

[1] E. D. Adrian. Discharges from vestibular receptors in the cat. *J Physiol*, 101(4):389–407, Mar 1943.

[2] J. Ahn, L. J. Kreeger, S. T. Lubejko, D. A. Butts, and K. M. MacLeod. Heterogeneity of intrinsic biophysical properties among cochlear nucleus neurons improves the population coding of temporal information. *J Neurophysiol*, 111(11):2320–2331, Jun 2014.

[3] D. E. Angelaki, G. A. Bush, and A. A. Perachio. Two-dimensional spatiotemporal coding of linear acceleration in vestibular nuclei neurons. *J Neurosci*, 13(4):1403–1417, Apr 1993.

[4] D. E. Angelaki and J. D. Dickman. Spatiotemporal processing of linear acceleration: primary afferent and central vestibular neuron responses. *J Neurophysiol*, 84(4):2113–2132, Oct 2000.

[5] E. Av-Ron and P. P. Vidal. Intrinsic membrane properties and dynamics of medial vestibular neurons: a simulation. *Biol Cybern*, 80(6):383–392, Jun 1999.

[6] Bruno B. Averbeck, Peter E. Latham, and Alexandre Pouget. Neural correlations, population coding and computation. *Nat Rev Neurosci*, 7(5):358–366, May 2006.

[7] Martha W. Bagnall, Lauren E. McElvain, Michael Faulstich, and Sascha du Lac. Frequency-independent synaptic transmission supports a linear vestibular behavior. *Neuron*, 60(2):343–352, Oct 2008.

[8] Martha W. Bagnall, Renna J. Stevens, and Sascha du Lac. Transgenic mouse lines subdivide medial vestibular nucleus neurons into discrete, neurochemically distinct populations. *J Neurosci*, 27(9):2318–2330, Feb 2007.

[9] R. A. Baird, G. Desmadryl, C. Fernandez, and J. M. Goldberg. The vestibular nerve of the chinchilla. ii. relation between afferent response properties and peripheral innervation patterns in the semicircular canals. *J Neurophysiol*, 60(1):182–203, Jul 1988.

[10] R. Baker, C. Evinger, and R. A. McCrea. Some thoughts about the three neurons in the vestibular ocular reflex. *Ann N Y Acad Sci*, 374:171–188, 1981.

[11] S. Bello, G. D. Paige, and S. M. Highstein. The squirrel monkey vestibulo-ocular reflex and adaptive plasticity in yaw, pitch, and roll. *Exp Brain Res*, 87(1):57–66, 1991.

[12] R. H. Blanks, I. S. Curthoys, and C. H. Markham. Planar relationships of the semicircular canals in man. *Acta Otolaryngol*, 80(3-4):185–196, 1975.

[13] R. Boyle, J. M. Goldberg, and S. M. Highstein. Inputs from regularly and irregularly discharging vestibular nerve afferents to secondary neurons in squirrel monkey vestibular nuclei. iii. correlation with vestibulospinal and vestibuloocular output pathways. *J Neurophysiol*, 68(2):471–484, Aug 1992.

[14] A. M. Bronstein and M. A. Gresty. Short latency compensatory eye movement responses to transient linear head acceleration: a specific function of the otolith-ocular reflex. *Exp Brain Res*, 71(2):406–410, 1988.

[15] A. N. Burkitt and G. M. Clark. Synchronization of the neural response to noisy periodic synaptic input. *Neural Comput*, 13(12):2639–2672, Dec 2001.

[16] Shawn D. Burton, G Bard Ermentrout, and Nathaniel N. Urban. Intrinsic heterogeneity in oscillatory dynamics limits correlation-induced neural synchronization. *J Neurophysiol*, 108(8):2115–2133, Oct 2012.

[17] Jon Cafaro and Fred Rieke. Noise correlations improve response fidelity and stimulus encoding. *Nature*, 468(7326):964–967, Dec 2010.

[18] Nicholas Carriero and David Gelernter. The s/net's linda kernel. *ACM Trans. Comput. Syst.*, 4(2):110–129, May 1986.

[19] Nicholas Carriero and David Gelernter. Linda in context. *Commun. ACM*, 32(4):444–458, April 1989.

[20] C. Chabbert, J. M. Chambard, A. Sans, and G. Desmadryl. Three types of depolarization-activated potassium currents in acutely isolated mouse vestibular neurons. *J Neurophysiol*, 85(3):1017–1026, Mar 2001.

[21] Mircea I. Chelaru and Valentin Dragoi. Efficient coding in heterogeneous neuronal populations. *Proc Natl Acad Sci U S A*, 105(42):16344–16349, Oct 2008.

[22] Sofiane Cherif, Kathleen E. Cullen, and Henrietta L. Galiana. An improved method for the estimation of firing rate dynamics using an optimal digital filter. *J Neurosci Methods*, 173(1):165–181, Aug 2008.

[23] M. C. Chubb, A. F. Fuchs, and C. A. Scudder. Neuron activity in monkey vestibular nuclei during vertical vestibular stimulation and eye movements. *J Neurophysiol*, 52(4):724–742, Oct 1984.

[24] R. A. Clendaniel, D. M. Lasker, and L. B. Minor. Horizontal vestibuloocular reflex evoked by high-acceleration rotations in the squirrel monkey. iv. responses after spectacle-induced adaptation. *J Neurophysiol*, 86(4):1594–1611, Oct 2001.

[25] Richard A. Clendaniel, David M. Lasker, and Lloyd B. Minor. Differential adaptation of the linear and nonlinear components of the horizontal vestibuloocular reflex in squirrel monkeys. *J Neurophysiol*, 88(6):3534–3540, Dec 2002.

[26] K. Cullen and S. Sadeghi. Vestibular system. *Scholarpedia*, 3(1):3013, 2008. revision 137650.

[27] K. E. Cullen and R. A. McCrea. Firing behavior of brain stem neurons during voluntary cancellation of the horizontal vestibuloocular reflex. i. secondary vestibular neurons. *J Neurophysiol*, 70(2):828–843, Aug 1993.

[28] Kathleen E. Cullen and Lloyd B. Minor. Semicircular canal afferents similarly encode active and passive head-on-body rotations: implications for the role of vestibular efference. *J Neurosci*, 22(11):RC226, Jun 2002.

[29] I. S. Curthoys, C. H. Markham, and E. J. Curthoys. Semicircular duct and ampulla dimensions in cat, guinea pig and man. *J Morphol*, 151(1):17–34, Jan 1977.

[30] C. de Waele, M. Serafin, A. Khateb, T. Yabe, P. P. Vidal, and M. Muhlethaler. Medial vestibular nucleus in the guinea-pig: apamin-induced rhythmic burst firing–an in vitro and in vivo study. *Exp Brain Res*, 95(2):213–222, 1993.

[31] Agnes Delahaies, David Rousseau, Jean-Baptiste Fasquel, and Francois Chapeau-Blondeau. Local-feature-based similarity measure for stochastic resonance in visual perception of spatially structured images. *J Opt Soc Am A Opt Image Sci Vis*, 29(7):1211–1216, Jul 2012.

[32] J David Dickman and Dora E. Angelaki. Dynamics of vestibular neurons during rotational motion in alert rhesus monkeys. *Exp Brain Res*, 155(1):91–101, Mar 2004.

[33] Marianne Dieterich and Thomas Brandt. Functional brain imaging of peripheral and central vestibular disorders. *Brain*, 131(Pt 10):2538–2552, Oct 2008.

[34] J. K. Douglass, L. Wilkens, E. Pantazelou, and F. Moss. Noise enhancement of information transfer in crayfish mechanoreceptors by stochastic resonance. *Nature*, 365(6444):337–340, Sep 1993.

[35] Ruth Anne Eatock and Karen M. Hurley. Functional development of hair cells. *Curr Top Dev Biol*, 57:389–448, 2003.

[36] Ruth Anne Eatock, Karen M. Hurley, and Melissa A. Vollrath. Mechanoelectrical and voltage-gated ion channels in mammalian vestibular hair cells. *Audiol Neurootol*, 7(1):31–35, 2002.

[37] Ruth Anne Eatock, Jingbing Xue, and Radha Kalluri. Ion channels in mammalian vestibular afferents may set regularity of firing. *J Exp Biol*, 211(Pt 11):1764–1774, Jun 2008.

[38] G Bard Ermentrout, Roberto F. Galan, and Nathaniel N. Urban. Reliability, synchrony and noise. *Trends Neurosci*, 31(8):428–434, Aug 2008.

[39] A. Aldo Faisal and Simon B Laughlin. Stochastic simulations on the reliability of action potential propagation in thin axons. *PLoS Comput Biol*, 3(5):e79, 05 2007.

[40] A Aldo Faisal, Luc P J. Selen, and Daniel M. Wolpert. Noise in the nervous system. *Nat Rev Neurosci*, 9(4):292–303, Apr 2008.

[41] P. FATT and B. KATZ. Some observations on biological noise. *Nature*, 166(4223):597–598, Oct 1950.

[42] C. Fernandez and J. M. Goldberg. Physiology of peripheral neurons innervating semicircular canals of the squirrel monkey. ii. response to sinusoidal stimulation and dynamics of peripheral vestibular system. *J Neurophysiol*, 34(4):661–675, Jul 1971.

[43] C. Fernandez and J. M. Goldberg. Physiology of peripheral neurons innervating otolith organs of the squirrel monkey. i. response to static tilts and to long-duration centrifugal force. *J Neurophysiol*, 39(5):970–984, Sep 1976.

[44] C. Fernandez and J. M. Goldberg. Physiology of peripheral neurons innervating otolith organs of the squirrel monkey. ii. directional selectivity and force-response relations. *J Neurophysiol*, 39(5):985–995, Sep 1976.

[45] C. Fernandez and J. M. Goldberg. Physiology of peripheral neurons innervating otolith organs of the squirrel monkey. iii. response dynamics. *J Neurophysiol*, 39(5):996–1008, Sep 1976.

[46] C. Fernandez, J. M. Goldberg, and W. K. Abend. Response to static tilts of peripheral neurons innervating otolith organs of the squirrel monkey. *J Neurophysiol*, 35(6):978–987, Nov 1972.

[47] Michael Fetter. Vestibulo-ocular reflex. *Dev Ophthalmol*, 40:35–51, 2007.

[48] A. F. Fuchs and J. Kimm. Unit activity in vestibular nucleus of the alert monkey during horizontal angular acceleration and eye movement. *J Neurophysiol*, 38(5):1140–1161, Sep 1975.

[49] H. L. Galiana, H. L. Smith, and A. Katsarkas. Comparison of linear vs. non-linear methods for analysing the vestibulo-ocular reflex (vor). *Acta Otolaryngol*, 115(5):585–596, Sep 1995.

[50] J. M. Goldberg and C. Fernandez. Physiology of peripheral neurons innervating semicircular canals of the squirrel monkey. 3. variations among units in their discharge properties. *J Neurophysiol*, 34(4):676–684, Jul 1971.

[51] J. M. Goldberg and C. Fernanndez. Efferent vestibular system in the squirrel monkey: anatomical location and influence on afferent activity. *J Neurophysiol*, 43(4):986–1025, Apr 1980.

[52] J. M. Goldberg, S. M. Highstein, A. K. Moschovakis, and C. Fernandez. Inputs from regularly and irregularly discharging vestibular nerve afferents to secondary neurons in the vestibular nuclei of the squirrel monkey. i. an electrophysiological analysis. *J Neurophysiol*, 58(4):700–718, Oct 1987.

[53] J. M. Goldberg, C. E. Smith, and C. Fernandez. Relation between discharge regularity and responses to externally applied galvanic currents in vestibular nerve afferents of the squirrel monkey. *J Neurophysiol*, 51(6):1236–1256, Jun 1984.

[54] D. Golomb, D. Hansel, B. Shraiman, and H. Sompolinsky. Clustering in globally coupled phase oscillators. *Phys. Rev. A*, 45:3516–3530, Mar 1992.

[55] B. P. Graham and M. B. Dutia. Cellular basis of vestibular compensation: analysis and modelling of the role of the commissural inhibitory system. *Exp Brain Res*, 137(3-4):387–396, Apr 2001.

[56] Andrea M. Green and Dora E. Angelaki. Internal models and neural computation in the vestibular system. *Exp Brain Res*, 200(3-4):197–222, Jan 2010.

[57] G. M. Halmagyi, I. S. Curthoys, P. D. Cremer, C. J. Henderson, M. J. Todd, M. J. Staples, and D. M. D'Cruz. The human horizontal vestibulo-ocular reflex in response to high-acceleration stimulation before and after unilateral vestibular neurectomy. *Exp Brain Res*, 81(3):479–490, 1990.

[58] D. Hansel, G. Mato, and C. Meunier. Synchrony in excitatory neural networks. *Neural Comput*, 7(2):307–337, Mar 1995.

[59] C. M. Harris and D. M. Wolpert. Signal-dependent noise determines motor planning. *Nature*, 394(6695):780–784, Aug 1998.

[60] LaurenceR. Harris, Karl Beykirch, and Michael Fetter. Levels of analysis of the vestibulo-ocular reflex: A postmodern approach. In Laurence Harris and Michael Jenkin, editors, *Levels of Perception*, pages 279–294. Springer New York, 2003.

[61] S. M. Highstein. Synaptic linkage in the vestibulo-ocular and cerebello-vestibular pathways to the vith nucleus in the rabbit. *Exp Brain Res*, 17(3):301–314, 1973.

[62] S. M. Highstein, J. M. Goldberg, A. K. Moschovakis, and C. Fernandez. Inputs from regularly and irregularly discharging vestibular nerve afferents to secondary neurons in the vestibular nuclei of the squirrel monkey. ii. correlation with output pathways of secondary neurons. *J Neurophysiol*, 58(4):719–738, Oct 1987.

[63] Stephen M. Highstein, Richard D. Rabbitt, Gay R. Holstein, and Richard D. Boyle. Determinants of spatial and temporal coding by semicircular canal afferents. *J Neurophysiol*, 93(5):2359–2370, May 2005.

[64] A. Him, A. R. Johnston, J. L. Yau, J. Seckl, and M. B. Dutia. Tonic activity and gaba responsiveness of medial vestibular nucleus neurons in aged rats. *Neuroreport*, 12(18):3965–3968, Dec 2001.

[65] Y. Hirata, J. M. Lockard, and S. M. Highstein. Capacity of vertical vor adaptation in squirrel monkey. *J Neurophysiol*, 88(6):3194–3207, Dec 2002.

[66] T. P. Hirvonen, H. Aalto, I. Pyykko, and M. Juhola. Phase difference of vestibulo-ocular reflex in head autorotation test. *Acta Otolaryngol Suppl*, 529:98–100, 1997.

[67] A. L. HODGKIN and A. F. HUXLEY. A quantitative description of membrane current and its application to conduction and excitation in nerve. *J Physiol*, 117(4):500–544, Aug 1952.

[68] Timothy M. Hospedales, Mark C W. van Rossum, Bruce P. Graham, and Mayank B. Dutia. Implications of noise and neural heterogeneity for vestibulo-ocular reflex fidelity. *Neural Comput*, 20(3):756–778, Mar 2008.

[69] T. E. Hullar and L. B. Minor. High-frequency dynamics of regularly discharging canal afferents provide a linear signal for angular vestibuloocular reflexes. *J Neurophysiol*, 82(4):2000–2005, Oct 1999.

[70] Timothy E. Hullar, Charles C. Della Santina, Timo Hirvonen, David M. Lasker, John P. Carey, and Lloyd B. Minor. Responses of irregularly discharging chinchilla semicircular canal vestibular-nerve afferents during high-frequency head rotations. *J Neurophysiol*, 93(5):2777–2786, May 2005.

[71] Hans Hultborn. Plateau potentials and their role in regulating motoneuronal firing. *Adv Exp Med Biol*, 508:213–218, 2002.

[72] Eric Hunsberger, Matthew Scott, and Chris Eliasmith. The competing benefits of noise and heterogeneity in neural coding. *Neural Comput*, 26(8):1600–1623, Aug 2014.

[73] Karen M. Hurley, Sophie Gaboyard, Meng Zhong, Steven D. Price, Julian R A. Wooltorton, Anna Lysakowski, and Ruth Anne Eatock. M-like k+ currents in type i hair cells and calyx afferent endings of the developing rat utricle. *J Neurosci*, 26(40):10253–10269, Oct 2006.

[74] Marko Huterer and Kathleen E. Cullen. Vestibuloocular reflex dynamics during high-frequency and high-acceleration rotations of the head on body in rhesus monkey. *J Neurophysiol*, 88(1):13–28, Jul 2002.

[75] M. Ito, N. Nisimaru, and M. Yamamoto. Pathways for the vestibulo-ocular reflex excitation arising from semicircular canals of rabbits. *Exp Brain Res*, 24:257–271, Jan 1976.

[76] M. Ito, N. Nisimaru, and M. Yamamoto. Specific patterns of neuronal connexions involved in the control of the rabbit's vestibulo-ocular reflexes by the cerebellar flocculus. *J Physiol*, 265(3):833–854, Mar 1977.

[77] A. R. Johnston, N. K. MacLeod, and M. B. Dutia. Ionic conductances contributing to spike repolarization and after-potentials in rat medial vestibular nucleus neurones. *J Physiol*, 481 (Pt 1):61–77, Nov 1994.

[78] G. M. Jones and J. H. Milsum. Frequency-response analysis of central vestibular unit activity resulting from rotational stimulation of the semicircular canals. *J Physiol*, 219(1):191–215, Dec 1971.

[79] O. Kiehn and T. Eken. Functional role of plateau potentials in vertebrate motor neurons. *Curr Opin Neurobiol*, 8(6):746–752, Dec 1998.

[80] David C. Knill and Alexandre Pouget. The bayesian brain: the role of uncertainty in neural coding and computation. *Trends Neurosci*, 27(12):712–719, Dec 2004.

[81] Andrei S. Kozlov, Thomas Risler, and A. J. Hudspeth. Coherent motion of stereocilia assures the concerted gating of hair-cell transduction channels. *Nat Neurosci*, 10(1):87–92, Jan 2007.

[82] David M. Lasker, Gyu Cheol Han, Hong Ju Park, and Lloyd B. Minor. Rotational responses of vestibular-nerve afferents innervating the semicircular canals in the c57bl/6 mouse. *J Assoc Res Otolaryngol*, 9(3):334–348, Sep 2008.

[83] Agenor Limon, Cristina Perez, Rosario Vega, and Enrique Soto. Ca2+-activated k+-current density is correlated with soma size in rat vestibular-afferent neurons in culture. *J Neurophysiol*, 94(6):3751–3761, Dec 2005.

[84] S. G. Lisberger and F. A. Miles. Role of primate medial vestibular nucleus in long-term adaptive plasticity of vestibuloocular reflex. *J Neurophysiol*, 43(6):1725–1745, Jun 1980.

[85] S. G. Lisberger, F. A. Miles, and L. M. Optican. Frequency-selective adaptation: evidence for channels in the vestibulo-ocular reflex? *J Neurosci*, 3(6):1234–1244, Jun 1983.

[86] S. G. Lisberger, T. A. Pavelko, H. M. Bronte-Stewart, and L. S. Stone. Neural basis for motor learning in the vestibuloocular reflex of primates. ii. changes in the responses of horizontal gaze velocity purkinje cells in the cerebellar flocculus and ventral paraflocculus. *J Neurophysiol*, 72(2):954–973, Aug 1994.

[87] Ariel M. Lyons-Warren, Michael Hollmann, and Bruce A. Carlson. Sensory receptor diversity establishes a peripheral population code for stimulus duration at low intensities. *J Exp Biol*, 215(Pt 15):2586–2600, Aug 2012.

[88] William W. Lytton. *From computer to brain : foundations of computational neuroscience*. Springer, New York, 2002.

[89] Corentin Massot, Maurice J. Chacron, and Kathleen E. Cullen. Information transmission and detection thresholds in the vestibular nuclei: single neurons vs. population encoding. *J Neurophysiol*, 105(4):1798–1814, Apr 2011.

[90] Mark D. McDonnell and Derek Abbott. What is stochastic resonance? definitions, misconceptions, debates, and its relevance to biology. *PLoS Comput Biol*, 5(5):e1000348, May 2009.

[91] Mark D. McDonnell and Lawrence M. Ward. The benefits of noise in neural systems: bridging theory and experiment. *Nat Rev Neurosci*, 12(7):415–426, Jul 2011.

[92] J. F. Mejias and A. Longtin. Optimal heterogeneity for coding in spiking neural networks. *Phys Rev Lett*, 108(22):228102, Jun 2012.

[93] John R W. Menzies, John Porrill, Mayank Dutia, and Paul Dean. Synaptic plasticity in medial vestibular nucleus neurons: comparison with computational requirements of vor adaptation. *PLoS One*, 5(10), 2010.

[94] Leonor Michaelis, Maud Leonora Menten, Kenneth A. Johnson, and Roger S. Goody. The original michaelis constant: translation of the 1913 michaelis-menten paper. *Biochemistry*, 50(39):8264–8269, Oct 2011.

[95] Americo A. Migliaccio, Michael C. Schubert, Patpong Jiradejvong, David M. Lasker, Richard A. Clendaniel, and Lloyd B. Minor. The three-dimensional vestibulo-ocular reflex evoked by high-acceleration rotations in the squirrel monkey. *Exp Brain Res*, 159(4):433–446, Dec 2004.

[96] W. H. Miltner, C. Braun, M. Arnold, H. Witte, and E. Taub. Coherence of gamma-band eeg activity as a basis for associative learning. *Nature*, 397(6718):434–436, Feb 1999.

[97] L. B. Minor and J. M. Goldberg. Vestibular-nerve inputs to the vestibulo-ocular reflex: a functional-ablation study in the squirrel monkey. *J Neurosci*, 11(6):1636–1648, Jun 1991.

[98] L. B. Minor, D. M. Lasker, D. D. Backous, and T. E. Hullar. Horizontal vestibuloocular reflex evoked by high-acceleration rotations in the squirrel monkey. i. normal responses. *J Neurophysiol*, 82(3):1254–1270, Sep 1999.

[99] Nhamoinesu Mtetwa and Leslie S. Smith. Precision constrained stochastic resonance in a feedforward neural network. *IEEE Trans Neural Netw*, 16(1):250–262, Jan 2005.

[100] S. Nagata. The vestibulothalamic connections in the rat: a morphological analysis using wheat germ agglutinin-horseradish peroxidase. *Brain Res*, 376(1):57–70, Jun 1986.

[101] A. A. Perachio, G. A. Bush, and D. E. Angelaki. A model of responses of horizontal-canal-related vestibular nuclei neurons that respond to linear head acceleration. *Ann N Y Acad Sci*, 656:795–801, May 1992.

[102] Sandra Pfanzelt, Christian Rossert, Martin Rohregger, Stefan Glasauer, Lee E. Moore, and Hans Straka. Differential dynamic processing of afferent signals in frog tonic and phasic second-order vestibular neurons. *J Neurosci*, 28(41):10349–10362, Oct 2008.

[103] W. Precht and H. Shimazu. Functional connections of tonic and kinetic vestibular neurons with primary vestibular afferents. *J Neurophysiol*, 28(6):1014–1028, Nov 1965.

[104] R. Quadroni and T. Knopfel. Compartmental models of type a and type b guinea pig medial vestibular neurons. *J Neurophysiol*, 72(4):1911–1924, Oct 1994.

[105] Ramnarayan Ramachandran and Stephen G. Lisberger. Normal performance and expression of learning in the vestibulo-ocular reflex (vor) at high frequencies. *J Neurophysiol*, 93(4):2028–2038, Apr 2005.

[106] Ramnarayan Ramachandran and Stephen G. Lisberger. Transformation of vestibular signals into motor commands in the vestibuloocular reflex pathways of monkeys. *J Neurophysiol*, 96(3):1061–1074, Sep 2006.

[107] Stephen J. Read and Darren I. Urada. A neural network simulation of the outgroup homogeneity effect. *Pers Soc Psychol Rev*, 7(2):146–169, 2003.

[108] H. Reisine, J. I. Simpson, and V. Henn. A geometric analysis of semicircular canals and induced activity in their peripheral afferents in the rhesus monkey. *Ann N Y Acad Sci*, 545:10–20, 1988.

[109] Jessica R. Risner and Jeffrey R. Holt. Heterogeneous potassium conductances contribute to the diverse firing properties of postnatal mouse vestibular ganglion neurons. *J Neurophysiol*, 96(5):2364–2376, Nov 2006.

[110] J. E. Roy and K. E. Cullen. Selective processing of vestibular reafference during self-generated head motion. *J Neurosci*, 21(6):2131–2142, Mar 2001.

[111] Soroush G. Sadeghi, Maurice J. Chacron, Michael C. Taylor, and Kathleen E. Cullen. Neural variability, detection thresholds, and information transmission in the vestibular system. *J Neurosci*, 27(4):771–781, Jan 2007.

[112] Soroush G. Sadeghi, Lloyd B. Minor, and Kathleen E. Cullen. Response of vestibular-nerve afferents to active and passive rotations under normal conditions and after unilateral labyrinthectomy. *J Neurophysiol*, 97(2):1503–1514, Feb 2007.

[113] Hitoshi Sasaki, Sadatsugu Sakane, Takuya Ishida, Masayoshi Todorokihara, Tahei Kitamura, and Ryozo Aoki. Suprathreshold stochastic resonance in visual signal detection. *Behav Brain Res*, 193(1):152–155, Nov 2008.

[114] Adam D. Schneider, Kathleen E. Cullen, and Maurice J. Chacron. In vivo conditions induce faithful encoding of stimuli by reducing nonlinear synchronization in vestibular sensory neurons. *PLoS Comput Biol*, 7(7):e1002120, Jul 2011.

[115] Tilo Schwalger, Karin Fisch, Jan Benda, and Benjamin Lindner. How noisy adaptation of neurons shapes interspike interval histograms and correlations. *PLoS Comput Biol*, 6(12):e1001026, 2010.

[116] C. A. Scudder and A. F. Fuchs. Physiological and behavioral identification of vestibular nucleus neurons mediating the horizontal vestibuloocular reflex in trained rhesus monkeys. *J Neurophysiol*, 68(1):244–264, Jul 1992.

[117] Chris Sekirnjak and Sascha du Lac. Intrinsic firing dynamics of vestibular nucleus neurons. *J Neurosci*, 22(6):2083–2095, Mar 2002.

[118] M. Serafin, C. de Waele, A. Khateb, P. P. Vidal, and M. Mhlethaler. Medial vestibular nucleus in the guinea-pig. i. intrinsic membrane properties in brainstem slices. *Exp Brain Res*, 84(2):417–425, 1991.

[119] M. Serafin, C. de Waele, A. Khateb, P. P. Vidal, and M. Mhlethaler. Medial vestibular nucleus in the guinea-pig. ii. ionic basis of the intrinsic membrane properties in brainstem slices. *Exp Brain Res*, 84(2):426–433, 1991.

[120] C.E. Shannon and W. Weaver. *The Mathematical Theory of Communication*. Number v. 1 in Illini books. University of Illinois Press, 1949.

[121] H. Shimazu and W. Precht. Tonic and kinetic responses of cat's vestibular neurons to horizontal angular acceleration. *J Neurophysiol*, 28(6):991–1013, Nov 1965.

[122] C. E. Smith and J. M. Goldberg. A stochastic afterhyperpolarization model of repetitive activity in vestibular afferents. *Biol Cybern*, 54(1):41–51, 1986.

[123] Fred Spoor, Theodore Garland, Jr, Gail Krovitz, Timothy M. Ryan, Mary T. Silcox, and Alan Walker. The primate semicircular canal system and locomotion. *Proc Natl Acad Sci U S A*, 104(26):10808–10812, Jun 2007.

[124] C. E. Stafstrom, P. C. Schwindt, M. C. Chubb, and W. E. Crill. Properties of persistent sodium conductance and calcium conductance of layer v neurons from cat sensorimotor cortex in vitro. *J Neurophysiol*, 53(1):153–170, Jan 1985.

[125] Richard B. Stein, E Roderich Gossen, and Kelvin E. Jones. Neuronal variability: noise or part of the signal? *Nat Rev Neurosci*, 6(5):389–397, May 2005.

[126] M. Stopfer, S. Bhagavan, B. H. Smith, and G. Laurent. Impaired odour discrimination on desynchronization of odour-encoding neural assemblies. *Nature*, 390(6655):70–74, Nov 1997.

[127] H. Straka, N. Vibert, P. P. Vidal, L. E. Moore, and M. B. Dutia. Intrinsic membrane properties of vertebrate vestibular neurons: function, development and plasticity. *Prog Neurobiol*, 76(6):349–392, Aug 2005.

[128] Hans Straka, Frans M. Lambert, Sandra Pfanzelt, and Mathieu Beraneck. Vestibulo-ocular signal transformation in frequency-tuned channels. *Ann N Y Acad Sci*, 1164:37–44, May 2009.

[129] J. Szentagothai. The elementary vestibulo-ocular reflex arc. *J Neurophysiol*, 13(6):395–407, Nov 1950.

[130] Hiromitsu Tabata, Kenji Yamamoto, and Mitsuo Kawato. Computational study on monkey vor adaptation and smooth pursuit based on the parallel control-pathway theory. *J Neurophysiol*, 87(4):2176–2189, Apr 2002.

[131] R. D. Tomlinson and D. A. Robinson. Signals in vestibular nucleus mediating vertical eye movements in the monkey. *J Neurophysiol*, 51(6):1121–1136, Jun 1984.

[132] J J Torres, J Marro, and J F Mejias. Can intrinsic noise induce various resonant peaks? *New Journal of Physics*, 13(5):053014, 2011.

[133] George Wells. Coordination languages: Back to the future with linda. In *Proceedings of WCAT05*, pages 87–98, 2005.

[134] V. J. Wilson, R. Boyle, K. Fukushima, P. K. Rose, Y. Shinoda, Y. Sugiuchi, and Y. Uchino. The vestibulocollic reflex. *J Vestib Res*, 5(3):147–170, 1995.

[135] V. J. Wilson, R. M. Wylie, and L. A. Marco. Synaptic inputs to cells in the medial vestibular nucleus. *J Neurophysiol*, 31(2):176–185, Mar 1968.

[136] Julian R A. Wooltorton, Sophie Gaboyard, Karen M. Hurley, Steven D. Price, Jasmine L. Garcia, Meng Zhong, Anna Lysakowski, and Ruth Anne Eatock. Developmental changes in two voltage-dependent sodium currents in utricular hair cells. *J Neurophysiol*, 97(2):1684–1704, Feb 2007.

[137] J. Yamada and H. Noda. Afferent and efferent connections of the oculomotor cerebellar vermis in the macaque monkey. *J Comp Neurol*, 265(2):224–241, Nov 1987.

[138] Yide Zhou, Dalian Ding, Kari Suzanne Kraus, Dongzhen Yu, and Richard J. Salvi. Functional and structural changes in the chinchilla cochlea and vestibular system following round window application of carboplatin. *Audiol Med*, 7(4):189–199, Dec 2009.

[139] E. Zohary, M. N. Shadlen, and W. T. Newsome. Correlated neuronal discharge rate and its implications for psychophysical performance. *Nature*, 370(6485):140–143, Jul 1994.